Temperature-induced priming during *Pinus radiata* somatic embryogenesis: integrating proteomic, metabolic and physiological approaches

Ander Castander Olarieta

2021

eman ta zabal zazu

Universidad del País Vasco

Euskal Herriko Unibertsitatea

Temperature-induced priming during *Pinus radiata* somatic embryogenesis: integrating proteomic, metabolic and physiological approaches

Directoras

Paloma Moncaleán

Itziar A. Montalbán

AGRADECIMIENTOS

Parece que fue ayer cuando entré por primera vez por la puerta de Neiker, entre nervios y una gran emoción por empezar este maravilloso camino que hoy llega a su fin. Por ello, no querría dejar de agradecer a todas esas personas e instituciones que, de una forma u otra, han contribuido a hacer posible todo lo que sigue a estas líneas:

Gracias al Departamento de Desarrollo Económico, Sostenibilidad y Medio Ambiente del Gobierno Vasco, por la concesión de la beca predoctoral (Programa de ayudas de formación a jóvenes investigadores y tecnólogos en el entorno científico-tecnológico y empresarial del sector agropesquero y alimentario vasco), y a Neiker-BRTA, por poner a mi disposición sus instalaciones y recursos.

Asimismo, esta tesis ha podido realizarse gracias a los proyectos PINEM (agl2016-76143-c4-3R) y MULTIFOREVER (MULTIFOREVER project, supported under the umbrella of ERANET Cofund ForestValue by ANR (FR), FNR (DE), MINCyT (AR), MINECO-AEI (ES), MMM (FI) and VINNOVA (SE). ForestValue has received funding from the European Union's Horizon 2020 research and innovation programme under Grant Agreement No. 773324), y la ayuda de la red de ciencia BIOALI (P117RT0522).

Agradecimientos a mis directoras de tesis: las doctoras Paloma Moncaleán e Itziar Montalbán. Me siento infinitamente afortunado por haberos tenido como directoras. Gracias por vuestra confianza, vuestras enseñanzas y por todo lo que habéis hecho por mí. Mil gracias, de corazón.

A mis compañeros de laboratorio y oficina: Isi, Alejandra, Sonia, Alba, Maider, Kepa, Mikel, Iratxe, Mónica, Leire, Maite, Bego, Diego, Ana, Javi… ¡gracias a todos! Gracias también a la mejor compañera de mesa, alias, la técnico de Samsung, mi Anita Herrán, por su disponibilidad y buen humor. Y sobre todo, gracias a mi chuggggi, a mi compañera de aventuras y espero que gran amiga por muchos años: Cátia Pereira. ¡Gracias por ayudarme a contar pinos bajo el fresno a las 6 de la tarde…gracias por hacerme las horas más amenas frente al osmómetro con tus "melodiosos" cánticos! Has sido sin duda uno de los mayores regalos de la tesis.

A toda esa gente de administración, mantenimiento, campo, limpieza, etc que me ha ayudado a resolver esos problemillas del día a día.

A todas esas personas que he tenido la inmensa suerte de conocer durante mis estancias:

Thanks to professor Petronia Carillo, Emilia, Luisa, Angelo, Marilena, Francesca and the rest of people from the Department of Environmental, Biological and Pharmaceutical Sciences and Technologies from Caserta. You made me feel at home. ¡Grazie mille! ¡Vi ricorderò sempre con tanto amore!

To all the people from Brazil and Portugal: professors Miguel Guerra, Jorge Canhoto and Neusa Steiner. To my "portuguesiños": João, Sandra, Mariana, Daniela… ¡Obrigado!

A la profesora Ester Sales, de la Universidad de Zaragoza, por enseñarme que el truco de las qPCR consiste en maridarlas con un buen "Gewürztraminer". A la profesora Isabel Arrillaga de la Universidad de Valencia, por acogerme en su laboratorio y deleitarme con una buena horchatita de Alboraya. Bromas a un lado, gracias a las dos por todo.

A los profesores Tomás Goicoa y María Dolores Ugarte de la Universidad Pública de Navarra, por su inestimable ayuda con los análisis estadísticos.

A esas profesoras que dejan huella: Ana Aranburu, por recordarnos que ser "tacañorrito" no es una opción, y Begoña Uria, por conseguir que la biología pasara de encantarme a fascinarme.

A mis amigos: Olatz, por esas tardes de "amamas" en el New York recargando pilas; mi Maritxu, por sus maravillosas dotes de diseñadora gráfica y esta preciosa portada de tesis; Óscar, por su ayuda con la dichosa resolución de las fotos; Javi, por prestarme su casa en mi intento por dominar la estadística; Urtzi, Irene, por ser de esos amigos que siempre están ahí para echarte una mano. ¡¡¡Gracias a todos!!!

A mi familia, mis lleidatans, y en especial a mis padres, mis mayores referentes…sobran las palabras. Sin vosotros nada de esto hubiera sido posible. Y también a los que ya no están, porque ellos me inculcaron el amor por las plantas: mila esker Atxitxe eta Amama, naizenaren parte handi bat zuei zor dizuedalako!

Y como no, a ti, Enrique, por estar siempre ahí, por apoyarme en todo, porque a tu lado todo es mejor.

Eskerrik asko danori, bihotz bihotzez!!!

INDEX

INTRODUCTION

INTRODUCTION

1. *Pinus radiata D. Don*

Plantation forests have become the key to meet the wood and fibre needs of society. This situation is reflected in the fact that during the last decades, the increasing demand of forest products has promoted a rise of planted forest areas from 167.5 million ha in 1990 to 277.9 million ha in 2015, with approximately 42% of this area composed of the *Pinaceae* family (Payn et al., 2015).

Apart from wood products, due to the current trend towards bio-economy, non-wood forest products have gained special attention as prompters of new business opportunities, and will have a significant role in the near future forest-based value chains. The use of forests has broadened from timber production to the application of non-wood products in human nutrition, energy production and creation of reusable and recyclable bio-materials. This could transform strategic sectors of the economy such as construction and manufacturing (e.g. automotive, textiles, packaging, etc.) and create job and income opportunities in rural areas (FAO 2019; Weiss et al., 2020).

In this context, radiata pine (*Pinus radiata* D. Don) (Figure 1), formerly referred to as Monterey pine or insignis pine, is a species of great economic relevance and has become the most widely planted pine species for forestry in the world (Mead, 2013). Even if it is native to the Central Coast of California and Mexico (Rogers, 2002), nowadays there are more than four million ha of planted radiata pine worldwide, extending from New Zealand to Chile (about 1.5 million ha each), Australia, South Africa or Spain. It is in the last country where 13% of the wood cut annually comes from this pine (Ministerio de Medio Ambiente, Gobierno de España) and in some areas like the Basque Country it covers around 115,000 ha (Mapa forestal CAE, 2019) (Figure 2).

In spite of its preference for deep acid loamy texture soils (Olarieta et al., 2006), this pine is adaptable to a broad spectrum of land characteristics, growing from the see level up onto 800 m and in temperate climatic areas where annual rainfall is greater than 800 mm (Ceballos & Ruíz de la Torre, 1979). It is a fast-growing tree species, achieving mean

annual increments of 25 m^3 ha^{-1} $year^{-1}$ on 25-30-year rotations (Schimleck et al., 2018). Besides, thanks to the development of numerous extensive breeding programs (Zamudio et al., 2002) and improvement of silvicultural practices such as control over initial planting density, improved site preparation, thinning and fertilization at mid-rotation (Fox, 2000), mean annual increments of more than 40 m^3 ha^{-1} $year^{-1}$ have been obtained in many countries (Moore & Clinton, 2015).

Figure 1. (A) 6-year-old radiata pine tree in Lemoa, Biscay, Spain **(B)** Immature cone of radiata pine.

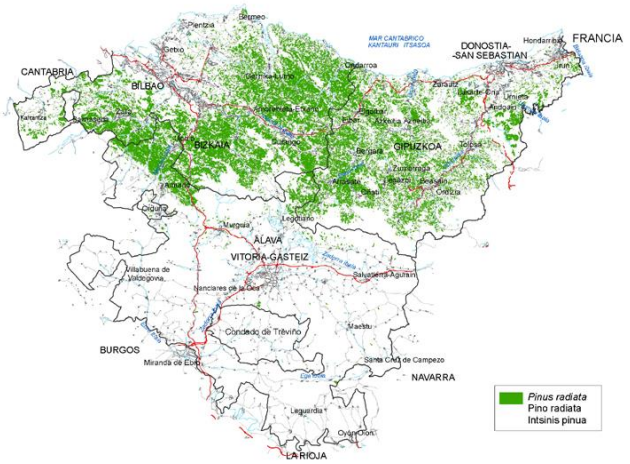

Figure 2. Distribution of radiata pine plantations in The Basque Country (Spain) (Inventario forestal de la Comunidad Autónoma del País Vasco 2005).

Radiata pine possesses medium-density, homogeneous and valued softwood, suitable for a wide range of uses. High-grade timber is used in house construction as weatherboards, posts or beams, but it can also be employed chipped to make particle board sheets, commonly used in flooring, together with thin high-grade ply suitable for furniture, cabinet work and boat building. Lower grade timber is usually converted to pulp to make paper. As a result, radiata pine plantations have become important sources of wood and fibre, which has stimulated the development of wood-using industries (Mead, 2013). Moreover, from the ecological point of view radiata pine is a valuable species in erosion control and carbon sink (Ausseil & Dymond, 2010).

Nonetheless, in recent years the area of planted radiata pine worldwide has remained static mainly due to poor returns (Mead, 2013). One of the multiple factors determining this situation is the impact of climate change, which is already threatening the viability and productivity of natural forests and plantations (Allen et al., 2010). Although gains in forest productivity are likely to occur as a result of CO_2 increases (Reyer, 2015), when the levels of CO_2 rise above 400 ppm, as already observed by Betts et al. (2016), the relative photosynthetic gains in C3 plants become progressively smaller (Watt et al., 2019). Besides, in many countries (Australia and Chile, for instance), climate is expected to become drier. Similar patterns have been described for Southern Europe, including Spain, where climate models predict lower precipitation (Tsanis & Tapoglou, 2018), and in some areas like the Bay of Biscay, heat wave episodes will become more frequent (Chust et al., 2011). This fact, coupled with alterations on the frequency and intensity of other damaging abiotic factors such as wind and fire will have a great impact in the survival of radiata pine plantations (Bender et al., 2010; Dupuy et al., 2020). Furthermore, climate change will influence the distribution and abundance of many pathogens such as *Fusarium circinatum*, *Diplodia pinea*, *Dothistroma pini*, *Dothistroma septosporum* and *Lecanosticta acicula*. These last three pathogens are responsible for the so-called red band and brown spot needle blight pine diseases, which are currently causing serious epidemics in many Atlantic pine ecosystems, including radiata pine plantations of the north of Spain (Ortíz de Urbina et al., 2016).

In consequence, a long-term strategy is required to maintain the productivity and health of forests. In this sense, tree breeding programmes should focus on the production of genotypes that will cope better with effects directly derived from climate change, such as drought, heat, or diseases (Codesido et al., 2012; Espinoza et al., 2013).

2. Forest biotechnology

Because of the often-poor correlation between juvenile and mature traits in conifers, proper testing in breeding programs generally requires at least about one-third to one-half the rotation age (Weng et al., 2008). This, coupled with the fact that conifer stem cuttings suitable for rooting are generally available only from juvenile plants has led to limitations in traditional breeding techniques. Conifer trees usually develop the characteristics to determine their suitability for clonal planting after phase-change (during maturity), a developmental moment when rooting of cuttings becomes unfeasible (Bonga et al., 2014). Moreover, the intrinsic heterozygosity found in conifers makes it difficult to fix desirable alleles by conventional techniques (Williams and Savolainen 1996).

Consequently, traditional breeding techniques should be combined with new biotechnological tools (forest biotechnology) such as *in vitro* tissue culture through organogenesis or somatic embryogenesis (SE) to effectively improve the performance, quality and health of commercially valued forest species (Giri et al., 2004).

Organogenesis has successfully been employed to propagate a wide variety of angiosperm species with high economic importance, such as *Eucalyptus* and *Populus*, and has also shown great potential with certain conifer species, including *P. radiata* (Aitken-Christie et al., 1988; Montalbán et al., 2011). However, in the *pinaceae* family this technique is restricted to zygotic embryos, parts of them, or young seedlings as explant sources, and attempts to clone selected adult individuals, albeit feasible, have not shown the desired results. In our laboratory, organogenesis from vegetative buds of various *Pinus* spp. was carried out (De Diego et al., 2008, 2010; Cortizo et al, 2009; Montalbán et al., 2013a), but after several months the resulting clonal plants showed

mature characteristics, denoting that the achieved rejuvenation was transient, leading to low rooting, acclimatization and growth rates.

As a result, during the last decades most research has focused on the development of SE systems, which have become the most commonly employed and the first biotechnology showing great potential for application in conifer forestry.

3. Somatic embryogenesis

SE is the process by which bipolar structures with no vascular connection with the surrounding tissue (somatic embryos) are formed from a single or a group of vegetative cells. Somatic embryos, unlike their zygotic counterparts, lack endosperm and an outer coat (Dodeman et al., 1997).

Induction of *in vitro* SE is usually triggered by the stress derived from the removal of the cells from their tissue environment and/or from the alteration of endogenous hormone balance. Under those conditions, cells are forced to adapt to their new environment, which leads to complex metabolic and genetic reprogramming coordinated by the action of transcription factors, DNA methylation, histone modifications and chromatin remodelling. In certain cases, those changes provoke a developmental transition in single cells or cell groups which are freed from the strong epigenetic repression that determines their somatic cell fate and enter the embryogenic program (Yang & Zhang, 2010; Fehér et al., 2015; Isah, 2016).

SE was first described in *Daucus carota* towards the middle of the 20th century independently by Steward et al. (1958) and Reinert (1958), and since then numerous protocols have been developed for a great variety of plants species, including conifers (i.e. in *Picea abies*; Hakman et al., 1985; Chalupa, 1985). In the genus *Pinus*, Smith et al. (1985) were the first describing the method of initiating SE by culturing intact megagametophytes enclosing immature zygotic embryos of *P. radiata.* Then, Gupta and Durzan (1986) first reported complete and successful SE in *P. lambertiana*. Following in their footsteps, many protocols have been published in the last years for other pine species: *P. taeda* (Li & Huang, 1996), *P. sylvestris* (Keinonen-Mettälä et al., 1996), *P.*

pinaster (Lelu-Walter, 1999), *P. pinea* (Carneros et al., 2009), *P. halepensis* (Montalbán et al., 2013b) and *P. canariensis* (Castander-Olarieta et al., 2020), among others.

SE can be accomplished either directly or indirectly. In the first case, somatic embryos directly arise from vegetative tissues while in indirect SE the original explants produce a calli of partially undifferentiated cells. The latter is the pathway followed by conifer species, and typically comprises five distinguishable steps: initiation, proliferation, maturation, germination and acclimatization *ex vitro* (Lelu-Walter et al., 2013). Masses of early-stage embryos, so-called proembryogenic masses (PEMs), are induced on culture media containing plant growth regulators (PGRs), usually a mix of cytokinins and auxins. After reaching a few millimetres in diameter, the embryogenic tissue is transferred to a semi-solid maintenance medium. Once the culture has been established, proliferation of the embryogenic tissue can be carried out in solid or liquid media (Stasolla & Yeung, 2003). Somatic embryo development is initiated by arresting cell proliferation trough removal of the PGRs used in previous phases and the application of abscisic acid, together with a reduction on water availability through increased gelling agent concentration or osmoticum in the culture medium (maturation) (Stasolla et al., 2002). Those mature somatic embryos will be separated from the remaining PEMs and transferred to a new culture medium most-frequently without PGRs. Once the embryos have developed roots and shoots, they should be transferred to *ex vitro* conditions onto suitable substrate under controlled conditions to avoid drastic changes and ensure a successful acclimatization (Klimaszewska et al., 2007).

In comparison with the other techniques, SE presents numerous advantages; it offers the possibility to obtain large amounts of somatic embryos from just one explant (Lelu-Walter et al., 2013) and it is a good solution when working with recalcitrant seeds from endangered species or valuable interspecific hybrid crosses that produce few seeds (Hargreaves et al., 2017; Egertsdotter et al., 2019). It is also a good source of material for genetic transformation (Álvarez et al., 2012), is cheaper and less time-consuming than other micropropagation techniques like organogenesis (Lelu-Walter et al., 2013) and avoids the appearance of premature aging traits typically encountered during vegetative

propagation by cuttings or vegetative buds that at the end result in high levels of plant material depreciation (Bonga et al., 2014).

Likewise, in the last years improvements have been made towards solving some bottlenecks of the process by enhancing initiation, maturation and germinations rates (Montalbán et al., 2010; 2012).

In spite of the abovementioned benefits of SE, one of the major features that has conditioned the commercial deployment of this propagation method in conifers is that, with a few exceptions, such as those observed in some adult somatic *Picea* spp trees (Klimaszewska et al. 2011; Varis et al., 2018), SE can only be successfully executed using juvenile initial explants (Salaj et al., 2015). However, this problem has been solved to a large degree thanks to the fact that SE enables the implementation of family and multi-varietal forestry.

Family forestry is based in the production of somatic plants from seeds of control-pollinated elite families, eliminating the lengthy clone testing periods that are required with the traditional techniques (Egertsdotter, 2018). On top of that, multi-varietal forestry allows for the deployment of tested varieties through vegetative propagation in intensively managed plantation forests (Park, 2016). This can only be achieved by its complementation with a method for long-term storage of plant material. In this sense, SE can be combined with the cryopreservation of PEMs (Häggman et al., 1998; Ford et al., 2000; Marum et al., 2004). In that way, somatic seedlings from the cryopreserved PEMs can be subjected to field trials and once the desired clones are selected, cryopreserved PEMs can be thawed, and somatic embryos produced. This technique offers the opportunity to obtain greater genetic gains than conventional tree breeding programs based on seed orchards and more flexibility regarding changing breeding goals and environmental conditions.

4. Induction of stress memory

In addition to being used as a propagation technique, in recent times SE has become a model system for studying numerous physiological, biochemical and developmental

events occurring during embryo development (Smertenko & Bozhkov, 2014; Trontin et al., 2016). SE is also an attractive system to study the effects of different abiotic factors in plants (Muilu-Mäkelä et al., 2015; Eliášová et al., 2017), as well as the epigenetic mechanisms integrating stress response and adaptation (Kvaalen & Johnsen, 2008).

In this context, embryo development and seed maturation appear to be key periods for the formation of stable epigenetic marks and stress memory, as reported in Norway spruce, the "model" conifer species for plant epigenetics (Johnsen et al., 2005; Kvaalen & Johnsen, 2008). These studies underlined that the environmental conditions during both zygotic and SE can modulate the timing of bud set and bud burst of plants years later by numerous epigenetic mechanisms, determining the climatic adaptation of this species. These epigenetic modifications include DNA and histone methylation, small RNAs and the differential expression of transposon-related genes (Yakovlev et al., 2010; 2011; 2016; Yakovlev & Fossdal, 2017).

This fact has opened the door to "engineer" plants at the embryo stage by the establishment of an epigenetic memory that could modulate their phenotype and adaptation capacity to different stress conditions years later (García-Mendiguren et al., 2017).

To this purpose, in previous studies carried out in our laboratory we have studied the effect of various stressful environmental conditions (temperature and water availability) along the different stages of *P. radiata* and *P. halepensis* SE: initiation (García Mendiguren et al., 2016a; Pereira et al., 2016, 2020), proliferation (Pereira et al., 2017), and maturation (Moncaleán et al., 2018). Results have shown that the application of specific environmental conditions at different stages of SE can provoke long-lasting effects that determine the success of further steps of the process months later, i.e., the production of somatic embryos or the germination capacity. Similar results were reported in *P. pinaster* (Arrillaga et al., 2019). Besides, those conditions seem to modulate the protein profile of the resulting somatic embryos, as observed in the levels of certain stress-related proteins (chaperones and ROS scavengers) (García-Mendiguren

et al, 2016b), as well as their auxin and cytokinin profiles, suggesting their role as mediators of stress response and adaptation (Moncaleán et al., 2018).

5. Mechanisms governing stress response and epigenetic memory

As sessile organisms, plants have acquired different strategies to cope with changing environmental conditions throughout evolution. Among them, phenotypic plasticity (short-term), epigenetic memory (mid-term) and local adaptation (long-term) are perhaps the most sophisticated, and epigenetics seems to have a determinant role in all of them (Sow et al., 2018).

Phenotypic plasticity is defined as the ability to express different phenotypes under changing environmental conditions by reversible changes in the epigenetic state of cells, modulating in that way the expression of specific genes. Once the stress factor in released, most of the epigenetic marks activated are reverted, but in some cases, plants can maintain part of those marks, developing the ability to remember the stress episode (priming), which results in a modified response upon a recurring stress or in a sustained response after the first exposure. This allows the plant to react more efficiently to future stress events (Amaral et al., 2020). This phenomenon covers both abiotic (Leuendorf et al., 2020; Marthandan et al., 2020) and biotic stresses (Wang et al., 2016; Morcillo et al., 2020), being referred to the former as systemic acquired resistance. Additionally, those epigenetic marks can become stable and even transmitted to the offspring as inter (environmental maternal effects; Zas et al., 2013) or transgenerational stress memory (Crisp et al., 2016), leading to local adaptation (Bose et al., 2020).

Due to the effect of epigenetic modifications on gene expression and phenotype determination, the study of phenotypic plasticity and epigenetic memory requires the integration of the different "omics" analyses (Fleta-Soriano & Munné-Bosch, 2016). This strategy increases the power of the study and could be used to validate epigenomics, by providing insights into the interactions between the multiple molecular regulation mechanisms underpinning these phenomena. In fact, transcriptomics offers an image of the direct effect of epigenetic changes on gene expression, while proteomics and

metabolomics are commonly used to link those effects with the phenotype by accounting for post-transcriptional and post-translational regulation mechanism (Perrone & Martinelli, 2020).

Transcriptomics, metabolomics and proteomics have been successfully applied in numerous tree species to shed light on the molecular mechanisms taking part in the response to a wide variety of stress factors, including heat, drought or UV light (Correia et al., 2016, 2018; Escandón et al., 2017, 2018; Pascual et al., 2016, 2017; Taïbi et al., 2015; Ujino-Ihara, 2020), but also as complement to the study of the epigenetic basis of stress memory (Lamelas et al., 2020).

In this regard, phytohormones have been demonstrated to play a key role not only during stress-sensing, response and adaptation, but also as a link between stress, epigenetics and its regulation (Galviz et al., 2020). Similarly, proteins, greatly due to their enzymatic nature, take part in almost all cellular processes, from signalling and direct stress responses (proteins involved in oxidative stress, cell structure and metabolism) (Hu et al., 2014), to gene expression control and memory acquisition (histones, transcription factors, heat shock proteins, etc) (Lamelas et al., 2020). All these modifications and readjustments are finally turned into changes at the metabolic level, among which, the function of certain carbohydrates and amino acids as compatible solutes and the synthesis of secondary metabolites such as phenolic compounds seem to be of great relevance under multiple stress factors (De Diego et al., 2013, 2015; Eliášová et al., 2017).

These approaches can be combined with traditional physiological analyses such as plant water-status, gas exchange parameters and photosynthetic activity determination (De Diego et al., 2012, 2013, 2015) to select physiological and molecular markers that could predict tolerance to stress early in the life of the plant (Taïbi et al., 2015, Escandón et al., 2017). Together with the implementation of advanced micropropagation techniques like SE, this strategy could improve genetic breeding programs and meet the current necessities derived from climate change.

6. General hypothesis and objectives

Based on this information the general hypothesis of the present work was the following:

- The application of high temperatures at initiation of radiata pine SE can trigger the formation of a stable epigenetic memory leading to the obtention of somatic plants with an altered capacity to cope with stress.

To this purpose, the objectives were:

1. To study the effect of high temperatures on the success of the different stages of the SE process (initiation, proliferation, maturation, germination).
2. To analyse the morphological features derived from heat-stress response in embryonal masses and somatic embryos.
3. To determine through physiological analyses if the resulting somatic plants present modified stress resilience.
4. To analyse the proteomic and metabolic basis of heat stress response and memory at different stages of SE.
5. To investigate if the application of heat has caused alterations in epigenetic marks along the whole embryogenic process.
6. To confirm whether the alteration of the epigenome has caused the differential expression of stress-related genes.

7. References

Aitken-Christie, J., Singh, A.P., and Davies, H. (1988). "Multiplication of meristematic tissue: a new tissue culture system for radiate pine" in Genetic manipulation of woody plants, eds. Hanover, J.W., Keathley, D.E. (Plenum Press, New York and London), 413-432.

Allen, C.D., Macalady, A.K., Chenchouni, H., Bachelet, D., McDowell, N., Vennetier, M., et al. (2010). A global overview of drought and heat-induced tree mortality reveals emerging climate change risks for forests. *For. Ecol. Manage.* 259, 660-684.

Álvarez, J.M., Cortizo, M., Ordás, R.J. (2012). Characterization of a type-A response regulator differentially expressed during adventitious caulogenesis in *Pinus pinaster*. *J. Plant Physiol.* 169, 1807-1814.

Amaral, J., Ribeyre, Z., Vigneaud, J., Sow, M.D., Fichot, R., Messier, C., et al. (2020). Advances and promises of epigenetics for forest trees. *Forests* 11, 976.

Arrillaga, I., Morcillo, M., Zanón, I., Lario, F., Segura, J., and Sales, E. (2019). New approaches to optimize somatic embryogenesis in maritime pine. *Front. Plant Sci.* 10, 138.

Ausseil, A.G.E., and Dymond, J.R. (2010). Evaluating ecosystem services of afforestation on erosion-prone land: a case study in the Manawatu Catchment, New Zealand. Proceedings: International Environmental Modelling and Software Society (IEMSS) 2010 *International Congress on Environmental Modelling and Software Modelling for Environment's Sake, Fifth Biennial Meeting, Ottawa, Canada, 5–8 July, 201*0 (available at: www.iemss.org/iemss2010/papers/S06/S.06.02.Evaluating ecosystem services of afforestation on erosionprone land a case study in the Manawatu catchment, New Zealand - ANNE-GAELLE AUSSEIL.pdf)

Bender, M.A., Knutson, T.R., Tuleya, R.E., Sirutis, J.J., Vecchi, G.A., Garner, S.T., et al. (2010). Modeled impact of anthropogenic warming on the frequency of intense Atlantic hurricanes. *Science* 327, 454-458.

Betts, R., Jones, C., Knight, J., Keeling, R.F., and Kennedy, J.J. (2016). El Niño and a record CO_2 rise. *Nature Clim. Change* 6, 806-810.

Bonga, J.M. (2014). A comparative evaluation of the application of somatic embryogenesis, rooting of cuttings, and organogenesis of conifers. *Can. J. For. Res.* 45, 379-383.

Bose, A.K., Moser, B., Rigling, A., Lehmann, M.M., Milcu, A., Peter, M., et al. (2020). Memory of environmental conditions across generations affects the acclimation potential of scots pine. *Plant Cell Environ*. 43, 1288-1299.

Carneros, E., Celestino, C., Klimaszewska, K., Park, Y.S., Toribio, M., and Bonga, J.M. (2009). Plant regeneration in Stone pine (*Pinus pinea* L.) by somatic embryogenesis. *Plant Cell Tiss. Organ Cult.* 98, 165–178.

Ceballos, L., and Ruíz De La Torre, J., 1979. Árboles y Arbustos de la España Peninsular. IFIE, España.

Chalupa, V. (1985). Somatic embryogenesis and plant regeneration from cultured immature and mature embryos of *Picea abies* (L.) Karst. *Commun. Inst. For. Czech.* 14, 57-63.

Chust, G., Borja, Á., Caballero, A., Irigoien, X., Sáenz, J., Moncho, R., et al. (2011). Climate change impacts on coastal and pelagic environments in the southeastern Bay of Biscay. *Clim Res.* 48, 307-332.

Codesido, V., Zas, R., and Fernández-López, J. (2012). Juvenile–mature genetic correlations in *Pinus radiata D. Don*. under different nutrient × water regimes in Spain. *Eur. J. Forest Res.* 131, 297-305.

Correia, B., Valledor, L., Hancock, R.D., Renaut, J., Pascual, J., Soares, A.M.V.M., et al. (2016). Integrated proteomics and metabolomics to unlock global and clonal responses of *Eucalyptus globulus* recovery from water deficit. *Metabolomics* 12, 141.

Correia, B., Hancock, R.D., Valledor, L., Pinto, G. (2018). Gene expression analysis in *Eucalyptus globulus* exposed to drought stress in a controlled and a field environment indicates different strategies for short- and longer-term acclimation. *Tree Physiol.* 38, 1623-1639.

Cortizo, M., de Diego, N., Moncaleán, P., and Ordás, R.J. (2009). Micropropagation of adult stone pine (*Pinus pinea* L.). *Trees - Struc. Funct.* 23, 835-842.

Crisp, P.A., Ganguly, D., Eichten, S.R., Borevitz, J.O., and Pogson, B.J. (2016). Reconsidering plant memory: intersections between stress recovery, RNA turnover, and epigenetics. *Sci. Adv.* 2, e1501340.

De Diego, N., Montalbán, I.A., Fernandez De Larrinoa, E., and Moncaleán, P. (2008). *In vitro* regeneration of *Pinus pinaster* adult trees. *Can. J. For. Res.* 38, 2607-2615.

De Diego, N., Montalbán, I.A., and Moncaleán, P. (2010). *In vitro* regeneration of adult *Pinus sylvestris* L. trees. *S. Afr. J. Bot.* 76, 158–162.

De Diego, N., Pérez-Alfocea, F., Cantero, E., Lacuesta, M., and Moncaleán, P. (2012). Physiological response to drought in radiata pine: Phytohormone implication at leaf level. *Tree Physiol.* 32, 435-449.

De Diego, N., Sampedro, M.C., Barrio, R.J., Saiz-Fernández, I., Moncaleán, P., and Lacuesta, M. (2013). Solute accumulation and elastic modulus changes in six radiata pine breeds exposed to drought. *Tree Physiol.* 33, 69-80.

De Diego, N., Saiz-Fernández, I., Rodríguez, J.L., Pérez-Alfocea, P., Sampedro, M.C., Barrio, R.J., et al. (2015). Metabolites and hormones are involved in the intraspecific variability of drought hardening in radiata pine. *J. Plant Physiol.* 188, 64-71.

Dodeman, V.L., Ducreux, G., and Kreis, M. (1997). Zygotic embryogenesis *versus* SE. *J. Exp. Bot.* 48, 1493-1509.

Dupuy, J., Fargeon, H., Martin-StPaul, N., Pimont, F., Ruffault, J., Guijarro, M., et al. (2020). Climate change impact on future wildfire danger and activity in southern Europe: a review. *Ann. For. Sci.* **77,** 35.

Egertsdotter, U. (2019). Plant physiological and genetical aspects of the somatic embryogenesis process in conifers. *Scand. J. For. Res.* 34, 360-369.

Egertsdotter, U., Ahmad, I., and Clapham, D. (2019). Automation and scale up of somatic embryogenesis for commercial plant production, with emphasis on conifers. *Front. Plant Sci*. 10, 109.

Eliášová, K., Vondráková, Z., Malbeck, J., Trávníčková, A., Pešek, B., Vágner, M., et al. (2017). Histological and biochemical response of Norway spruce somatic embryos to UV-B irradiation. *Trees - Struct. Funct.* 31, 1279-1293.

Escandón, M., Valledor, L., Pascual, J., Pinto, G., Cañal, M.J., and Meijón, M. (2017). System-wide analysis of short-term response to high temperature in *Pinus radiata*. *J. Exp. Bot.* 68, 3629-3641.

Escandón, M., Meijón, M., Valledor, L., Pascual, J., Pinto, G., and Cañal, M.J. (2018). Metabolome integrated analysis of high-temperature response in *Pinus radiata*. *Front. Plant Sci.* 9, 485.

Espinoza, S., Magni, C.R., Martínez, V., Ivković, M., and Gapare, W. (2013). Genetic parameters for early growth and biomass traits of *Pinus radiata* D. Don under different water regimes. *Silvae Genet.* 62, 110-116.

Fehér, A. (2015). Somatic embryogenesis - stress-induced remodeling of plant cell fate. *Biochim. Biophys. Acta - Gene Regul. Mech*. 1849, 385-402.

Fleta-Soriano, E., and Munné-Bosch, S. (2016) Stress memory and the inevitable effects of drought: a physiological perspective. *Front Plant Sci.* 15, 7-143.

Ford, C., Jones, N. and van Staden, J. (2000). Cryopreservation and plant regeneration from somatic embryos of *Pinus patula*. *Plant Cell Rep.* 19, 610–615.

Fox, T.R. (2000). Sustained productivity in intensively managed forest plantations. *Forest Ecol. Manag.* 138, 187-202.

Galviz, Y.C.F., Ribeiro, R.V., and Souza, G.M. (2020) Yes, plants do have memory. *Theor. Exp. Plant Physiol.* 32, 195-202.

García-Mendiguren, O., Montalbán, I.A., Goicoa, T., Ugarte, M.D., and Moncaleán, P. (2016). Environmental conditions at the initial stages of *Pinus radiata* somatic embryogenesis affect the production of somatic embryos. *Trees - Struct. Funct.* 30, 949-958.

García-Mendiguren, O., Montalbán, I.A., Goicoa, T., Ugarte, M.D., and Moncaleán, P. (2017). Are we able to modulate the response of somatic embryos of pines to drought stress? *Acta Hortic.* 1155, 77-84.

Giri, C.C., Shyamkumar, B., and Anjaneyulu, C. (2004). Progress in tissue culture, genetic transformation and applications of biotechnology to trees: an overview. *Trees – Struct. Funct.* 18, 115-135.

Gupta, P.K., and Durzan, D.J. (1986). Somatic polyembryogenesis from callus of mature sugar pine embryos. *Bio/Technol*. 4, 643-645.

Häggman, H.M., Ryynänen, L.A., Aronen, T.S., and Krajnakova, J. (1998). Cryopreservation of embryogenic cultures of Scots pine. *Plant Cell Tiss. Organ Cult.* 54, 45-53.

Hakman, I., Fowke, L.C., von Arnold, S., and Eriksson, T. (1985). The development of somatic embryos in tissue cultures initiated from immature embryos of *Picea abies* (Norway spruce). *Plant Science* 38, 53-59.

Hargreaves, C., Reeves, C., Gough, K., Montalbán, I.A., Low, C., van Ballekom, S., et al. (2017). Nurse tissue for embryo rescue: testing new conifer somatic embryogenesis methods in a F1 hybrid pine. *Trees - Struct. Funct.* 31, 273-283.

Hu, W.J., Chen, J., Liu, T.W., Simon, M., Wang, W.H., Chen, J., et al. (2014). Comparative proteomic analysis of differential responses of *Pinus massoniana* and *Taxus wallichiana* var. *mairei* to simulated acid rain. *Int. J. Mol. Sci.* 15, 4333-4355.

Isah, T. (2016). Induction of somatic embryogenesis in woody plants. *Acta Physiol. Plant.* 38, 118.

Johnsen, Ø., Fossdal, C.G., Nagy, N., Mølmann, J., Dæhlen, O.G., and Skrøppa, T. (2005). Climatic adaptation in *Picea abies* progenies is affected by the temperature during zygotic embryogenesis and seed maturation. *Plant Cell Environ*. 28, 1090-1102.

Keinonen-Mettälä, K., Jalonen, P., Eurola, P., von Arnold, S., and von Weissenberg, K. (1996). Somatic embryogenesis of *Pinus sylvestris*. *Scand. J. For. Res.* 11, 242-250.

Klimaszewska K., Trontin J.F., Becwar M., Devillard C., Park Y.S., and Lelu-Walter M.A. (2007). Recent progress on somatic embryogenesis of four *Pinus* sp. *Tree For. Sci. Biotechnol.* 1, 11-25.

Klimaszewska, K., Overton, C., Stewart, D., and Rutledge, R.G. (2011). Initiation of somatic embryos and regeneration of plants from primordial shoots of 10-year-old somatic white spruce and expression of 11 genes followed during the tissue culture process. *Planta* 233, 635-647.

Kvaalen, H., and Johnsen, Ø. (2008). Timing of bud set in *Picea abies* is regulated by a memory of temperature during zygotic and somatic embryogenesis. *New Phytol.* 177, 49-59.

Lamelas, L., Valledor, L., Escandón, M., Pinto, G., Cañal, M.J., and Meijón, M. (2020). Integrative analysis of the nuclear proteome in *Pinus radiata* reveals thermopriming coupled to epigenetic regulation. *J. Exp. Bot.* 71, 2040-2057.

Lelu, M.A., Bastien, C., Drugeault, A., Gouez, M.L. and Klimaszewska, K. (1999). Somatic embryogenesis and plantlet development in *Pinus sylvestris* and *Pinus pinaster* on medium with and without growth regulators. *Physiol. Plant.* 105, 719-728.

Lelu-Walter, MA., Thompson, D., Harvengt, L., Sanchez, L., Toribio, M., Pâques, L.E. (2013). Somatic embryogenesis in forestry with a focus on Europe: state-of-the-art, benefits, challenges and future direction. *Tree Genet. Genomes* 9, 883-899.

Leuendorf, J.E., Frank, M., and Schmülling, T. (2020). Acclimation, priming and memory in the response of *Arabidopsis thaliana* seedlings to cold stress. *Sci. Rep.* 10, 689.

Li, X.Y., and Huang, F.H. (1996). Induction of somatic embryogenesis in loblolly pine (*Pinus taeda* L.). *In Vitro Cell Dev. Biol. - Plant* 32, 129-135.

Marthandan, V., Geetha, R., Kumutha, K., Renganathan, V.G., Karthikeyan, A., and Ramalingam, J. (2020). Seed priming: A feasible strategy to enhance drought tolerance in crop plants. *Int. J. Mol. Sci.* 21, 8258.

Marum, L., Estêvão, C., Oliveira, M.M., Amâncio, S., Rodrigues, L., and Miguel, C. (2004). Recovery of cryopreserved embryogenic cultures of maritime pine: effect of cryoprotectant and suspension density. *Cryo Letters* 25, 363-374.

Mead, D.J. (2013). Sustainable management of *Pinus radiata* plantations. *FAO Forestry Paper* 1-51.

Moncaleán, P., García-Mendiguren, O., Novák, O., Strnad, M., Goicoa, T., Ugarte, M.D., et al. (2018). Temperature and water availability during maturation affect the cytokinins and auxins profile of radiata pine somatic embryos. *Front. Plant Sci.* 9, 1-13.

Montalbán, I.A., De Diego, N., and Moncaleán, P. (2011). Testing novel cytokinins for improved in vitro adventitious shoots formation and subsequent ex vitro performance in *Pinus radiata*. *Forestry* 84, 363-373.

Montalbán, I.A., Novák, O., Rolčik, J., Strnad, M. and Moncaleán, P. (2013a), Endogenous cytokinin and auxin profiles during in vitro organogenesis from vegetative buds of *Pinus radiata* adult trees. *Physiol. Plantarum* 148, 214-231.

Montalbán, I.A., Setién-Olarra, A., Hargreaves, C.L., and Moncaleán, P. (2013b) Somatic embryogenesis in *Pinus halepensis* Mill.: an important ecological species from the Mediterranean forest. *Trees- Struct. Funct.* 27, 1339-1351.

Montalbán, I.A., García-Mendiguren, O., and Moncaleán, P. (2016). "Somatic embryogenesis in *Pinus* spp." in Methods in Molecular Biology, eds. Lambardi, M., Germanà, M.A. (Humana Press-Springer: New York), 405-415.

Moore, J., and Clinton, P. (2015). Enhancing the productivity of radiata pine forestry within environmental limits. *N. Z. J. For.* 60, 35-41.

Morcillo, M., Sales, E., Ponce, L., Guillén, A., Segura, J., and Arrillaga, I. Effect of elicitors on holm oak somatic embryo development and efficacy inducing tolerance to *Phytophthora cinnamomi*. *Sci. Rep.* 10, 15166.

Muilu-Mäkelä, R., Vuosku, J., Hamberg, L., Latva-Mäenpää, H., Häggman, H., and Sarjala, T. (2015). Osmotic stress affects polyamine homeostasis and phenolic content in proembryogenic liquid cell cultures of Scots pine. *Plant Cell. Tiss. Org.* 122, 709-726.

Olarieta, J.R., Besga, G., Rodríguez-Ochoa, R., Aizpurua, A. and Usón, A. (2006). Land evaluation for forestry: a study of the land requirements for growing *Pinus radiata* D. Don in the Basque Country, northern Spain. *Soil Use Manage.* 22, 238-244.

Ortíz de Urbina, E., Mesanza, N., Aragonés, A., Raposo, R., Elvira-Recuenco, M., Boqué, R., et al. (2017). Emerging needle blight diseases in Atlantic *Pinus* ecosystems of Spain. *Forests* 8, 18.

Park, Y.S., BeauLieu, J., and Bousquet, J. (2016). "Multi-varietal forestry integrating genomic selection and somatic embryogenesis" in Vegetative Propagation of Forest Trees, eds. Park, Y.S., Bonga, J.M., Moon, H.K. (National Institute of Forest Science: Seoul), 302-322.

Pascual, J., Alegre, S., Nagler, M., Escandón, M., Annacondia, M.L., Weckwerth, W., et al. (2016). The variations in the nuclear proteome reveal new transcription factors and mechanisms involved in UV stress response in *Pinus radiata*. *J. Proteomics* 143, 390-400.

Pascual, J., Canal, M.J., Escandon, M., Meijon, M., Weckwerth, W., and Valledor, L. (2017). Integrated physiological, proteomic, and metabolomic analysis of ultra violet (UV) stress responses and adaptation mechanisms in *Pinus radiata*. *Mol. Cell. Proteomics* 16, 485-501.

Payn, T., Carnus, J.M., Freer-Smith, P., Kimberley, M., Kollert, W., Liu, S., et al. (2015). Changes in planted forests and future global implications. *Forest Ecol. Manag.* 352, 57-67.

Pereira, C., Montalbán, I.A., García-Mendiguren, O., Goicoa, T., Ugarte, M.D., Correia, S., et al. (2016). *Pinus halepensis* somatic embryogenesis is affected by the physical and chemical conditions at the initial stages of the process. *J. For. Res.* 21, 143-150.

Pereira, C., Castander-Olarieta, A., Montalbán, I.A., Pěnčík, A., Petřík, I., Pavlović, I., et al. (2020) Embryonal masses induced at high temperatures in Aleppo pine: Cytokinin profile and cytological characterization. *Forests* 11, 807.

Perrone, A., and Martinelli, F. (2020) Plant stress biology in epigenomic era. *Plant Sci*. 294, 110376.

Pullman, G.S., and Bucalo, K. (2014). Pine somatic embryogenesis: analyses of seed tissue and medium to improve protocol development. *New Forests* 45, 353-377.

Reinert, J. (1958). Morphogenese und ihre kontrolle an gewebekulturen aus carotten. *Naturwissenschaft* 45, 344-345.

Reyer, C.P.O. (2015). Projections of changes in forest productivity and carbon pools under environmental change - A review of stand scale modelling studies. *Curr. For. Rep.* 1, 53-68.

Rogers, D.L. (2002). *In situ* genetic conservation of Monterrey pine (*Pinus radiata* D. Don): information and recommendations. Report 26. Davis, California, USA, University of California, Division of Agriculture and Natural Resources, Genetic Resources Conservation Program.

Salaj, T., Matusova, R., and Salaj, J. (2015). Conifer somatic embryogenesis – an efficient plant regeneration system for theoretical studies and mass propagation. *Dendrobiology* 74, 69-76.

Schimleck, L., Antony, F., Dahlen, J., and Moore, J. (2018). Wood and fiber quality of plantation-grown conifers: a summary of research with an emphasis on loblolly and radiata pine. *Forests* 9, 298.

Smertenko, A., and Bozhkov, P.V. (2014). Somatic embryogenesis: life and death processes during apical-basal pattering. *J. Exp. Bot.* 65, 1343-1360.

Smith, D., Singh, A.P., and Wilton, L. (1985). Zygotic embryos of *Pinus radiata in vivo* and *in vitro*. Abstracts 3rd meeting International conifer tissue culture work group, Rotorua, 12-16.

Sow, M.D., Allona, I., Ambroise, C., Conde, D., Fichot, R., Gribkova, S., et al. (2018). "Epigenetics in forest trees: State of the art and potential implications for breeding and management in a context of climate change" in Advances in botanical research. Plant epigenetics coming of age for breeding applications, eds. Gallusci, P., Bucher, E., Mirouze, M. (Academic Press, Elsevier: Amsterdam), 387-453.

Stasolla, C., Kong, L., Yeung, E.C., Thorpe, T.A. (2002). Maturation of somatic embryos in conifers: Morphogenesis, physiology, biochemistry, and molecular biology. *In Vitro Cell.Dev.Biol.-Plant* 38, 93-105.

Stasolla, C., and Yeung, E.C. (2003). Recent advances in conifer somatic embryogenesis: improving embryo quality. *Plant cell Tiss. Org. Cult.* 74, 15-35.

Steward, F.C., Mapes, M.O., and Smith, J. (1958). Growth and organized development of cultured cells. II. Organization in cultures grown from freely suspended cells. *Amer. J. Bot.* 45, 705-708.

Taïbi, K., del Campo, A.D., Aguado, A., and Mulet, J.M. (2015). The effect of genotype by environment interaction, phenotypic plasticity and adaptation on *Pinus halepensis* reforestation establishment under expected climate drifts. *Ecol. Eng.* 84, 218-228.

Trontin, J.F., Klimaszewska, K., Morel, A., Hargreaves, C., and Lelu-Walter, M.A. (2016). "Molecular aspects of conifer zygotic and somatic embryo development: A review of genome-wide approaches and recent insights" in *In Vitro* Embryogenesis in Higher Plants, eds. Germana, M., Lambardi, M. (Humana Press, New York), 167-207.

Tsanis, I., and Tapoglou, E. (2019). Winter North Atlantic Oscillation impact on European precipitation and drought under climate change. *Theor. Appl. Climatol.* 135, 323-330.

Ujino-Ihara, T. (2020). Transcriptome analysis of heat stressed seedlings with or without pre-heat treatment in *Cryptomeria japonica*. *Mol. Genet. Genomics* 295, 1163-1172.

Varis, S., Klimaszewska, K., and Aronen, T. (2018). Somatic embryogenesis and plant regeneration from primordial shoot explants of *Picea abies* (L.) H. Karst. somatic trees. *Front. Plant Sci.* 871, 1551.

Wang, X.Y., Li, D.Z., Li, Q., Ma, Y.Q., Yao, J.W., Huang, X., et al. (2016). Metabolomic analysis reveals the relationship between AZI1 and sugar signalling in systemic acquired resistance of *Arabidopsis*. *Plant Physiol. Biochem.* 107, 273-287.

Watt, M.S., Kirschbaum, M.U.F., Moore, J.R., Pearce, H.G., Bulman, L.S., Brockerhoff, E.G., et al. (2019). Assessment of multiple climate change effects on plantation forests in New Zealand. *Int. J. For. Res.* 92, 1-15.

Weiss, G., Emery, M.R., Corradini, G., and Živojinović, I. (2020). New values of non-wood forest products. *Forests* 11, 165.

Weng, Y.H., Park, Y.S., Krasowski, M.J., Tosh, K.J., and Adams, G. (2008). Partitioning of genetic variance and selection efficiency for alternative vegetative deployment strategies for white spruce in eastern Canada. *Tree Genet. Genomes* 4, 809-819.

Williams, C.G., and Savolainen, O. (1996). Inbreeding depression in conifers: implications for using selfing as a breeding strategy. *For. Sci.* 42, 102-117.

Yakovlev, I.A., Fossdal, C.G., and Johnsen, Ø. (2010). MicroRNAs, the epigenetic memory and climatic adaptation in Norway spruce. *New Phytol.* 187, 1154-1169.

Yakovlev, I.A., Asante, D.K.A., Fossdal, C.G., Junttila, O., and Johnsen, T. (2011). Differential gene expression related to an epigenetic memory affecting climatic adaptation in Norway spruce. *Plant Sci.* 180, 132-139.

Yakovlev, I.A., Carneros, E., Lee, Y.K., Olsen, J.E., and Fossdal, C.G. (2016). Transcriptional profiling of epigenetic regulators in somatic embryos during temperature induced formation of an epigenetic memory in Norway spruce. *Planta* 243, 1237-1249.

Yakovlev, I.A., and Fossdal, C.G. (2017). *In silico* analysis of small RNAs suggest roles for novel and conserved miRNAs in the formation of epigenetic memory in somatic embryos of Norway spruce. *Front. Physiol.* 8.

Yang, X., and Zhang, X. (2010). Regulation of somatic embryogenesis in higher plants. *Crit. Rev. Plant Sci.* 29, 1, 36-57.

Zamudio, F., Baettyg, R., Vergara, A., Guerra, F., and Rozenberg, P. (2002). Genetic trends in woody density and radial growth with cambial age in a radiata pine progeny test. *Ann. For. Sci.* 59, 541-549.

Zas, R., Cendán, C., and Sampedro, L. (2013). Mediation of seed provisioning in the transmission of environmental maternal effects in Maritime pine (*Pinus pinaster* Aiton). *Heredity (Edinb).* 111, 248-255.

CHAPTER 1

Effect of thermal stress on tissue ultrastructure and metabolite profiles during initiation of radiata pine somatic embryogenesis

---

The content of this chapter corresponds to the published article "Castander-Olarieta, A., Montalbán, I.A., De Medeiros Oliveira, E., Dell'Aversana, E., D'Amelia, L., Carillo, P., Steiner, N., Fraga, H.P.D.F., Guerra, M.P., Goicoa, T., Ugarte, M.D., Pereira, C., and Moncaleán, P. (2019). Effect of thermal stress on tissue ultrastructure and metabolite profiles during initiation of radiata pine somatic embryogenesis. *Frontiers in Plant Science* 9, 1-16".

1. INTRODUCTION

Radiata pine (*Pinus radiata* D. Don) is a species native to the Central Coast of California and Mexico. Due to its rapid, versatile growth and the desirable quality of its pulp and lumber, it is suitable for a great range of uses and it is the most widely planted pine in the world (Escandón et al., 2017), extending from New Zealand to Chile, Australia, South Africa, and Spain. Owing to its great economic relevance, major emphasis has been placed during the past 50 years on the development of breeding programs (Espinel et al., 1995; Dungey et al., 2009). However, expected future climate change conditions will seriously threaten the survival and productivity of radiata pine plantations because of increased wind damage, more severe fungal infections, and a high frequency of fierce drought periods (Booth & McMurtrie, 1988; Spinoni et al., 2018). Accordingly, plant capacity to cope with environmental variations will be a key factor for the success of the plantations, with drought being one of the major limiting factors (Mena-Petite et al., 2004).

Somatic embryogenesis (SE) is an effective method for the large-scale propagation of "elite" plants and it can be combined with other technologies such as cryopreservation and selection of clones in field tests (Park, 2002). Moreover, it has been widely used as a model system for understanding the physiological and biochemical events occurring both during plant embryo development and in response to different abiotic stresses (Eliášová et al., 2017). SE in *Pinus radiata* was reported for the first time in by Smith (1997) and in recent years several studies have been made seeking to overcome various obstacles in the process (Hargreaves et al., 2002; Montalbán et al., 2010, 2012, 2015; Montalbán & Moncaleán, 2017, 2018).

Epigenetic variation is thought to be one of the main evolutionary strategies that endow plants with high phenotypic plasticity and an adaptive capacity to changing environments (Boyko & Kovalchuk, 2008; Bräutigam et al., 2013; García-Mendiguren et al., 2017) and clear examples, such as the phenomenon of what is traditionally called plant hardening (Villar-Salvador et al., 2004; Conrath et al., 2015) support this idea. In

the so-called deficit irrigation watering strategy, long-term drought tolerance can be induced by transient or partial drying, which could similarly be explained in terms of epigenetic mechanisms (Davies et al., 2010). These mechanisms do not involve mutation or other types of genome-related alterations. They are, by contrast, an active part in the formation of an epigenetic memory that results in modified metabolic and hormonal profiles. These modifications are responsible for the abovementioned long-lasting response which is observed in plants after an initial induction. Under different kinds of stress, which usually lead to the formation of oxygen radicals and osmotic imbalances, plants adjust many of their biochemical pathways and accumulate elevated amounts of metabolites. In many forest species, organic solutes, specifically soluble carbohydrates and free amino acids, are the principal compounds involved in this process (Patakas et al., 2002).

It has been reported that in some tree species such as Norway spruce (*Picea abies*), the temperature during zygotic embryogenesis appears to establish an adaptive epigenetic memory which may regulate the bud phenology and thus, the cold acclimation of the progeny, making this species well adapted to a large range of climatic and geographic areas (Kvaalen & Johnsen, 2008). Colder than normal conditions during zygotic embryogenesis result in plants presenting an early bud set and cold hardiness in autumn along with an early dehardening and bud flushing during spring, whilst higher temperatures delay these processes. Besides, it has been observed that the alterations are durable in progeny with identical genetic background (Johnsen et al., 2005; Yakovlev et al., 2011). In other long-lived plants such as Scots pine or Maritime pine it has been proved that maternal environmental conditions have a direct effect on the performance and phenotype of the offspring (Dormling & Johnsen, 1992; Zas et al., 2013). This "natural hardening" process suggests that embryogenesis may be a critical stage in modulating future plant behaviour, thus becoming, in combination with an appropriate propagation system, a valuable strategy for the production of "elite" plants adapted to different environmental conditions.

Following the experiments performed previously in our laboratory (García-Mendiguren et al., 2017), in this work we hypothesize that the application of high temperatures, which are known to reduce water availability (García-Mendiguren et al., 2016b), during the initiation stage of SE, may induce an epigenetic mark that could result in the formation of plantlets with a different capacity to tolerate drought stress through the accumulation of specific metabolites. SE at different induction temperatures has already been studied at a genetic and a transcriptional level for Norway spruce to explain the climatic adaptation of this species (Yakovlev et al., 2011, 2016); moreover, previous studies carried out in our laboratory suggest that the temperature at the initial stages of SE strongly influences the success of the subsequent steps (García-Mendiguren et al., 2016b; Pereira et al., 2016), even determining the protein profile of the obtained somatic embryos (Se's) (García-Mendiguren et al., 2016a). Some authors also emphasize the idea that stress could be an essential force to switch on the machinery required for SE (Fehér et al., 2003). In further studies the same authors pointed out that temperature exerts a selective pressure during the initial SE stages that result in lower rates of initiation but an improved yield for the forthcoming steps (Fehér, 2015).

Taking into account the abovementioned information, the aim of this work was to evaluate the effect of high temperatures (30, 40, 50, and 60°C) applied during the initial steps of SE in terms of initiation, proliferation and maturation rates, as well as the quantity and quality of the Se's obtained. In the same way, we have tried to elucidate if the stresses applied provoke any type of morphological or ultrastructural alteration in the embryogenic cultures at cellular level. Finally, an analysis of carbohydrate, amino acid and protein profiles has been carried out at initial steps of SE to analyse their behaviour under different temperatures.

2. MATERIALS AND METHODS

2.1. Plant material and initiation experiment

One year-old green female cones of *P. radiata* D.Don were collected in July 2016 and 2017 from four different open-pollinated trees (7, 12, 14, and 42) in a seed orchard

established by Neiker-Tecnalia in Deba (Spain; latitude: 43°16′59″N, longitude: 2°17′59″W, elevation: 50 m). Cones were wrapped in filter paper and stored at 4°C for one month following Montalbán et al. (2015). They were then surface-sterilized with 70% (v/v) ethanol, split into quarters and all the immature seeds were extracted and surface sterilized following Montalbán et al. (2012). Seed coats were removed and intact megagametophytes were excised out aseptically and placed horizontally onto EDM initiation medium (Walter et al., 2005) supplemented with 3.5 gL^{-1} gellan gum (Gelrite®; Duchefa).

Experiment 1

For this experiment, cones collected in 2016 were utilized and the assessment of temperatures and the duration of the treatments were based on preliminary studies carried out in our laboratory. In this case, the treatments were as follows: 23°C (8 weeks, control), 30°C (4 weeks), 40°C (4 days), and 50°C (5 min). The Petri dishes with medium were warmed up to the desired temperatures prior to placing the explants on the surface of the medium. Once the different treatments had finished, all the megagametophytes were kept at 23°C for 8 weeks in darkness. In summary, the experiment included four different treatments and four seed families, comprising a total of 960 megagametophytes.

After 8 weeks on the initiation medium, initiation rates were calculated and the emerging embryonal masses (EMs) bigger than 3–5 mm in diameter were separated from the megagametophytes and subcultured to a fresh EDM initiation medium. After 14 days, the EMs were subcultured onto an EDM proliferation medium (the same composition as the initiation medium but a 4.5 gL^{-1} of gellan gum (Gelrite®; Duchefa) every 2 weeks until maturation, as described by Montalbán et al. (2010). Following four periods of subculturing, actively growing EMs were recorded as established cell lines (ECLs), and the percentage of proliferating lines respect to the EMs initiated was calculated. For maturation, 8 replicates were prepared per embryogenic cell line (ECL) and each replicate contained 80 mg of EM. Proliferation and maturation were both

conducted in darkness at 23°C. After 12–16 weeks, the maturation success was evaluated and the number of Se's per gram of EM were calculated.

Experiment 2

In this second experiment, cones from 2017 were used and, based on the result of Experiment 1, higher temperatures and shorter time periods were tested. Therefore, the megagametophytes were cultured at 23°C (8 weeks), 40°C (4 h), 50°C (30 min), and 60°C (5 min). The following steps were carried out in the same way as in Experiment 1 with slight differences. In this case, just before their placement onto an EDM proliferation medium, a small part of all the proliferating ECLs was frozen in liquid nitrogen and stored at -80°C. In addition, after assessing the maturation success, the morphology of the obtained Se's was studied. There were 10 Se's per each of the four selected ECLs per temperature treatment (4). In summary, 160 Se's were analysed. For this purpose, two measurements were made using a Leica DMS 1000 microscope and the LAS V4.12 (Leica Application Suite) software: the total length of the Se's and the width, measured just under the cotyledons.

2.2. Micromorphological study

Light microscopy analyses were carried out with EMs which had been frozen after the first proliferation subculture following the procedure described by Fraga et al. (2015). Three ECLs were used per treatment, comprising a total of 12 ECLs. Samples of approximately 3–5 mm in diameter were collected and fixed in formaldehyde (2.5%) in 0.1 M sodium phosphate buffer (pH 7.2) overnight at 4°C. Subsequently, the material was washed twice for 15 min in buffer without fixative and then dehydrated in an increasing series of ethanol aqueous solutions (30–100%), comprising a total of six different solutions, each being applied for 30 min. Then, the samples were infiltrated with Historesin (Leica Historesin, Heidelberg, Germany) and sections of 5 µm were obtained using a rotatory microtome (Slee Technik). After adhesion to histological slides, sections were stained with 1% toluidine blue in an aqueous solution of 1% Borax pH 9. Samples were analysed and photographed using an Olympus BX 40 microscope equipped with a computer-controlled Olympus DP 71 digital camera.

2.3. Ultrastructural analysis

The same 12 ECLs were subjected to transmission electron microscopy (TEM). To this end, samples of 3–5 mm in diameter were fixed in 2.5% v/v glutataldehyde in 0.1% w/v sodium cacodylate buffer and 0.6% w/v sucrose overnight. After five washing steps, each of 20 min, with decreasing concentrations of glucose in 0.1% w/v sodium cacodylate buffer, the samples were post-fixed using 1% osmium tetroxide and 0.1 M sodium cacodylate for 4 h, washed again three times with the same concentration of sodium cacodylate and dehydrated in an increasing series of acetone aqueous solutions (30–100%), following the same procedure described above for light microscopy assays. Then, the material was embedded in Spurr's resin (Spurr, 1969) and ultrathin sections (60 nm) were collected and stained on grinds using aqueous uranyl acetate followed by lead citrate (Reynolds, 1963). The samples were then examined under TEM JEM 1011 (JEOL Ltd., Tokyo, Japan, at 80 kV).

2.4. Metabolites analysis

Metabolite analysis was performed with the same frozen 12 ECLs used for the micromorphological and ultrastructural analyses. Frozen samples were powdered and diluted 1/12 in ethanol 80% as described by Carillo et al. (2012) with slight modifications. This solution, which will be referred to below as main extract, was used to determine amino acid, total proteins, and carbohydrates.

Amino acid content determination

For primary amino acids (alanine, arginine, asparagine, aspartate, ethanolamine, phenylalanine, GABA, glycine, glutamate, glutamine, isoleucine, histidine, leucine, lysine, methionine, ornithine, proline, serine, tyrosine, threonine, tryptophane and valine), distilled water was added to the main extract so that the final concentration was ethanol: water in a ratio of 2:3 (v/v). Following this, all samples were centrifuged for 30 s at 14,000 rpm and diluted by ½ in ethanol 40%. Amino acids were estimated by HPLC after pre-column derivatization by *o*-phthaldialdehyde (OPA) according to Carillo et al. (2011b) using a reverse phase 5 μm ZORBAX Eclipse Plus C18 (250 × 4.6 mm internal

diameter; Agilent Technologies). The extract was injected into the column and eluted at a flow rate of 0.85 ml/min at 27°C with a discontinuous gradient. Solvent A was a mixture of 50 mM sodium acetate, 20% (v/v) methanol and 3% (v/v) tetrahydrofuran. Solvent B was pure methanol. The amino acid-OPA derivatives were detected by their fluorescence with excitation at 330 nm and emission at 450 nm.

Proline was determined following the procedure of Bates et al. (1973) and described in Carillo et al. (2011a) with slight modifications. Briefly, aliquots of ethanol (containing 2/3 water) previously prepared for amino acid analysis were used. Three replicates of 40 µl were taken from each sample and 80 µl of a reaction mix prepared with ninhydrin 1% (w/v) in acetic acid 60% (v/v) and ethanol 20% (v/v) were added. Then, the samples were kept in the heating block at 90°C and mixed for 20 min at 1,400 rpm. After cooling at room temperature, centrifugation was carried out at 14,000 rpm for 1 min. Following this, 100 µl of each sample were dispensed in a polypropylene microplate and introduced in a Safas Monaco microplate reader for absorbance measurement at 520 nm.

Total protein content determination

Total protein content was determined by the method described by Bradford (1976) with bovine serum albumin as standard as described by Augusti et al. (1999).

Carbohydrate content quantification

Sugars and starch were measured from the main extract according to Pietrini et al. (1999) with slight modifications. After subsequent extraction steps using decreasing concentrations of ethanol, mixing at 80°C for 20 min and centrifugation at 14,000 rpm for 5 min, the supernatant was immediately analysed for soluble sugars (glucose, sucrose, and fructose) or stored at -20°C until analysis. The pellet, containing starch, was re-suspended in KOH 0.1M, heated for 2 h at 94°C and centrifuged for 1 min at 10,000 rpm. pH correction (pH 7) was carried out using acetic acid. To dissolve starch, 50 mM of sodium acetate buffer, containing four units of β-amilase and 40 units of amyloglucosidase were added and the mixture was incubated at 30°C for 2 days to allow

complete starch hydrolysis. Following this, the samples were centrifuged and the supernatant analysed for glucose. Soluble sugars, as well as glucose resulting from the hydrolysis of starch, were analysed enzymatically as described by Jones et al. (1977). Sucrose and fructose were determined by the addition of 2 units of invertase and 1 unit of isomerase, respectively. The assay was performed using a Safas Monaco microplate reader with wavelength fixed at 340 nm and a measurement interval of 1 min.

2.5. Data collection and statistical analysis

Once the initiation and proliferation rates had been calculated in Experiments 1 and 2, a logistic regression was performed to assess the effect of temperature on both parameters. The mother tree was introduced into the model as a block variable to reduce variability, and temperature was considered as the variable factor. Multiple comparisons were based on predictable linear functions of model coefficients, and Tukey's *post-hoc* test ($\alpha = 0.05$) was used. *p* values were conveniently adjusted according to the Benjamini and Hochberg (1995) method.

In relation to maturation results, a logistic regression and the corresponding analysis of deviance were conducted to assess the effect of temperature on the number of mature Se's per gram of EM. The ECL was included in the model as a random effect with a different variance for each temperature level. The inclusion of the ECL improved the fit and helped to analyse the effect of temperature more accurately.

As for the evaluation of Se's morphology, the length and length/width ratio measurements were analysed following the same procedure described for maturation. A logistic regression including the ECL as a random effect with the corresponding analysis of deviance was carried out to evaluate the effect of temperature on both measurements. In this case a different variance was considered for each ECL level. Multiple comparisons were based on a Tukey *post-hoc* test ($\alpha = 0.05$).

Finally, for the data obtained from metabolites analysis, a linear mixed effect model with the ECL as a random effect and the corresponding analysis of variance were performed

to assess the effect of temperature on the amount of each metabolite in logarithmic scale. Multiple comparisons were based on Tukey *post hoc* tests.

3. RESULTS

3.1. Initiation experiment

Experiment 1

It should be mentioned that megagametophytes subjected to 40°C for 4 days failed to initiate, so no results could be obtained for proliferation and maturation (Table 1). As for the other three treatments, statistically significant differences were found at initiation percentages between treatments 23 and 30°C, and 50°C and 30°C ($p < 0.05$) (Table 2). 30°C was the treatment with the lowest initiation rate, compared with the values obtained for 50 and 23°C, which did not show significant differences between them (Table 1). Concerning proliferation, similar results were observed but differences were significant between all the treatments ($p < 0.05$) (Table 2). Once again, treatment 30°C presented the lowest values and the highest proliferation rates were obtained when treatment at 50°C was applied, followed by treatment 23°C (Table 1).

Table 1. Embryonal mass initiation and proliferation (%) in *P. radiata* megagametophytes cultured at different temperatures in EDM for Experiment 1 and Experiment 2. Data are presented as mean values ± SE. Significant differences at p < 0.05 are indicated by different letters for initiation and by different numbers for proliferation.

Experiment 1			Experiment 2		
Treatment	**Initiation %**	**Proliferation %**	**Treatment**	**Initiation %**	**Proliferation %**
23°C, 8 weeks	56.9 ± 3.12[a]	29.9 ± 2.89[2]	23°C, 8 weeks	12 ± 2.14[a]	10.6 ± 2.12[1]
30°C, 4 weeks	23.3 ± 3.20[b]	6.2 ± 1.86[3]	40°C, 4 h	9.6 ± 2.24[a]	6.7 ± 1.64[1]
40°C, 4 days	0 ± 0	0 ± 0	50°C, 30 min	5.9 ± 1.59[a]	4.1 ± 1.26[1]
50°C, 5 min	54.7 ± 3.44[a]	37.2 ± 3.46[1]	60°C, 5 min	10.8 ± 2.35[a]	8.5 ± 2.10[1]

Maturation showed no variations with respect to temperature, as 59 out of the 64 ECLs (92.2%) accomplished maturation. No significant differences were found for the number of Se's produced per gram of EM either ($p < 0.05$) (Supplementary Table 1). However, it

is noteworthy that ECLs derived from treatments 50 and 30°C produced the highest number of Se's, compared with those from treatment 23°C (Table 3).

Table 2. Analysis of deviance of the logistic regression for initiation and proliferation (%) of *Pinus radiata* embryonal masses in Experiment 1 and Experiment 2 according to temperature.

Experiment 1				Experiment 2			
Source	**df**	**X^2 test**	***p* value**	**Source**	**df**	**X^2 test**	***p* value**
Initiation				**Initiation**			
Temperature (T)	2	112.845	$< 2.2\times10^{-16}$	Temperature (T)	3	5.8749	0.11786
Proliferation				**Proliferation**			
Temperature (T)	2	124.13	$< 2.2\times10^{-16}$	Temperature (T)	3	7.7246	0.05206

Table 3. Number of somatic embryos per gram of embryonal mass obtained under different initiation temperatures in Experiment 1 and Experiment 2. Data are presented as mean values ± SE.

Experiment 1		Experiment 2	
Treatment	**Se's/g EM**	**Treatment**	**Se's/g EM**
23°C, 8 weeks	334.55 ± 27.13	23°C, 8 weeks	207.12 ± 32.74
30°C, 4 weeks	520.88 ± 63.1	40°C, 4 h	283.68 ± 72.22
40°C, 4 days	-	50°C, 30 min	256.25 ± 40.3
50°C, 5 min	564.71 ± 56.96	60°C, 5 min	216.32 ± 22.33

Experiment 2

The initiation percentage did not show statistically significant differences between the assayed temperatures ($p < 0.05$) (Table 2). The same results were obtained for proliferation, despite the fact that the differences observed for proliferation percentages are bordering on being statistically significant ($p = 0.05206$). However, it is remarkable that both initiation and proliferation rates showed the same decreasing pattern when high temperatures were applied, with 23°C being the treatment with the highest initiation and proliferation percentages and 50°C the one with the lowest percentages. With respect to the other two treatments (40 and 60°C), they displayed an intermediate behaviour, with the results obtained for 60°C more similar to the ones for 23°C (Table 1).

Regarding maturation, 23 out of the 24 ECLs subjected to this process (95.8%) produced Se's, which clearly shows that temperature had no effect on the maturation capacity of the ECLs. As for the number of Se's per gram of EM, no significant differences were found between the different temperatures ($p < 0.05$) (Supplementary Table 1). All average values were around 200–300 Se's per gram of EM, with 23°C being the treatment with the lowest and the highest value corresponding to 40°C (Table 3).

Nevertheless, statistically significant differences were found for the length and the length/width ratio of the obtained Se's ($p < 0.05$). Se's derived from ECLs initiated at 50°C were significantly longer (3.76 ± 0.1 mm) than those from control treatments (2.34 ± 0.16 mm). Se's derived from treatments 40 and 60°C presented intermediate values (3.08 ± 0.13 and 3.05 ± 0.12 mm, respectively). With respect to length/width ratio, Se's from initiation temperatures 23 and 50°C showed the lowest values (2.408 ± 0.06 and 2.435 ± 0.1), denoting a barrel-like shape, especially those corresponding to treatment 50°C. On the other hand, Se's from treatments 40 and 60°C resulted in the highest values (2.872 ± 0.09 and 2.703 ± 0.09), denoting a more elongated shape (Figure 1).

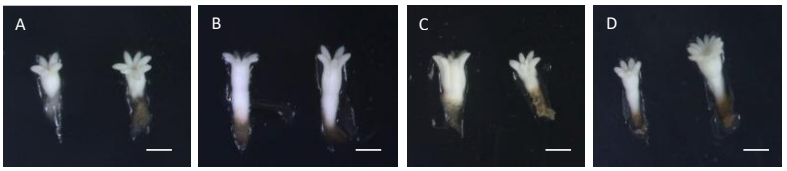

Figure 1. Somatic embryos produced under different initiation temperatures: 23°C, 8 weeks **(A)**, bar = 1 mm; 40°C, 4 h **(B)**, bar = 1.4 mm; 50°C, 30 min **(C)**, bar = 2.2 mm; and 60°C, 5 min **(D)**, bar = 1.7 mm. Notice the different morphologies between temperatures. Embryos from temperatures 40 and 60°C showing an elongated shape, while embryos from temperature 23°C are short and embryos from 50°C are big but barrel-shaped.

3.2. Micromorphological study

Micromorphological analyses revealed the presence of three cell types in the embryogenic cultures:

1. Embryogenic cells (ECs), which were small, round-shaped and had a dense cytoplasm, with large central nuclei (N), characteristics, all these being typical of meristematic cells.

2. Suspensor cells (SCs), which were elongated, according to their degree of vacuolation, and which had neither N nor organelles (in some cases a few degraded organelles were detected).
3. Embryonal tube-like cells (TLCs), seemed to be in transition between ECs and SCs as they share characteristics of both cell types. They had a big central N and a dense cytoplasm, but they showed an increase in length and in the number of vacuoles (V).

All these cells were attached to each other forming aggregates called proembryogenic masses (PEMs) and in all cases three developmental and organizational stages of PEMs were observed: PEMI, PEMII, and PEMIII. PEMI were characterized by the presence of small groups of ECs linked to one or two SCs, while PEMII and PEMIII consisted of a higher number of ECs and increased numbers of SCs, forming large cell clusters in the case of PEMIII. However, characteristics in terms of cell organization, polarization and structure differed significantly between the treatments.

In the case of the ECLs initiated at 23°C, all three stages of PEMs could be observed in the analysed samples and polarity was evident for all of them, especially for PEMIII. These structures showed a clear organization, divided into three regions, with an embryogenic dense mass composed of ECs at the top, followed by a transitional region formed by TCLs and a suspensor region at the end (Figure 2A). The cells at the embryogenic areas presented a smooth surface with a thick layer of polysaccharides and a high metabolic and mitotic activity (Figure 2B). SCs were long and most of them remained attached to the structure.

At 40°C, however, polarized structures were not always present. Even though a small grade of polarization was observed in some cases, most of the PEMs could not be divided into three regions. The reason for this was the appearance of SCs near embryogenic areas, without a clear and thick transition region dividing them, or just the formation of SCs directly from embryogenic areas, disturbing the cell cluster. It is also noticeable that ECs presented a decrease in mitotic activity and an increase in vacuolation (Figure 3).

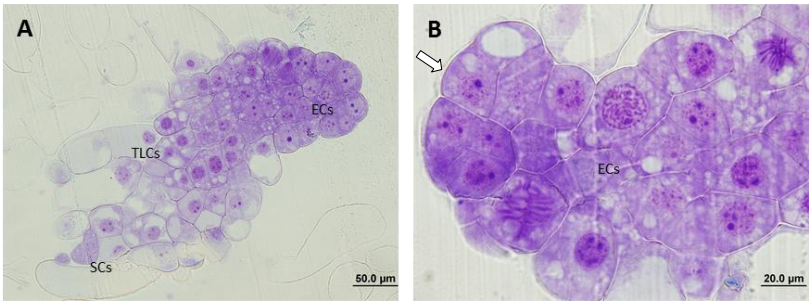

Figure 2. Light microscopy and histochemical analyses of proembryogenic masses (PEMs) of *Pinus radiata* induced at 23°C. **(A)** PEMIII showing clear polarization and a well divided structure: compact embryogenic area formed by embryogenic cells (ECs), transition region formed by tube-like cells (TLCs) and suspensor cells (SCs). **(B)** Detail of an embryogenic mass with high mitotic activity and thick layer of polysaccharides (arrow).

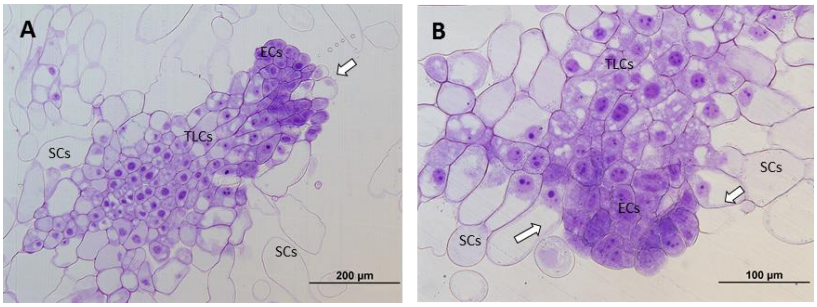

Figure 3. Light microscopy and histochemical analyses of PEMs of *P. radiata* induced at 40°C during 4 h. **(A)** Clear examples of PEMIIIs starting to lose polarization with SCs arising directly from embryonal areas, or close to them **(B)** (arrows). Note the increase of vacuolation and the decrease of mitotic activity in ECs.

At 50°C, polarization was non-existent. No cell organization could be observed. SCs arose directly from embryonal areas and most of them appeared detached from PEMs, presenting an advanced state of degradation in many cases. The number of SCs was also much higher than in the other treatments and embryonal areas were significantly smaller in this case, creating an unbalanced proportion between embryonal areas and suspensors (Figure 4A). Embryonal areas showed symptoms of early vacuolar programmed cell death (PCD) and loss of embryogenic state, such as an increase of vacuolation and a decrease of mitotic activity, as described by Smertenko & Bozhkov (2014). As well as this, in some of the cells, small blue-stained spots were detected

attached to the inner faces of tonoplasts, highlighting the presence of phenolic compounds (Figure 4B).

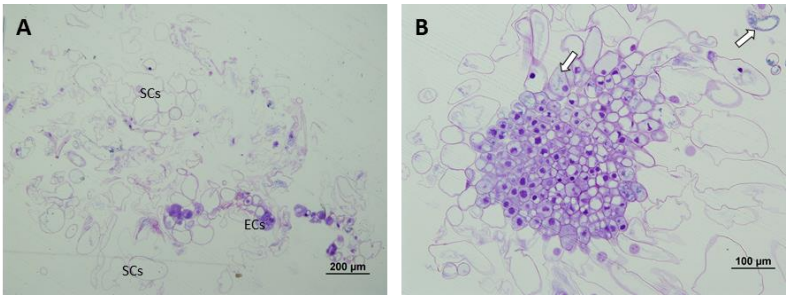

Figure 4. Light microscopy and histochemical analyses of PEMs of *P. radiata* induced at 50°C for 30 min. **(A)** General view of a sample presenting supernumerary SCs detached from small embryonal areas. Notice the great number of degraded SCs. **(B)** Embryonal area that has completely lost polarization and presents symptoms of PCD. Cells have a high rate of vacuolation, start to elongate to form SCs and heterochromatin becomes more visible. Small phenolic grains start to appear (arrows).

Finally, for ECLs initiated at 60°C, both polarized and non-polarized areas were detected. In the case of non-polarized areas, the same degeneration pattern was observed as in samples initiated at 50°C, as well as the accumulation of abovementioned phenolic compounds (Figure 5B). In the case of polarized areas however, embryonal areas were even bigger than in the control samples and were tightly attached to each other, forming more developed structures that resembled early globular Se's (Figure 5A).

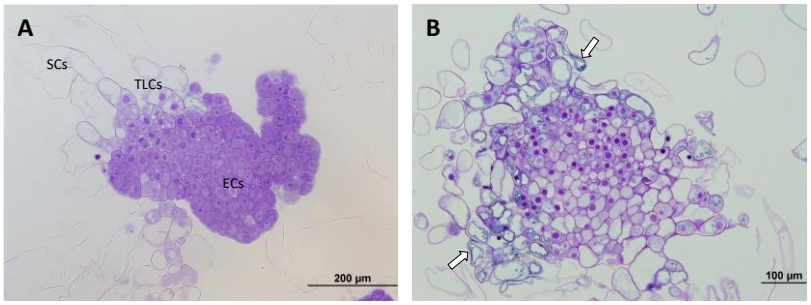

Figure 5. Light microscopy and histochemical analyses of PEMs of *P. radiata* induced at 60°C for 5 min. **(A)** PEMIII formed by a huge cluster of compact ECs resembling the first steps of somatic embryo development. **(B)** Detail of a group of ECs that have lost their embryogenic state and are developing into SCs. Note the absence of polarization, the non-organized formation of SCs and the presence of large amounts of phenolic compounds attached to the inner layer of vacuole membranes, stained in blue (arrows).

3.3. Ultrastructural analysis

As a general trend, TEM enabled observations of three cell types: ECs, TLCs and SCs. The ECs morphology, as briefly described previously, was characterized by a dense cytoplasm with a large, prominent central N, high ratio nuclei: cytoplasm, and distinguishable heterochromatin and euchromatin regions. Big nucleoli and intact nuclear envelope could also be observed (Figure 6A). In the cytoplasm many organelles such as, mitochondria (M), rough endoplasmic reticulum, Golgi bodies (G), small V and plastids, both with and without, starch grains (S) were present (Figures 6B,D). The cell wall was thin with a few plasmodesmata and a visible middle lamella (Figure 6C).

Ultrastructural characterization of TCs and SCs, however, showed that these cells were undergoing different degrees of cellular disassembly as compared to cellular organization of ECs (Filonova et al., 2000). TLCs differed from ECs by being more elongated, with a thicker and less organized cell wall and a higher number and larger V. At the same time, many leucoplasts developed into amyloplasts, presenting huge S, and the number of G increased significantly, which resulted in the formation of large amounts of vesicles (Figure 6E). In SCs, engulfment of those vesicles and portions of cytoplasm by V gave rise to the formation of a big autolytic vacuole, that together with plastolysome-like structures (portions of cytoplasm surrounded by one or several double membranes arising from a plastid-like leucoplast) started to progressively destroy the cytosol and organelles, taking up the majority of the cell volume until its collapse and the formation of a hollow-walled corpse (Figures 6F–H).

Despite these general characteristics of each cell type, some differences were detected among treatments, supporting the results obtained from light microscopy assays. As a general trend, ECs from control samples (23°C), presented a dense cytoplasm with no or just a few V. Neither amyloplasts nor plastids with small grains of starch could be detected in these samples (Figure 7A). In the case of samples subjected to high temperatures, however, G became more numerous, the number of small V increased noticeably, and the presence of a big S around the N was noticeable (Figure 7B). Even though small amounts of phenolic compounds could be detected in the inner face of

tonoplasts, as described before in light microscopy experiments, no clear differences were seen among treatments in TEM analysis. For ECLs initiated at 50 and 60°C, big plastolysome-like structures (Figure 7D) and the formation of whorls by cytoplasmic membranes (Figure 7C) were identified. No clear differences among the treatments were observed for tube-like cells and SCs.

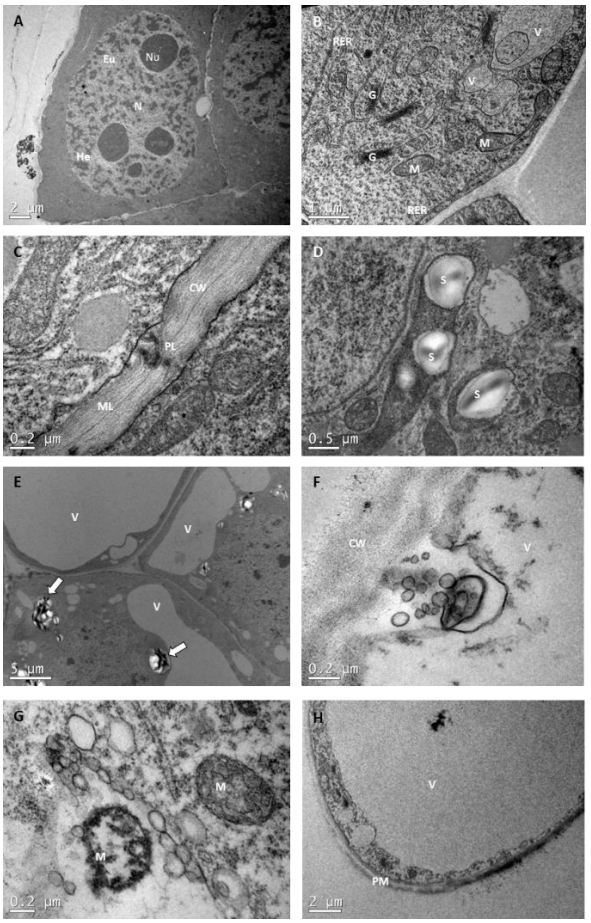

Figure 6. Transmission electron microscopy images of *P. radiata* ECs, TLCs, and SCs. **(A)** EC with huge central nuclei (N) presenting four nucleolus (Nu), heterochromatin (He) and euchromatin (Eu). Notice the high nuclei: cytoplasm ratio and the dense cytoplasm. **(B)** Detail of the EC cytoplasm with rough endoplasmic reticulum (RER), Golgi bodies (G), small vacuoles (V) and mitochondria (M). Observe the "sickle-like mitochondria" close to the plasma membrane (arrow). **(C)** Detail of the cell wall (CW), with well-organized fibers, visible middle lamella (ML) and some plasmodesmata (PL). **(D)** Image of plastids containing starch grains (S). **(E)** TLCs with big vacuoles and amyloplasts (arrows). **(F,G)** showing clear examples of cell dismantling and organelle degradation. Notice the disorganization of cell wall fibers. **(H)** Image of an SC with a huge central vacuole taking up most of the cell volume. The cytoplasm, with a few quite degenerated organelles occupies a narrow layer confined between tonoplast and plasma membrane (PM).

TEM analysis also revealed different types of M morphologies. Besides the typical cylindrical shaped with well-organized cristae morphology, we observed swollen M, mainly in cells undergoing PCD such as tube-like cells or SCs, and "sickle-like M" (Figure 6B).

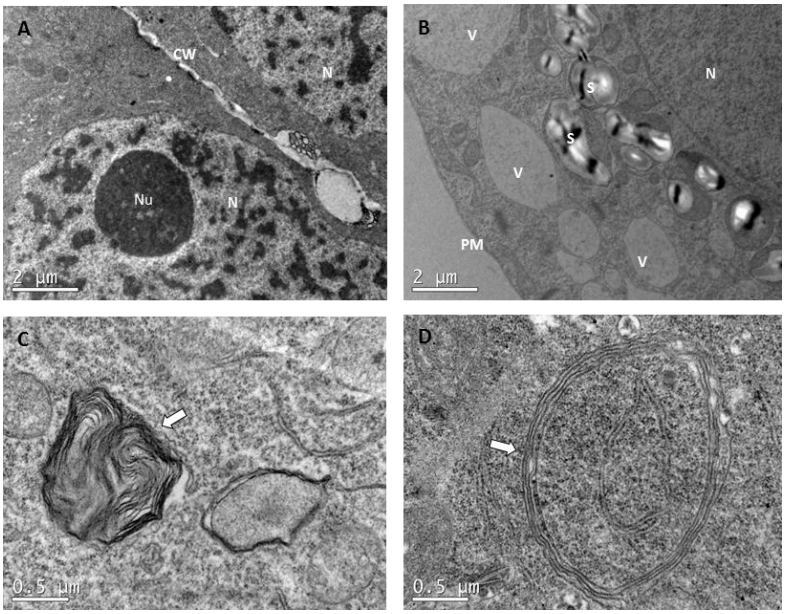

Figure 7. Transmission electron microscopy images comparing ECs that came from PEMs initiated at different temperatures. **(A)** EC from 23°C treatment. Observe the presence of a dense cytoplasm, with no or just a few small provacuoles. No starch grains can be detected. **(B)** EC from 40°C for 4 h with a lot of vacuoles, bigger than in the control treatment, and many plastids containing starch grains surrounding the nuclei. Both symptoms of PCD. **(C,D)** are details of the cytoplasm of ECs from 50°C for 30 min, showing whorls of cytoplasmic membranes and plastolysome-like structures, respectively.

3.4. Metabolites analysis

Among all the metabolites analysed, soluble sugars, starch, total protein, and the amino acids alanine, arginine, asparagine, aspartate, ethanolamine, phenylalanine, GABA, glycine, glutamate, glutamine, lysine, methionine, ornithine, proline, serine, threonine, tryptophan, and valine presented no significant differences (Tables 4, 5 and Supplementary Table 2). However, the applied stress resulted in significantly different contents of leucine, isoleucine, tyrosine and histidine (Table 5 and Supplementary Table 2).

Table 4. Carbohydrates (µmol/g FW) and soluble proteins (mg/g FW) in *Pinus radiata* embryonal masses under different initiation temperatures (23°C, 8 weeks; 40°C, 4 h; 50°C, 30 min; 60°C, 5 min). Data are presented as mean values ± SE. Significant differences at $p < 0.05$ are indicated by different letters.

	Treatment (°C)			
Carbohydrates (µmol/g FW)	**23**	**40**	**50**	**60**
Starch	6.4 ± 2.681[a]	3.36 ± 0.89[a]	5.77 ± 3.88[a]	5.32 ± 2.61[a]
Glucose	37.17 ± 2.91[a]	33.53 ± 2.28[a]	31.85 ± 4.65[a]	33.13 ± 1.7[a]
Fructose	40.48 ± 3.98[a]	38.86 ± 1.48[a]	44.77 ± 4.24[a]	41.63 ± 1.75[a]
Sucrose	7.73 ± 0.37[a]	6.74 ± 0.12[a]	7 ± 0.6[a]	7.17 ± 0.28[a]
Proteins (mg/g FW)				
Total protein	1.06 ± 0.16[a]	1.02 ± 0.08[a]	0.99 ± 0.03[a]	1.05 ± 0.12[a]

Regarding these differences, diverse patterns could be observed. In the case of tyrosine (Figure 8A), cell lines initiated at 23°C presented significantly ($p < 0.05$) lower amounts of this amino acid when compared to lines initiated at higher temperatures, showing a clear accumulation when embryogenic masses were initiated under high temperatures. With respect to isoleucine (Figure 8B), lines initiated at 40 and 60°C showed significantly higher values than those initiated at control temperature. Leucine, for its part (Figure 8C), showed significantly ($p < 0.05$) lower amounts in the case of lines initiated at 50°C when compared to those initiated at 23, 40 and 60°C. Despite not being significantly different from the control temperature, leucine followed the same pattern described for isoleucine as the greatest amounts of this amino acid were found in lines subjected to 40 and 60°C. Finally, statistically significant ($p < 0.05$) differences were found for the levels of histidine between treatments 40 and 50°C (Figure 8D). Lines initiated at 50°C presented the lowest levels of histidine, whereas those subjected to 40°C accumulated the highest ones. Application of the control treatment and 60°C resulted in intermediate values, but following once again the tendency described above for leucine and isoleucine.

Table 5. Free amino acids (µmol/g FW) in *Pinus radiata* embryonal masses under different initiation temperatures (23°C, 8 weeks; 40°C, 4 h; 50°C, 30 min; 60°C, 5 min). Data are presented as mean values ± SE. Significant differences at $p < 0.05$ are indicated by different letters.

	Treatment (°C)			
Amino acids (µmol/g FW)	**23**	**40**	**50**	**60**
Alanine	8.33 ± 3.83^{a}	7.6 ± 3.42^{a}	7.38 ± 1.45^{a}	6.09 ± 1.49^{a}
Arginine	1.19 ± 0.5^{a}	0.48 ± 0.18^{a}	0.62 ± 0.24^{a}	1.51 ± 0.68^{a}
Asparagine	16.6 ± 4.11^{a}	11.1 ± 3.38^{a}	12.23 ± 2.11^{a}	13.79 ± 3.48^{a}
Aspartate	0.12 ± 0.02^{a}	0.08 ± 0.02^{a}	0.09 ± 0.02^{a}	0.12 ± 0.01^{a}
Ethanolamine	0.19 ± 0.01^{a}	0.3 ± 0.12^{a}	0.15 ± 0.02^{a}	0.29 ± 0.09^{a}
Phenylalanine	0.1 ± 0.01^{a}	0.12 ± 0.01^{a}	0.1 ± 0^{a}	0.11 ± 0.01^{a}
GABA	0.06 ± 0^{a}	0.07 ± 0.02^{a}	0.07 ± 0^{a}	0.08 ± 0^{a}
Glycine	1.02 ± 0.08^{a}	1.1 ± 0.05^{a}	1.06 ± 0.11^{a}	0.97 ± 0.14^{a}
Glutamate	0.18 ± 0.02^{a}	0.29 ± 0.1^{a}	0.17 ± 0.03^{a}	0.21 ± 0.04^{a}
Glutamine	6.89 ± 0.73^{a}	8.51 ± 1.44^{a}	10.63 ± 3.37^{a}	7.46 ± 3.89^{a}
Isoleucine	0.15 ± 0.01^{c}	0.2 ± 0.01^{a}	0.16 ± 0.01^{bc}	0.19 ± 0.02^{ab}
Histidine	1.33 ± 0.21^{ab}	2.16 ± 0.59^{a}	1.26 ± 0.13^{b}	1.48 ± 0.14^{ab}
Leucine	0.16 ± 0.02^{a}	0.19 ± 0.01^{a}	0.1 ± 0.01^{b}	0.2 ± 0.02^{a}
Lysine	0.22 ± 0^{a}	0.24 ± 0.02^{a}	0.22 ± 0^{a}	0.27 ± 0.02^{a}
Methionine	0.06 ± 0^{a}	0.06 ± 0^{a}	0.07 ± 0.01^{a}	0.07 ± 0.01^{a}
Ornithine	0.25 ± 0^{a}	0.24 ± 0.02^{a}	0.25 ± 0.01^{a}	0.24 ± 0.03^{a}
Proline	2.32 ± 0.53^{a}	1.42 ± 0.61^{ab}	1.88 ± 1.09^{ab}	0.86 ± 0.12^{b}
Serine	0.49 ± 0.08^{a}	0.54 ± 0.07^{a}	0.51 ± 0.17^{a}	0.68 ± 0.21^{a}
Tyrosine	0.13 ± 0.01^{b}	0.25 ± 0.03^{a}	0.24 ± 0.02^{a}	0.21 ± 0.03^{a}
Threonine	0.48 ± 0.06^{a}	0.41 ± 0.03^{a}	0.71 ± 0.21^{a}	0.5 ± 0.2^{a}
Tryptophane	0.12 ± 0.01^{a}	0.16 ± 0.04^{a}	0.12 ± 0.01^{a}	0.15 ± 0.03^{a}
Valine	0.24 ± 0.05^{ab}	0.34 ± 0.07^{a}	0.18 ± 0.02^{b}	0.28 0.03^{a}

4. DISCUSSION

Somatic embryogenesis is a complex network of genetic, physiological and developmental processes that are strongly regulated and affected by internal and external factors. Small alterations of these factors could result in a complete failure of SE, especially conditioning critical but at the same time highly challenging steps such as initiation (Santa-Catarina et al., 2012). However, different stress conditions could presumably be beneficial and in some cases almost crucial for SE success; thus, heat

stress is one of the significant stresses for microspore embryogenesis induction in *Brassica napus* due to changes in DNA methylation (Li et al., 2016). This, in combination with the idea that conditions at the initiation step have long-term effects, could be used as a tool for improvement by increasing the efficiency of the process or the diversity of the plants produced.

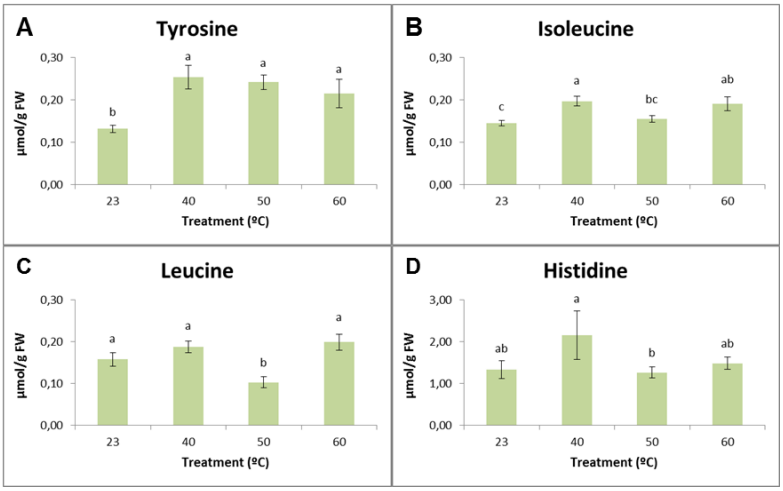

Figure 8. The effect of temperature (23°C, 8 weeks; 40°C, 4 h; 50°C, 30 min; 60°C, 5 min) on tyrosine **(A)**, isoleucine **(B)**, leucine **(C)**, and histidine **(D)** content of *P. radiata* embryonal masses. Data are presented as mean values ± SE. Significant differences at $p < 0.05$ are indicated by different letters.

Following the same tendency observed in previous studies (García-Mendiguren et al., 2016b; Pereira et al., 2016, 2017), significant differences in initiation and proliferation rates were found when different temperatures were applied during the initiation of SE in *P. radiata*. García-Mendiguren et al. (2016b) concluded that low temperatures (18 and 23°C) give rise to higher initiation rates when compared to those obtained when it was carried out at 28°C.

In the results obtained in Experiment 1, we observed that high temperatures applied for long periods of time resulted in the total (40°C, 4 days) or partial (30°C, 4 weeks) decrease of both initiation and proliferations rates. Thus, we could refer to these treatments as representing strong stresses. In Experiment 2 the effect was not so clear, maybe because the treatments applied were shorter, but we could also observe a slight

decrease in both parameters when temperatures above the standard were applied for the longest periods (40°C, 4 h and 50°C, 30 min). In fact, the differences observed for proliferation at 50°C were on the verge of statistical significance. As a result, we can conclude that when high temperatures are applied small differences in the duration of the treatment can be critical and when that point is exceeded the effects can be detrimental for the first steps of SE, compromising the genetic diversity that could be achieved in standard conditions.

In previous experiments carried out in our laboratory (García-Mendiguren et al., 2016b), the opposite effect was observed for proliferation and maturation phases, where high temperatures resulted in considerably higher proliferation rates and larger number of Se's. Despite proliferation following the same pattern as initiation in our study, maturation results were similar to those from the abovementioned study. Although not statistically significant, in both experiments the number of Se's obtained per gram of EM was slightly higher when stress was present, increasing the efficiency of the process. These results reinforce the idea postulated by Fehér (2015), according to which temperature exerts a selective pressure in the SE initial stages, resulting in an initiation decrease but higher rates for the forthcoming steps. It is worth mentioning that both authors, Fehér and García-Mendiguren, obtained better proliferation rates when stress was applied, which is in contradiction to our results. This suggests that the treatments applied in our experiments could have provoked a more severe effect at cellular level and as a result, had a more long-lasting effect on the EMs.

In contrast to these results, we have the ones obtained when high temperatures were applied for short periods of time, which we could refer to as mild stresses (50°C for 5 min in Experiment 1 and 40°C for 4 h and 60°C for 5 min in Experiment 2). In these cases, the values obtained for initiation and proliferation rates were not statistically different from those obtained at control temperatures, with the exception of 50°C for 5 min in Experiment 1 at proliferation, which were even higher than in control temperatures, dismissing the detrimental effect previously described for high temperatures during long time periods. Surprisingly, the beneficial effect observed

during maturation when high temperatures were applied for long time periods was also noticeable for mild stresses.

It is also noticeable that mild stresses had the effect of forming big, well-formed elongated Se's, while long-term applied high temperatures gave rise to big but barrel-shaped Se's. This kind of morphology is known to be a symptom of low-quality embryos (Pullman et al., 2003) and it is usually accompanied by low germination rates, especially with regard to rooting. Thus, even though stress induces the formation of Se's, long-lasting stresses provoke negative morphological alterations, while mild stresses enhance the quality of Se's. Microscopic observations and analysis of cellular ultrastructure may be able to shed light on this.

Light microscopy analysis revealed the presence of three cell types (ECs, TLCs, and SCs) and three organizational structures called PEMI, PEMII and PEMII, as described for *P. abies* by Filonova et al. (2000). These authors described PEMIII as enlarged clumps of densely cytoplasmic cells loosely attached to each other that do not present polarity, whereas in the case of *P. radiata* the ECs observed formed compact clumps which showed, in most cases, a well-organized structure with a clear polarization. A similar model was described by Steiner et al. (2016) for early Se's of *Araucaria angustifolia*, but no polarization was observed in PEMs, which could be explained in terms of interspecific differences.

In both light microscopy and TEM analysis, high temperatures during early stages of SE resulted in loss of polarity and mitotic activity, and an increase in V, G, plastolysome-like structures, whorls by cytoplasmic membranes and S around the N. These events are usually accompanied by nuclear degradation, which is reflected by the normally round N becoming lobed, with large clusters of nuclear pore complexes and contents of chromatin leaking into the cytoplasm (Filonova et al., 2000). Even though many anucleated SCs were observed, none of the above-mentioned symptoms of nuclear degradations were detected in our analysis.

With all this information, we can conclude that heat shock treatments may trigger PCD of ECs. Interestingly, DaMatta & Ramalho (2006) pointed out that strong high temperature-based stresses are known to activate signalling pathways related to plant PCD. An increased PCD leads to an early loss of embryogenic potential and the formation of supernumerary SCs, which in turn may compromise proliferation and maturation of PEMs. This supernumerary suspensor cell scenario may be caused by a disturbed polar auxin transport, which stimulates division of ECs adjacent to the tube-like cells, as described by Abrahamsson et al. (2012). Similar morphologies were described by Merino et al. (2018) for Norway spruce early Se's leading to abnormal Se's. These authors pointed out that there is a strong relationship among early Se's morphology, its capacity to develop into a mature embryo and the expression of certain transcripts. Up-regulation of EXPB1 and RIC3, transcripts suggested to be involved in the cleavage process during zygotic embryogenesis, resulted in the disintegration of EMs, the presence of highly vacuolated cells in the embryonal clusters and the formation of supernumerary SCs. Down-regulation of CYP78A7 or TT7 on the other hand, caused the formation of embryos with disturbed apical-basal polarization. This information indicates that heat-shock treatments may have provoked alterations in the expression pattern of some gens involved in the correct development of PEMs and thus, in the correct development of future Se's.

The idea that the accumulation of S around N is a symptom of loss of embryogenic competence was also described by Morel et al. (2014). These authors noticed that starch accumulation occurs mainly during the first weeks of the maturation process, not during the proliferation phase, in which the glycolytic pathway is enhanced, and this accumulation occurs basically in SCs and in the basal part of the embryos. Embryos accumulating S around the N were linked with the appearance of dead cells in meristematic centres.

All these aspects could, to some extent, explain the results obtained for initiation and proliferation rates. The increase in PCD and the loss of embryogenic competence observed in EMs submitted to heat shock treatments, and especially those initiated at

high temperatures during longer periods of time, such as those at 50°C in Experiment 2, may be the reason for the slight decrease in both parameters. Previous studies (Breton et al., 2006; Carneros et al., 2017) suggest that these effects could be more relevant during future stages, especially during maturation, where cellular organization may play a crucial role in the success of embryo formation. However, alterations observed during maturation were not as relevant as those observed during initiation or proliferation. The only remarkable aspect was the formation of barrel-shaped Se's when long term stresses were applied, which supports the idea that cellular organization of PEMs, at least in our case, had a major impact on the morphology of the forming Se's, rather than on the success of the maturation itself.

It is worth noting that in spite of the cellular dismantling aspects observed at 60°C, light microscopy demonstrated the presence of some bigger and more developed embryogenic areas when compared to control samples, which could explain the improvements observed for embryo production and embryo morphology in the case of mild stress temperatures. This is in line with results of authors that pointed out the idea of temperature based mild stresses having a beneficial effect during production of Se's. Besides, it is known that some stresses induce *de novo* synthesis of ABA and therefore enhance endogenous abscisic acid levels (Dronne et al., 1997), which could explain the formation of structures that resembled earlier globular Se's in 60°C samples.

It is also interesting to take into account the differential accumulation of phenolic compounds observed in light microscopy, especially for treatments 50 and 60°C. Accumulation of this type of molecules is described as playing an essential role in the prevention of oxidative damage caused by different types of stresses (Eliášová et al., 2017; Falahi et al., 2018).

Finally, different mitochondrial morphologies were observed by TEM. These morphologies were described for the first time in plant embryogenic cultures by Fraga et al. (2015). Alterations in mitochondrial structure in response to heat shock treatments have already been reported (Welch & Suhan, 1985). However, the alterations observed in our experiment were homogeneously distributed among all treatments,

which suggest that other stress factors may be the reason for such changes. *In vitro* culture represents an unusual combination of stress factors (Zavattieri et al., 2010), so it is difficult to assess whether externally applied stresses are responsible for altered mitochondrial conformations or if *in vitro* culture itself promotes those changes.

With regard to the metabolite analysis, significant differences were found for several metabolites for different temperature treatments. The accumulation of metabolites in response to abiotic stresses, and in particular to osmotic stress, is well documented (Delauney & Verma, 1993). Osmotic stress can be provoked due to different kinds of environmental conditions such as drought, salinity, or flooding. Drought is usually accompanied by other stresses such as heat, and recent studies have shown that both these stresses have overlapping roles (Jia et al., 2017). Heat involves complex mechanisms including multiple protective pathways which seem to be essential for homeostasis preservation (Ahuja et al., 2010).

In this regard, sugars seem to be among the most stress-responsive metabolites, as they play an essential role as osmolytes, stress response signals, and they are responsible for membrane stabilization and oxygen radical scavengers (Moradi et al., 2017; Woodrow et al., 2017). However, no differences were found either for soluble sugars, or for starch in our samples. Microscopic observations highlighted the accumulation of bigger amounts of S in samples subjected to higher temperatures, but this could be more related to PCD events rather than to protective ones. Furthermore, the lack of significant differences for HPLC analysis of these molecules might have been caused by the specific localization of starch, principally in cells starting to undergo PCD. This could all be explained by an unbalanced number of cell types among the treatments. In fact, samples submitted to high temperatures were those with the biggest amount of highly degraded SCs, most of which formed hollow-walled corpses.

Amino acid metabolism may also play an important role in plant stress tolerance through the accumulation of compatible metabolites, intracellular pH regulation, and detoxification of reactive oxygen species. These molecules are also known to be precursors of secondary metabolites (Campalans et al., 1999; Nuccio et al., 1999).

Among amino acids, it is proline which has been studied most extensively (Corcuera et al., 2012; De Diego et al., 2015), and apart from the abovementioned functions, it may also be involved in the protection of cell structures and cell proteins (Bandurska et al., 2009). Nevertheless, no differences could be observed for this amino acid study. It is worth mentioning, however, that when metabolites were statistically analysed, the introduction of the cell line in the model improved the adjustment, suggesting that there is variability that could be explained in terms of genetic background. This genetic background could have a great influence when there is exposure to temperature-based stress treatments. Besides, it is known that the accumulation of osmolytes is dependent on the cell or tissue type, developmental status, the particular environment, and the nature of the stress (Burg & Ferraris, 2008). In this sense, studies carried out with tobacco and *Arabidopsis* concluded that heat stress was not effective to promote proline accumulation (Krasensky & Jonak, 2012).

Despite being the most frequently studied amino acid, proline is not the only one whose accumulation pattern is altered in response to stress. Relative increases in branched-chain amino acids (BCAAs) (leucine, valine, and isoleucine) under drought stress have previously been studied in *Arabidopsis* by Nambara et al. (1998), and many studies conclude that the accumulation of this type of amino acid can be much greater under certain stress conditions than proline accumulation (Shen et al., 1989). It is noteworthy that the accumulation of BCAAs is more common in young tissues and reproductive ones (Singh & Shaner, 1995), where cells have high mitotic and metabolic activity, characteristic of EMs.

Our results suggest a slight accumulation, especially for isoleucine, in treatments that we have described as mild stresses (40°C, 4 h and 60°C, 5 min). It has been proposed that accumulation of BCAAs may serve as substrate for the synthesis of stress-induced proteins and that BCAAs may act as signalling molecules to regulate gene expression (Joshi et al., 2010). We have also observed a decrease in BCAA content when strong stress conditions were applied (50°C for half an hour), especially for leucine. The reason for this could be an increased consumption of this amino acid for the synthesis of

enzymes or secondary metabolites that could help to cope with stress (Falahi et al., 2018). Some studies reported a transient increase in BCAAs during stress conditions followed by a rapid decrease once the stress was eliminated. The explanation for this may be that BCAA catabolism leads to the formation of energetic compounds that could be very useful during plant recovery (Taylor et al., 2004).

Differences were also observed for the levels of tyrosine and histidine. The first amino acid presented a clear accumulation in all heat-shock treatments. Some authors, like Falahi et al. (2018), detected the same pattern when plants of *Scrophularia striata* were submitted to water deficit. Tyrosine is a precursor for a wide range of secondary metabolites. Among these metabolites, we can highlight the presence of phenolic compounds, which were detected in light microscopy assays as being highly accumulated in samples initiated under stress conditions. With regard to histidine, the greatest values were observed for the 40°C treatment. In previous studies carried out in *Pinus halepensis* seedlings, histidine showed higher concentrations in drought-tolerant plants (Taïbi et al., 2015).

To summarize, we can state that heat-based treatments applied during the initial stages of SE of *P. radiata* had varying effects throughout the process. Long-lasting stress treatments had detrimental effects during the initial stages due to clear symptoms of increased PCD and loss of embryogenic potential, as opposed to mild stresses. Despite both kinds of treatments slightly improving the production of Se's, those obtained when mild stresses were applied were of better quality. Moreover, alterations in the metabolic profile of samples subjected to heat-shock treatments were detected. These metabolites include amino acids such as leucine, isoleucine, histidine and tyrosine and phenolic compounds, which could be involved in osmotic adjustment and antioxidative processes. These metabolic alterations reinforce the idea that long-lasting metabolic memory could endow future plants with an increased capacity to cope with adverse environmental situations.

5. REFERENCES

Abrahamsson, M., Valladares, S., Larsson, E., Clapham, D., and von Arnold, S. (2012). Patterning during somatic embryogenesis in Scots pine in relation to polar auxin transport and programmed cell death. *Plant Cell Tissue Organ Cult.* 109, 391-400.

Ahuja, I., de Vos, R.C.H., Bones, A.M., and Hall, R.D. (2010). Plant molecular stress responses face climate change. *Trends Plant Sci.* 15, 664-674.

Augusti A., Lauteri M., Spaccino L., and Brugnoli E. (1999). "Short- and long-term responses of carbon isotope discrimination photosynthetic energy dissipation to elevated CO2 concentration" in Ecosystem response to CO2: the MAPLE results, eds. Raschi, A., Vaccari, F.P., Miglietta, F. (Office for Official publications of the European Communities: Luxembourg), 117-132.

Bandurska, H., Płachta, M., and Woszczyk, M. (2009). Seasonal patterns of free proline and carbohydrate levels in cherry laurel (*Prunus laurocerasus*) and ivy (*Hederea helix*) leaves and resistance to freezing and water deficit. *Dendrobiology* 62, 3-9.

Bates, L.S., Waldren, R.P., and Teare, I.D. (1973). Rapid determination of free proline for water-stress studies. *Plant Soil* 39, 205-207.

Benjamini, Y., and Hochberg, Y. (1995). Controlling the false discovery rate: a practical and powerful approach to multiple testing. *J. Roy. Stat. Soc.* B. 57, 289-300.

Booth, T.H., and McMurtrie, R.E. (1988). "Climatic change and *Pinus radiata* plantations in Australia", in Greenhouse: Planning for Climate Change, eds. Pearman, G.I. (CSIRO Publications, Melbourne), 534-545.

Boyko, A., and Kovalchuk, I. (2008). Epigenetic control of plant stress response. *Environ. Mol. Mutagen.* 49, 61-72.

Bratford M.M. (1976). A rapid and sensitive method for the quantification of microorganism quantities of protein utilizing the principle of protein dye binding. *Anal. Biochem.* 72, 248-254.

Bräutigam, K., Vining, K.J., Lafon-Placette, C., Fossdal, C.G., Mirouze, M., Marcos, J.G., et al. (2013). Epigenetic regulation of adaptive responses of forest tree species to the environment. *Ecol. Evol.* 3, 399-415.

Breton, D., Harvengt, L., Trontin, J.F., Bouvet, A., and Favre, J.M. (2006). Long-term subculture randomly affects morphology and subsequent maturation of early somatic embryos in maritime pine. *Plant Cell Tissue Organ Cult.* 87, 95-108.

Burg, M.B., and Ferraris, J.D. (2008). Intracellular organic osmolytes: Function and regulation. *J. Biol. Chem.* 283, 7309-7313.

Campalans, A., Messeguer, R., Goday, A., and Pagès, M. (1999). Plant responses to drought, from ABA signal transduction events to the action of the induced proteins. *Plant Physiol. Biochem.* 37, 327-340.

Carillo, P., Parisi, D., Woodrow, P., Pontecorvo, G., Massaro, G., Annunziata, M., et al. (2011a). Salt-induced accumulation of glycine betaine is inhibited by high light in durum wheat. *Funct. Plant Biol.* 38, 139-150.

Carillo P., Gibon Y., PrometheusWiki contributors (2011b). Extraction and determination of proline. Available at http://prometheuswiki.publish.csiro.au/tiki index.php?page=Extraction+and+determination+of+proline (accessed 07/10/2016)

Carillo, P., Cacace, D., De Pascale, S., Rapacciuolo, M., and Fuggi, A. (2012). Organic vs. traditional potato powder. *Food Chem.* 133, 1264-1273.

Carneros, E., Toribio, M., and Celestino, C. (2017). Effect of ABA, the auxin antagonist PCIB and partial desiccation on stone pine somatic embryo maturation. *Plant Cell Tissue Organ Cult.* 131, 445-458.

Conrath, U., Beckers, G.J.M., Langenbach, C.J.G., and Jaskiewicz, M.R. (2015). Priming for Enhanced Defense. *Annu. Rev. Phythopathol.* 53, 97-119.

Corcuera, L., Gil-Pelegrin, E., and Notivol, E. (2012). Aridity promotes differences in proline and phytohormone levels in *Pinus pinaster* populations from contrasting environments. *Trees - Struct. Funct.* 26, 799-808.

DaMatta, F.M., and Ramalho, J.C. (2006). Impact of drought and temperature stress on coffee physiology and production: a review. *Braz. J. Plant Physiol.* 18, 55-81.

Davies, W.J., Zhang, J., Yang, J., and Dodd I.C. (2010). Novel crop science to improve yield and resource use efficiency in water-limited agriculture. *J Agric Sci.* 149, 123-131.

De Diego, N., Sampedro, M.C., Barrio, R.J., Saiz-Fernández, I., Moncaleán, P., and Lacuesta, M. (2013). Solute accumulation and elastic modulus changes in six radiata pine breeds exposed to drought. *Tree Physiol.* 33, 69-80.

De Diego, N., Saiz-Fernández, I., Rodríguez, J. L., Pérez-Alfocea, P., Sampedro, M.C., Barrio, R.J., et al. (2015). Metabolites and hormones are involved in the intraspecific variability of drought hardening in radiata pine. *J. Plant Physiol.* 188, 64-71.

Delauney, A.J., and Verma, D.P.S. (1993). Proline biosynthesis and osmoregulation in plants. *Plant J.* 4, 215–223.

Dormling, I., and Johnsen, O. (1992). Effects of the parental environment on full-sib families of *Pinus sylvestris*. *Can. J. For. Res.* 22, 88-100.

Dronne, S., Label, P., and Lelu, M.A. (1997). Desiccation decreases abscisic acid content in hybrid larch (*Larix X leptoeuropaea*) somatic embryos. *Physiol. Plant.* 99, 433-438.

Dungey, H.S., Brawner, J.T., Burger, F., Carson, M., Henson, M., Jefferson, P., et al. (2009). A new breeding strategy for *Pinus radiata* in New Zealand and New South Wales. *Silvae Genet.* 58, 28-38.

Eliášová, K., Vondráková, Z., Malbeck, J., Trávníčková, A., Pešek, B., Vágner, M., et al. (2017). Histological and biochemical response of Norway spruce somatic embryos to UV-B irradiation. *Trees - Struct. Funct.* 31, 1279-1293.

Escandón, M., Valledor, L., Pascual, J., Pinto, G., Cañal, M.J., and Meijón, M. (2017). System-wide analysis of short-term response to high temperature in *Pinus radiata*. *J. Exp. Bot.* 68, 3629-3641.

Espinel, S., Aragonés, A., and Ritter, E. (1995). Performance of different provenances and of the local population of the Monterrey pine (*Pinus radiata* D Don) in northern Spain. *Ann. For. Sci.* 52, 515-519.

Falahi, H., Sharifi, M., Maivan, H.Z., and Chashmi, N.A. (2018). Phenylethanoid glycosides accumulation in roots of *Scrophularia striata* as a response to water stress. *Environ. Exp. Bot.* 147, 13-21.

Fehér, A. (2015). Somatic embryogenesis - stress-induced remodeling of plant cell fate. *Biochim. Biophys. Acta - Gene Regul. Mech.* 1849, 385-402.

Fehér, A., Pasternak, T.P., and Dudits, D. (2003). Transition of somatic plant cells to an embryogenic state. *Plant Cell Tissue Organ Cult.* 74, 201-228.

Filonova, L.H., Bozhkov, P.V., Brukhin, V.B., Daniel, G., Zhivotovsky, B., and von Arnold, S. (2000). Two waves of programmed cell death occur during formation and development of somatic embryos in the gymnosperm, Norway spruce. *J. Cell Sci.* 113, 4399-4411.

Fraga, H.P.F., Vieira, L.N., Puttkammer, C.C., Oliveira, E.M., and Guerra, M.P. (2015). Time-lapse cell tracking reveals morphohistological features in somatic embryogenesis of *Araucaria angustifolia* (Bert) O. Kuntze. *Trees - Struct. Funct.* 29, 1613-1623.

García-Mendiguren, O., Montalbán, I.A., Correia, S., Canhoto, J., and Moncaleán, P. (2016a). Different environmental conditions at initiation of radiata pine somatic embryogenesis determine the protein profile of somatic embryos. *Plant Biotechnol.* 33, 143-152.

García-Mendiguren, O., Montalbán, I.A., Goicoa, T., Ugarte, M.D., and Moncaleán, P. (2016b). Environmental conditions at the initial stages of *Pinus radiata* somatic embryogenesis affect the production of somatic embryos. *Trees - Struct. Funct.* 30, 949-958.

García-Mendiguren, O., Montalbán, I. A., Goicoa, T., Ugarte, M.D., and Moncaleán, P. (2017). Are we able to modulate the response of somatic embryos of pines to drought stress? *Acta Hortic.* 1155, 77-84.

Hargreaves, C.L., Grace, L.J., and Holden, D.G. (2002). Nurse culture for efficient recovery of cryopreserved *Pinus radiata* D. Don embryogenic cell lines. *Plant Cell Rep.* 21, 40-45.

Jia, J., Zhou, J., Shi, W., Cao, X., Luo, J., Polle, A., et al. (2017). Comparative transcriptomic analysis reveals the roles of overlapping heat-/drought-responsive genes in poplars exposed to high temperature and drought. *Sci. Rep.* 7, 43215.

Johnsen, Ø., Fossdal, C.G., Nagy, N., Mølmann, J., Dæhlen, O.G., and Skrøppa, T. (2005). Climatic adaptation in *Picea abies* progenies is affected by the temperature during zygotic embryogenesis and seed maturation. *Plant Cell Environ.* 28, 1090-1102.

Jones, M.G.K., Outlaw, W.H., and Lowry, O.H. (1977). Procedure for assay of sucrose in the range 10-1-10-14 moles. *Plant Physiol.* 6, 379-383.

Joshi, V., Joung, J.G., Fei, Z., and Jander, G. (2010). Interdependence of threonine, methionine and isoleucine metabolism in plants: Accumulation and transcriptional regulation under abiotic stress. *Amino Acids* 39, 933-947.

Krasensky, J., and Jonak, C., (2012). Drought, salt, and temperature stress-induced metabolic rearrangements and regulatory networks. *J. Exp. Bot.* 63, 1593-1608.

Kvaalen, H., and Johnsen, Ø. (2008). Timing of bud set in *Picea abies* is regulated by a memory of temperature during zygotic and somatic embryogenesis. *New Phytol.* 177, 49-59.

Li J., Huang Q., Mengxiang S., Zhang T., Li H., Chen B., Xu K., Gao G., Li F., Yan G., Qiao J., Cai Y., and Wu X. (2016). Global DNA methylation variations after short-term heat shock treatment in cultured microspores of *Brassica napus* cv. Topas. *Sci. Rep.* 6, 38401.

Mena-Petite, A., Estavillo, J.M., Duñabeitia, M., González-Moro, B., Muñoz-Rueda, A., and Lacuesta, M. (2004). Effect of storage conditions on post planting water status and performance of *Pinus radiata* D. Don stock-types. *Ann. For. Sci.* 61, 695-704.

Merino, I., Abrahamsson, M., Larsson, E., and von Arnold, S. (2018). Identification of molecular processes that differ among Scots pine somatic embryogenic cell lines leading to the development of normal or abnormal cotyledonary embryos. *Tree Genet. Genomes* 14.

Montalbán, I.A., De Diego, N., and Moncaleán, P. (2010). Bottlenecks in *Pinus radiata* somatic embryogenesis: Improving maturation and germination. *Trees - Struct. Funct.* 24, 1061-1071.

Montalbán, I.A., de Diego, N., and Moncaleán, P. (2012). Enhancing initiation and proliferation in radiata pine (*Pinus radiata* D. Don) somatic embryogenesis through seed

family screening, zygotic embryo staging and media adjustments. *Acta Physiol. Plant.* 34, 451-460.

Montalbán, I.A., García-Mendiguren, O., Goicoa, T., Ugarte, M.D., and Moncaleán, P. (2015). Cold storage of initial plant material affects positively somatic embryogenesis in *Pinus radiata*. *New For.* 46, 309-317.

Montalbán, I.A., and Moncaleán, P. (2017). Long term conservation at -80°C of *Pinus radiata* embryogenic cell lines: recovery, maturation and germination. *CryoLetters* 38, 202-209.

Montalbán, I.A., and Moncaleán, P. (2018). Rooting of *Pinus radiata* somatic embryos: factors involved in the success of the process. *J. For. Res.* 30, 65-71.

Moradi, P., Ford-Lloyd, B., and Pritchard, J. (2017). Metabolomic approach reveals the biochemical mechanisms underlying drought stress tolerance in thyme. *Anal. Biochem.* 527, 49-62.

Morel, A., Teyssier, C., Trontin, J.F., Eliášová, K., Pešek, B., Beaufour, M., et al. (2014). Early molecular events involved in *Pinus pinaster* Ait. somatic embryo development under reduced water availability: Transcriptomic and proteomic analyses. *Physiol. Plant.* 152, 184-201.

Nambara, E., Kawaide, H., Kamiya, Y., and Naito, S. (1998). Characterization of an *Arabidopsis thaliana* mutant that has a defect in ABA accumulation: ABA-dependent and ABA-independent accumulation of free amino acids during dehydration. *Plant Cell Physiol.* 39, 853-858.

Nuccio, M.L., Rhodes, D., McNeil, S.D., and Hanson, A.D. (1999). Metabolic engineering of plants for osmotic stress resistance. *Curr. Opin. Plant Biol.* 2, 128-134.

Park, Y.S. (2002). Implementation of conifer somatic embryogenesis in clonal forestry: Technical requirements and deployment considerations. *Ann. For. Sci.* 59, 651-656.

Patakas, A., Nikolaou, N., Zioziou, E., Radoglou, K., and Noitsakis, B. (2002). The role of organic solute and ion accumulation in osmotic adjustment in drought-stressed grapevines. *Plant Sci.* 163, 361-367.

Pereira, C., Montalbán, I.A., García-Mendiguren, O., Goicoa, T., Ugarte, M.D., Correia, S., et al. (2016). *Pinus halepensis* somatic embryogenesis is affected by the physical and chemical conditions at the initial stages of the process. *J. For. Res.* 21, 143-150.

Pereira, C., Montalbán, I.A., Goicoa, T., Ugarte, M.D., Correia, S., Canhoto, J.M., et al. (2017). The effect of changing temperature and agar concentration at proliferation stage in the final success of Aleppo pine somatic embryogenesis. *For. Syst.* 26, 1-4

Pietrini, F., Iannelli, M.A., Battistelli, A., Moscatello, S., Loreto, F., and Massacci, A. (1999). Effects on photosynthesis, carbohydrate accumulation and regrowth induced by temperature increase in maize genotypes with different sensitivity to low temperature. *Aust. J. Plant Physiol.* 26, 367-373.

Pullman, G.S., Johnson, S., Peter, G., Cairney, J., and Xu, N. (2003). Improving loblolly pine somatic embryo maturation: Comparison of somatic and zygotic embryo morphology, germination, and gene expression. *Plant Cell Rep.* 21, 747-758.

Reynolds, E.S. (1963). The use of lead citrate at light pH as an electron opaque stain in electron microscopy. *J Cell Biol.* 17, 208-212.

Santa-Catarina, C., Silveira, V., Guerra, M.P., Steiner, N., Ferreira Macedo, A., Iochevet Segal Floh, E., and Wendt Dos Santos, A.L. (2012). The use of somatic embryogenesis for mass clonal propagation and biochemical and physiological studies in woody plants. *Curr. Top. Plant Biol.* 13, 103-119.

Shen, L., Foster, J.G., and Orcutt, D.M. (1989). Composition and distribution of free amino acids in flatpea (*Lathyrus sylvestris* L.) as influenced by water deficit and plant age. *J. Exp. Bot.* 40, 71-79.

Singh, B.K., and Shaner, D.L. (1995). Biosynthesis of branched chain amino acids: From test tube to field. *Plant Cell* 7, 935-944.

Smertenko, A., and Bozhkov, P.V. (2014). Somatic embryogenesis: life and death processes during apical-basal pattering. *J. Exp. Bot.* 65, 1343-1360.

Smith, D.R. (1997). The role of in vitro methods in pine plantation establishment: the lesson from New Zealand. *Plant Tissue Cult. Biotechnol.* 3, 63-73.

Spinoni, J., Vogt, J.V., Naumann, G., Barbosa, P., and Dosio, A. (2018). Will drought events become more frequent and severe in Europe? *Int. J. Climatol.* 38, 1718-1736.

Spurr, A.R. (1969). A low-viscosity epoxy resin embedding medium for electron microscopy. *J. Ultra. Mol. Struct. R.* 26, 31-43.

Steiner, N., Farias-Soares, F.L., Schmidt, É.C., Pereira, M.L.T., Scheid, B., Rogge-Renner, G. D., et al. (2016). Toward establishing a morphological and ultrastructural characterization of proembryogenic masses and early somatic embryos of *Araucaria angustifolia* (Bert.) O. Kuntze. *Protoplasma* 253, 487-501.

Taïbi, K., del Campo, A.D., Aguado, A., and Mulet, J.M. (2015). The effect of genotype by environment interaction, phenotypic plasticity and adaptation on *Pinus halepensis* reforestation establishment under expected climate drifts. *Ecol. Eng.* 84, 218-228.

Taylor, N.L., Heazlewood, J.L., Day, D.A., and Millar, A.H. (2004). Lipoic acid-dependent oxidative catabolism of α-keto acids in mitochondria provides evidence for branched-chain amino acid catabolism in *Arabidopsis*. *Plant Physiol.* 134, 838-848.

Villar-Salvador, P., Planelles, R., Oliet, J., Peñuelas-Rubira, J.L., Jacobs, D.F., and González, M. (2004). Drought tolerance and transplanting performance of holm oak (*Quercus ilex*) seedlings after drought hardening in the nursery. *Tree Physiol.* 24, 1147-1155.

Walter, C., Find, J.I., and Grace, L.J. (2005). "Somatic embryogenesis and genetic transformation in *Pinus radiata*" in Protocols for somatic embryogenesis in woody plants, eds. Jain, S.M., Gupta, P.K. (Springer, Dordrecht), 491-504.

Welch, W.I., and Suhan, J.P. (1985). Morphological study of the mammalian stress response: Characterization of changes in cytoplasmic organelles, cytoskeleton, and nucleoli, and appearance of intranuclear actin filaments in rat fibroblasts after heat-shock treatment. *J. Cell Biol.* 101, 1198-1211.

Woodrow, P., Ciarmiello, L.F., Annunziata, M.G., Pacifico, S., Iannuzzi, F., Mirto, A., D'Amelia, L., Dell'Aversana, E., Piccolella, S., Fuggi, A.; Carillo, P. (2017). Durum wheat seedling responses to simultaneous high light and salinity involve a fine reconfiguration of amino acids and carbohydrate metabolism. *Physiol. Plant.* 159, 290-312.

Yakovlev, I.A., Asante, D.K.A., Fossdal, C.G., Junttila, O., and Johnsen, T. (2011). Differential gene expression related to an epigenetic memory affecting climatic adaptation in Norway spruce. *Plant Sci.* 180, 132-139.

Yakovlev, I.A., Carneros, E., Lee, Y.K., Olsen, J.E., and Fossdal, C.G. (2016). Transcriptional profiling of epigenetic regulators in somatic embryos during temperature induced formation of an epigenetic memory in Norway spruce. *Planta* 243, 1237-1249.

Zas, R., Cendán, C., and Sampedro, L. (2013). Mediation of seed provisioning in the transmission of environmental maternal effects in Maritime pine (*Pinus pinaster* Aiton). *Heredity* 111, 248-255.

Zavattieri, M.A., Frederico, A.M., Lima, M., Sabino, R., and Arnholdt-Schmitt, B. (2010). Induction of somatic embryogenesis as an example of stress-related plant reactions. *Electron. J. Biotechnol.* 13, 1-9.

6. SUPPLEMENTARY MATERIAL

Supplementary Table 1. Analysis of variance for the number of somatic embryos per gram of embryonal mass according to temperature (T).

Experiment 1				Experiment 2			
Source	**df**	**F value**	***p* value**	**Source**	**df**	**F value**	***p* value**
Temperature (T)	2	3.1399	0.2081	Temperature (T)	3	0.30725	0.8198

Supplementary Table 2. Analysis of variance for the amount of each metabolite according to temperature (T).

Source: Temperature (T)			
Variable	**df**	**F value**	***p* value**
Starch	3	0.2664	0.8479
Glucose	3	0.4731	0.7095
Fructose	3	0.6372	0.6119
Sucrose	3	1.7803	0.1707
Total protein	3	0.0856	0.9660
Alanine	3	0.1068	0.9538
Arginine	3	1.0016	0.4405
Asparagine	3	0.5551	0.6591
Aspartate	3	1.3577	0.3232
Ethanolamine	3	1.0437	0.4243
Phenylalanine	3	1.0696	0.3758
GABA	3	1.1567	0.3415
Glycine	3	0.3786	0.7690
Glutamate	3	0.7953	0.5301
Glutamine	3	0.3765	0.7726
Isoleucine	3	5.8760	0.0026
Histidine	3	3.4462	0.0281
Leucine	3	1.0562	0.0001
Lysine	3	1.6620	0.1948
Methionine	3	0.6562	0.5850
Ornithine	3	0.0342	0.9914
Proline	3	1.0770	0.4120
Serine	3	0.3494	0.7909
Tyrosine	3	9.4533	0.0001
Threonine	3	0.7276	0.5637
Tryptophane	3	1.0492	0.3843
Valine	3	2.7466	0.1126

CHAPTER 2

Cytokinins are involved in drought tolerance of *Pinus radiata* plants originating from embryonal masses induced at high temperatures

---

The content of this chapter corresponds to the published article "Castander-Olarieta, A., Moncaleán, P., Pereira, C., Pěnčík, A., Petřík, I., Pavlović, I., Novák, O., Strnad, M, Goicoa, T., Ugarte, M.D., Montalbán, I.A. (2020). Cytokinins are involved in drought tolerance of *Pinus radiata* plants originating from embryonal masses induced at high temperatures. *Tree Physiology* 1-15".

1. INTRODUCTION

Somatic embryogenesis (SE) is currently considered as one of the most successful methods for large-scale vegetative propagation of plants, and especially in some economically relevant woody conifer species such as *Pinus radiata*. SE combined with cryopreservation of embryonal masses (EMs) gives the opportunity for scaling-up production of genetically improved varieties that have been fully tested at field (Santa-Catarina et al., 2012; Montalbán et al., 2016). The rising demand for forest products worldwide may be partially addressed by the deployment of tested varieties through vegetative propagation in intensively managed plantation forests, a strategy referred to as multi-varietal forestry (Park 2002). In the last years, our team has overcome different bottlenecks in conifer SE by adjusting the composition of culture media and the culture conditions in *Pinus radiata* (Montalbán et al., 2010, 2012, 2015, García-Mendiguren et al., 2016a; Montalbán & Moncaleán, 2017, 2018) and also in *Pinus halepensis* (Pereira et al., 2016, 2017).

In vitro setups are often used as models systems for the complex field environments in which plants are subjected to stress (Claeys et al., 2014). Furthermore, it is well known that plant response is highly dependent on both the type and the intensity of stress (Claeys & Inzé, 2013) which can be controlled better and more easily in *in vitro* assays. Likewise, SE has been widely used not only as a proxy for understanding the physiological, biochemical and molecular events occurring during conifer embryo development (Morel et al., 2014; Reza et al., 2018), but also in response to different abiotic stresses (Muilu-Mäkelä et al., 2015; Eliášová et al., 2017; Castander-Olarieta et al., 2019).

Besides, stress is reported to be beneficial and, in some cases, even crucial for the embryogenic competence of different plant species by the activation of the molecular machinery required for the transition of somatic cells to an embryogenic state (Fehér et al., 2003; Ochatt, 2017). Moreover, stress can also act like a selective pressure during initial steps of SE determining the quantity and quality of the somatic embryos (Se's)

(Fehér, 2015; García-Mendiguren et al., 2016a; Pereira et al., 2016; Arrillaga et al., 2019; Castander-Olarieta et al., 2019).

In this regard, the relatively short period of embryogenesis in the life of a tree seems to be a critical stage to modulate plant behaviour *ex vitro* (García-Mendiguren et al., 2017). There is some strong evidence in the model conifer species *Picea abies* that environmental conditions during embryogenesis can establish an epigenetic memory that modulates different developmental traits (Johnsen et al., 2005; Kvaalen & Johnsen, 2008; Yakovlev et al., 2010, 2011). These epigenetic marks can be inherited as a pre-adaption to environmental conditions by subsequent generations as a form of maternal effect (Zas et al., 2013; Gosal & Wani, 2018). This middle-term memory, together with short term (developmental plasticity) and long-term (local adaptation) epigenetic developmental responses, are responsible for the great phenotypic plasticity and adaptation capacity observed in plants (Le-Gac et al., 2018), which pave the way for the production of plants pre-adapted to different environmental conditions (Pascual et al., 2014).

Among all types of stress conditions, heat and drought represent perhaps some of the most common abiotic stresses in plants and they have overlapping roles (Jia et al., 2017). Furthermore, it has been documented that increased tolerance to different kinds of stresses may rely on similar metabolic adjustments like cold and drought stresses (Shinozaki et al., 2003).

Because of climate change, the intensity and frequency of extreme weather events, such as heat waves and long drought periods, are predicted to increase (Duliè et al., 2013). High temperatures and drought are known to alter the fluidity and permeability of cell membranes (Sangwan et al., 2002), to produce imbalances in osmotic and water relations (De Diego et al., 2013; Feller & Vaseva, 2014), to increase the production of reactive oxygen species (ROS) (Larkindale & Knight, 2002) and trigger senescence, inhibition of photosynthesis and programmed cell death (Vacca et al., 2004). All these alterations could have significant implications in the viability, productivity and regeneration of all kind of forests, from planted to semi-natural forests (Allen et al.,

2010). Because of the complexity of stress tolerance traits, conventional breeding techniques combined with new biotechnological tools could offer more effective options for improving the performance, quality and health of commercially valued forest species and varieties.

The physiological mechanisms underlying heat and drought stress tolerance are still poorly understood. Integration of environmental stimuli, signal transduction and stress response are partially mediated by intense cross-talk among plant hormones (Wahid et al., 2007), which are considered the most important endogenous substances for modulating physiological, developmental and molecular responses (Wani et al., 2016). Apart from the well documented function of phytohormones in different *in vitro* assays such as organogenesis (Moncaleán et al., 2003, 2005; Montalbán et al., 2011) and SE (Carneros et al., 2017; Zhou et al., 2017; Moncaleán et al. 2018), they are active part in numerous stress response processes (Bielach et al., 2017; Corcuera et al., 2012; De Diego et al., 2012; 2015).

Particularly, cytokinins (CKs) are considered as master regulators during plant growth and development (Kieber & Schaller, 2018) and despite not being traditionally considered part of the stress response machinery, recent research has demonstrated that CKs directly participate in stress tolerance of plants (Wani et al., 2016). Although external application has been the most frequent method to study plant responses to CKs, stress-mediated alteration of endogenous levels of CKs indicates their involvement in abiotic stress, including drought (Kang et al., 2012). Current evidence supports that CKs could be primary receptors in temperature sensing (Černý et al., 2014) and cytokinin (CK) crosstalk with ethylene and other so-called "stress-hormones" such as abscisic acid (ABA), salicylic acid (SA), jasmonic acid (JA) and ethylene, has been observed (O'Brien & Benková, 2013).

The aim of this work was to evaluate if application of high-temperature regimes during initiation of radiata pine SE, which are known to reduce water availability (García-Mendiguren et al., 2016a; Moncaleán et al., 2018), could result in the production of somatic plants with different adaptation to drought stress. Isoprenoid CKs profiles were

investigated to assess the possible involvement of these phytohormones in the early response of initiated EMs to applied temperature stress determining the ongoing SE steps as well as *ex vitro* plant behaviour.

2. MATERIALS AND METHODS

2.1. Plant material production

Drought experiment

The somatic plants employed for this experiment originated from the procedure described in Materials and Methods section (Experiment 1) from Castander-Olarieta et al. (2019). Briefly, one year-old green female cones of *Pinus radiata* D.Don were collected in July 2016 from 4 genetically different open-pollinated trees in a seed orchard established by Neiker-Tecnalia in Deba (Spain; latitude: 43°16´59"N, longitude: 2°17´59"W, elevation: 50 m). Immature cones and seeds were processed following Montalbán et al. (2012) and the resulting dissected megagametophytes were placed horizontally in Petri dishes (9 mm x 14 mm) containing 19 ml of sterile EDM initiation medium (Walter et al., 2005) supplemented with 3.5 gL^{-1} gellan gum (Gelrite®; Duchefa). Eight megagametophytes were employed per Petri dish and transparent plastic film was used for a proper closure of Petri dishes. At this point, megagametophytes were incubated at different temperature regimes: 23°C (8 weeks, control), 30°C (4 weeks), 40°C (4 days) and 50°C (5 min). The Petri dishes containing the culture medium were pre-warmed before the start of the incubation period. Once finished, all the megagametophytes were kept at 23°C for 8 weeks in darkness. Further SE steps were carried out at standard conditions following the procedures described by Moncaleán et al. (2018) (Figure 1). For this experiment only well-formed mature Se's with similar morphologies were employed. After germination, somatic plantlets were transferred to 43 cm^3 (35 mm x 25 mm) individual pots containing blond peat moss (Pindstrup): perlite (7:3, v/v) and acclimatized in a greenhouse under controlled conditions (T = 23 ± 2°C and RH = 70 ± 5%) (Figure 1). Growing saplings bigger than 5 cm were transplanted to 2.18 L (90 mm x 270 mm) pots containing blond peat moss (Pindtrup): perlite (8:2, v/v) and 3 g L^{-1} Osmocote® Topdress fertilizer (Everris), and

watered regularly for one year until they had a minimum leader shoot length of 10 cm to conduct the drought experiment (Figure 1).

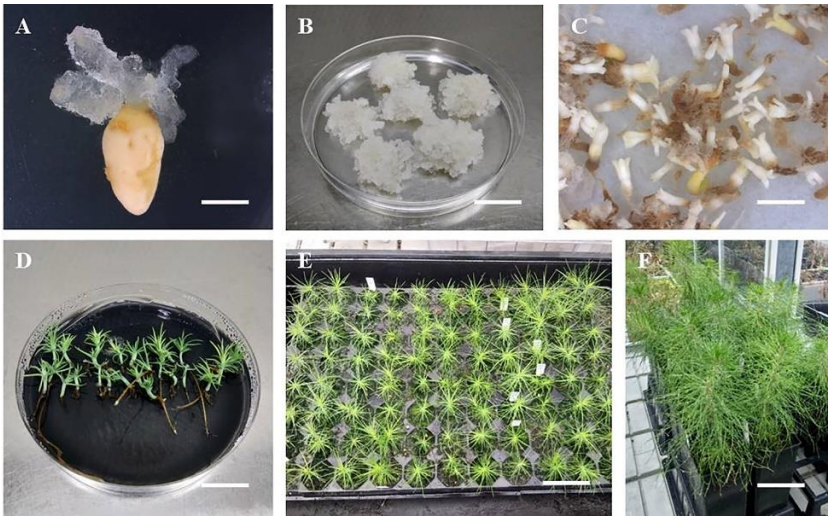

Figure 1. Extrusion of *Pinus radiata* embryonal masses from megagametophytes (bar = 4.5 mm; 8 weeks) **(A)**, proliferating embryonal masses (bar = 2.4 cm; 12 weeks) **(B)**, cotyledonary somatic embryos (bar = 5.5 mm; 12 weeks) **(C)**, germinated somatic plantlets (bar = 2.3 cm; 5 weeks) **(D)**, acclimatized somatic seedlings (bar = 5.5 cm; 8 weeks) **(E)** and two-year-old somatic plants ready for the drought experiment (bar = 6 cm) **(F)**.

Hormone analysis

The plant material used for the hormone analysis originated from the procedure described in Materials and Methods section (Experiment 2) from Castander-Olarieta et al. (2019). In this experiment green cones collected in July 2017 were employed. Sampled mother trees and procedures were the same as in 2.1.1 but applying adjusted temperature regimes based on the results obtained from the drought experiment: 23°C (8 weeks, control), 40°C (4 h), 50°C (30 min) and 60°C (5 min). In this case, just before maturation, part of the proliferating EMs (three ECLs per treatment and 40 mg from 4 different EMs of the same ECL) was put aside and frozen in liquid nitrogen. The samples were stored at -80°C until extraction, purification and quantification of endogenous phytohormones following the methodology described in Moncaleán et al. (2018).

2.2. Drought experiment

Experiment design, plant survival and growth rate

Two-year-old somatic saplings growing in the greenhouse and generated under the conditions previously described in section 2.1.1 were involved in a 3-months drought stress experiment between June to September 2019. Seven plants, each one from a different ECL, were randomly selected per treatment and per duplicate, comprising a total of 42 plants (7 ECLs x 2 biological replicates x 3 treatments). Half of them (each biological replicate) were subjected to a drought stress treatment by the complete suppression of watering, and the remainder were kept watered weekly (control plants). These control plants were used to verify if plants coming from different treatments could present varying behaviours in control conditions, and thus, interfere with the results obtained at drought conditions. The ECLs from the control temperature regime treatment (23°C, 8 weeks) originated from the 4 mother trees employed in section 2.1.1, while the ECLs from the temperature regimes of 30°C for 4 weeks and 50°C for 5 mins originated from 2 and 3 mother trees, respectively. All plants were watered to maximum retention capacity of the substrate before the start of the experiment and drought conditions were maintained for 12 weeks until plantlets from each treatment started to present external symptoms of drought stress such as needle epinasty or apical curvature (De Diego et al., 2012). After that period, all saplings were rewatered and plant survival was recorded one month later.

Total aerial height (cm) of each plant was measured at the beginning and at the end of the drought treatment (12 weeks) and the growth rate (GR) was calculated as follows:

$$GR\ (\%) = ((H2-H1) / H1) \times 100$$

where H represents the height of the plants at the beginning (H1) and at the end (H2) of the experiment.

Plant water potential and relative water content

Plant water potential was determined at the beginning and at the end of the treatment at predawn (from 5:00 to 7:00 a.m.) (Ψ_{pd}, MPa) from needles collected from the apical area using a Scholander chamber (PMS Instrument Company) and the pressure-equilibration technique (Scholander et al., 1965).

Relative water content (RWC (%)) was measured in two needles collected from the apical area of each sapling at the end of the drought period following the method described by De Diego et al., (2012). At harvesting time, needle fresh weight (FW) was recorded and then samples were immersed in de-ionized water and maintained overnight in dark. On the second day, after carefully removing the excess of water from needles surface by gently pressing them over filter paper, turgid weight (TW) was registered and needles were dried at 60°C for 48 h. After drying, needles were reweighed and dry weight (DW) recorded. RWC was estimated using the following equation:

RWC (%) = (FW – DW) / (TW – DW) × 100

Gas exchange parameters

Stomatal conductance (g_s, mmol H_2O m^{-2} s^{-1}), instant leaf transpiration (E, mmol H_2O m^{-2} s^{-1}) and instant net photosynthesis (A_N, µmol CO_2 m^{-2} s^{-1}) were measured at the beginning and at the end of the drought period at midday using the LI-6400XT Portable Photosynthesis System (Li-Cor Biosciences) equipped with the 6400-05 Clear Conifer Chamber (Li-Cor Niosciences). Intrinsic water use efficiency (WUE, µmol CO_2 $mmol^{-1}$ H_2O) was determined as the ratio between A_N and E.

2.3. Extraction, purification and quantification of endogenous CKs

Samples obtained in section 2.1.2 were analysed for the following 25 CKs types: N^6-Isopentenyladenine (iP), N^6-Isopentenyladenosine (iPR), N^6-Isopentenyladenine7-glucoside (iP7G), N^6-Isopentenyladenine-9-glucoside (iP9G), and N^6-Isopentenyladenosine-5'-monophosphate (iPMP), *cis*-Zeatin (cZ), *cis*-Zeatin riboside (cZR), *cis*-Zeatin *O*-glucoside (cZOG),), *cis*-Zeatin-7-glucoside (tZ7G), *cis*-Zeatin-9-

glucoside (cZ9G), *cis*-Zeatin riboside *O*-glucoside (cZROG), *cis*-Zeatin riboside-5'-monophosphate (cZRMP), *trans*-Zeatin (tZ), *trans*-Zeatin riboside (tZR), *trans*-Zeatin *O*-glucoside (tZOG), *trans*-Zeatin-7-glucoside (tZ7G), *trans*-Zeatin-9-glucoside (tZ9G), *trans*-Zeatin riboside *O*-glucoside (tZROG), *trans*-Zeatin riboside-5'-monophosphate (tZRMP), Dihydrozeatin (DHZ), Dihydrozeatin riboside (DHZR), Dihydrozeatin *O*-glucoside (DHZOG), Dihydrozeatin-7-glucoside (DHZ7G), Dihydrozeatin-9-glucoside (DHZ9G), Dihydrozeatin riboside *O*-glucoside (DHZROG), Dihydrozeatin riboside-5'-monophosphate (DHZMP). Isoprenoid CK types and their functional groups are shown in Table 1.

Table 1. Classification of isoprenoid CK types by functional groups analysed by mass spectrometry.

	Functional group				
Isoprenoid CK type	**Bases**	**Transport**	**Precursors**	**Storage**	**Irreversible metabolites**
N^6-Isopentenyladenine	iP	iPR	iPMP		iP7G, iP9G
cis-Zeatin	cZ	cZR	cZRMP	cZOG, cZROG	tZ7G, cZ9G
trans-Zeatin	tZ	tZR	tZRMP	tZOG, tZROG	tZ7G, tZ9G
Dihydrozeatin	DHZ	DHZR	DHZMP	DHZOG, DHZROG	DHZ7G, DHZ9G

Each sample was divided in two technical replicates of 10 mg and were analysed according to the protocol described by Svačinová et al. (2012), using miniaturized purification (pipette tip solid-phase extraction). Samples were extracted in 1 ml of modified Bieleski solvent and homogenized using a MM 301 vibration mill (Retsch GmbH & Co. KG, Haan, Germany) at a frequency of 27 Hz for 5 min at 4°C after adding 3 mm ceria-stabilized zirconium oxide bead. Samples were extracted with the addition of stable isotope-labelled internal standards (0.2 pmol for base, ribosides and 9- and 7-glucoside CKs; 0.5 pmol for *O*-glucoside and CK nucleotides). The extracts were ultrasonicated for 3 min and incubated at 4°C with continuous shaking for 30 min at 20 rpm. After centrifugation (15 min, 20,000 rpm, 4°C), from the supernatants of each sample, another three technical replicates of 300 µl were transferred onto Stage Tips and purified according to the aforementioned protocol, consisting of C18, SDB-RPS, and Cation-SR sorbents (Empore™). As a result, our experiment was carried out using 3

ECLs per treatment and 6 technical replicates per ECL, comprising a total number of 72 samples analysed.

Prior to loading the samples, the StageTip sorbents were conditioned with 50 µl acetone (by centrifugation at 2,000 rpm, 10 min, 8°C), 50 µl methanol (2,000 rpm, 10 min, 8°C), 50 µl water (2,200 rpm, 15 min, 8°C), equilibrated with 50 µl 50% (v/v) nitric acid (2,500 rpm, 20 min, 8°C), 50 µl water (2,500 rpm, 20 min, 8°C) and 50 µl modified Bieleski solvent (2,500 rpm, 20 min, 8°C). After the application of 300 µl of sample (3,500 rpm, 30 min, 8°C), the tips were washed using 50 µl of water and methanol (3,500 rpm, 20 min, 8°C). Samples were then eluted with 50 µl of 0.5 M NH_4OH in 60% methanol (3,500 rpm, 20 min, 8°C) and eluates were collected into new clean microcentrifuge tubes, evaporated to dryness and dissolved in 30 µl of mobile phase prior to UHPLC-MS/MS analyses.

Mass analysis was carried out following the procedure described by Moncaleán et al. (2018), using an Acquity UPLC® System (Waters, Milford, MA, United States), and a triple-quadrupole mass spectrometer Xevo™ TQ-S MS (Waters MS Technologies, Manchester, United Kingdom). All MS data were processed using the MassLynxTM software with TargetLynx™ program (version 4.2. Waters, Milford, MA, United States), and compounds were quantified by standard isotope dilution analysis (Rittenberg & Foster, 1940).

2.4. Statistical analysis

The results from all the physiological traits analysed during the drought experiment (growth rate, relative water content, water potential, A_N, g_s, E and WUE), a usual analysis of variance was conducted to assess the effect of the treatments on each parameter. A Tukey´s post-hoc test ($\alpha = 0.05$) was used for multiple comparisons. In the case of growth rate (for watered plants) and RWC (for plants subjected to drought stress), the analysis of variance did not fulfil the normality hypothesis, and thus, a Kruskal-Wallis test was performed.

Regarding the data obtained from the hormonal study, several models were considered for each hormone type. For cZR, the same usual analysis of variance described in the drought experiment section was performed, followed by multiple comparisons based on Tukey's post-hoc test ($\alpha = 0.05$).

To assess the effect of temperature regimes during the induction step on the levels of iPR, iPMP and cZ, the embryogenic cell line (ECL) was included in the model as a random effect. The inclusion of the ECL improved the fit and helped to analyse the effect of treatments more accurately by accounting for heteroscedasticity in the data. For total CK ribosides, the same model was performed, but including additional variance parameters for each level of temperature to correct for heteroscedasticity. In the case of total CK bases, total CK nucleotides and DZ, different variance parameters for each cell line were used to correct for heteroscedasticity.

In relation to tZR and DZR, the same procedure as described above for CK ribosides was followed, that is, a linear mixed effects model including the ECL as a random effect with different variance parameters for each temperature level. Multiple comparisons were also based on a Tukey post-hoc test ($\alpha = 0.05$) and predictable linear functions of the coefficients with *p*-values conveniently adjusted (Benjamini & Hochberg, 1995). The analysis of total iP and iP bases was equally conducted but considering different variance parameters for each cell line (ECL) in normal and logarithmic scale respectively.

3. RESULTS

3.1. Drought experiment

The application of 40°C for 4 days resulted in the complete failure of embryogenic tissue initiation. As a result, no plants could be obtained from that treatment and thus, the drought experiment was carried out only with the other three treatments (23°C, 8 weeks, control; 30°C, 4 weeks; 50°C, 5 min).

All the ECLs used in this experiment presented germination rates around 70-80% and the acclimatization success was >90% for all the plants originating from different induction treatments.

In general terms, comparing regularly watered plants with plants subjected to the drought period, clear differences were observed for all the parameters tested. Survival was 100% in watered plants, while plants subjected to drought stress presented survival rates of 66.7%. Growth rates of stressed plants decreased almost 3 times in relation to control plants, changing from an average growth rate of 77.9% ± 8 to 28.2% ±2.9, respectively (Table 2). Average Ψ_{pd} of plants at the beginning of the experiment (watered to maximum retention capacity of the substrate) was -0.63 ± 0.02 MPa, while the same parameter at the end of the drought period was -1.4 ± 0.08 MPa (Table 2), ranging from -2 MPa for the most stressed plants to -0.9 MPa for the less stressed. Likewise, RWC of plants in drought conditions was about 13% lower than control plants, and all gas exchange parameters analysed (A_N, g_s and E) decreased drastically after 12 weeks (Table 2).

Table 2. Survival, growth rate and physiological parameters of two-year-old *P. radiata* somatic plants grown in well-watered (W) or drought stress (D) conditions for 12 weeks. 21 plants were used for each condition (seven plants from each treatment, each one from a different ECL). Data are presented as mean values ± SE.

	Survival	**Growth rate**	**Ψ_{pd}**	**RWC**	**A_N**	**g_s**	**E**	**WUE**
W	100	77.9 ± 13.9	-0.63 ± 0.02	76.9 ± 1.3	17.4 ± 0.9	0.52 ± 0.06	5.45 ± 0.29	3.22 ± 0.15
D	66.7	28.2 ± 2.9	-1.4 ± 0.08	63.7 ± 4.1	1.8 ± 0.9	0.02 ± 0.005	0.58 ± 0.11	2.38 ± 0.49

Survival (%); Growth rate (%); Ψ_{pd}, water potential (MPa); RWC, relative water content (%); A_N, instant net photosynthesis (μmol CO_2 m^{-2} s^{-1}); g_s, stomatal conductance (mmol H2O m-2 s-1); E, instant leaf transpiration (mmol H_2O m^{-2} s^{-1}); WUE, water use efficiency (μmol CO_2 $mmol^{-1}$ H_2O).

Considering watered plants, no significant differences were detected (ANOVA, not shown) for most physiological traits between control (23°C, 8 weeks) and tested induction treatments (temperature regimes of 30°C, 4 weeks and 50°C, 5 min). Only growth rate was significantly higher for plants originating from the induction treatment at 30°C compared to the 23°C and 50°C treatments (Figure 2).

With respect to drought conditions, significant differences were observed for three of the 8 physiological traits evaluated (survival, A_N and WUE) (Table 3). It is worth mentioning that plants originating from standard induction conditions (23°C, 8 weeks) showed few visual symptoms of drought stress, with slight needle epinasty in some cell lines, but not apparent apical curvature. Plants originating from the 30°C treatment for 4 weeks presented the most heterogeneous aspect. Some plants presented similar symptoms to control plants, while others showed clear apical curvature and needle epinasty. Plants originating from the temperature regime of 50°C for 5 min were the ones presenting the greatest drought stress symptoms (Figure 3). Accordingly, clear differences in plants survival were detected. 100% of the plants coming from control conditions (23°C, 8 weeks) recovered after rewatering, while plants from induction treatments at 30°C and 50°C showed lower survival rates of 57.1% and 42.9%, respectively.

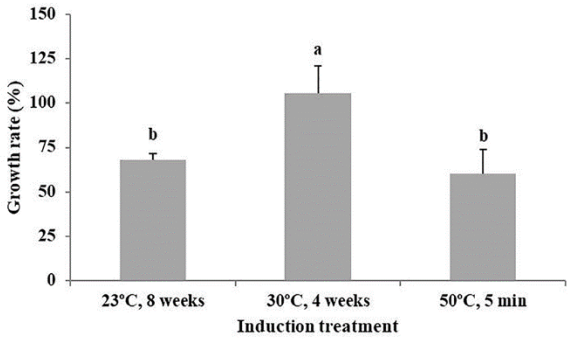

Figure 2. Growth rate (%) of two-year-old somatic plants produced under different induction temperature regimes (23°C, 8 weeks, control; 30°C, 4 weeks; 50°C, 5 mins) and grown in the greenhouse for 12 weeks in watered conditions. Seven plants were used per treatment and data are presented as mean values ± SE. Significant differences at $p < 0.05$ are indicated by different letters.

A_N and WUE presented significant differences among treatments at the end of the drought period. Plants coming from ECLs initiated at 50°C showed significant lower A_N values than those from control conditions (23°C), even reaching values near 0 for most of the individuals. Plants originating from the 30°C induction treatment showed intermediate values and high variability, denoting that some plants were close to the values obtained at 50°C while others were more like those at 23°C (Figure 4A).

Table 3. ANOVA of different physiological parameters obtained after the drought period (12 weeks) according to the 3 temperature induction treatments from which plants were obtained. Seven two-year-old plants from different ECLs were tested per treatment.

Source	df	F value	*p* value
Growth rate			
Temperature (T)	2	3.21	0.064
Ψ_{pd}			
Temperature (T)	2	1.39	0.274
A_N			
Temperature (T)	2	3.63	0.047
g_s			
Temperature (T)	2	3.38	0.057
E			
Temperature (T)	2	3.45	0.054
WUE			
Temperature (T)	2	5.45	0.014
RWC*			
Temperature (T)	2	2.23*	0.327*

Ψ_{pd}, water potential; RWC, relative water content; A_N, instant net photosynthesis; g_s, stomatal conductance; E, instant leaf transpiration; WUE, water use efficiency
*The values for RWC in the table correspond to the Kruskal-Wallis test. The normality assumption for this variable could not be assumed.

Figure 3. Two-year-old *P. radiata* somatic plants originating from the induction treatment of 50°C for 5 min grown in either well-watered control condition (bar = 2.72 cm) **(A)** or drought-stress conditions for 12 weeks (bar = 2.5 cm) **(B)**. See the apparent needle epinasty and apical curvature in drought condition.

Regarding WUE, similar results were obtained, being the 50°C induction treatment the one with the lowest values and 23°C the one with the highest ones. In this case the difference observed between the 50°C and control treatments was also statistically significant (Figure 4B).

Despite not statistically significant, it is noticeable that the differences obtained in the case of g_s, *E* and growth rate showed *p*-values of 0.0568, 0.0537 and 0.0645 respectively (Table 3), so we could assume that they are on the verge of statistical significance. All of them followed the same tendency previously described for A_N and WUE. Plants originating from the 50°C treatment showed the lowest values and control plants (23°C treatment) the highest ones. Considering the 30°C treatment, plants presented intermediate values for g_s and E, while the results in the case of growth were very similar to those of control plants (Table 3).

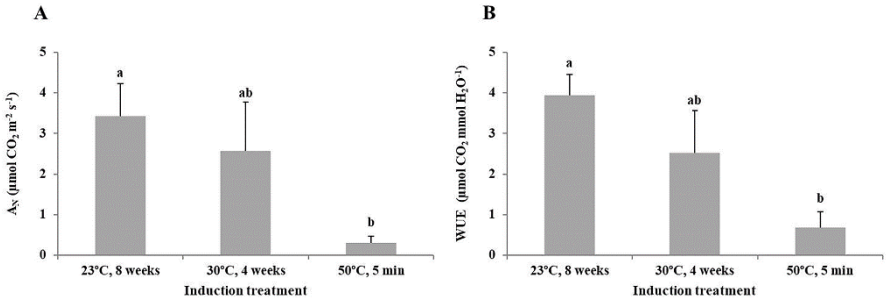

Figure 4. Instant net photosynthesis (A_N) **(A)** and water use efficiency (WUE) **(B)** of two-year-old *P. radiata* somatic plants originating from different induction treatments (23°C, 8 weeks, control; 30°C, 4 weeks; 50°C, 5 mins) and grown in drought-stress conditions for 12 weeks. Seven plants were used per treatment and data are presented as mean values ± SE. Significant differences at $p < 0.05$ are indicated by different letters.

3.2. Hormone analysis

The levels of CK N-glucosides (7G/9G) and most of CK *O*-glucosides (OG), which are known to be irreversible and storage metabolites of the active forms, were under limit of detection in all samples analysed. In the case of tZ, tZRMP, DHZMP and cZRMP, more than the 40% of the samples analysed were under limit of detection as well, thus no

statistical analysis could be performed. Because of the lack of some CK groups, the analysis of total CK types could not be performed either.

Regarding the amount of each CK type, it should be noted that the most abundant cytokinins in EMs were iP-type CKs, and specially the precursor forms (iPMP), along with cZ-type CKs in the base form (cZ). The levels of tZ and DHZ-type CKs were much lower than the two groups previously mentioned, and in the case of these two CK types the most abundant functional groups were the ribosides (tZR) and bases (DHZ), respectively (Table 4).

Table 4. Detectable endogenous cytokinins (pmol g^{-1} FW) in *P. radiata* EMs initiated under different induction treatments (23°C, 8 weeks; 40°C, 4 h; 50°C, 30 mins; 60°C, 5 mins). Three ECLs per treatment and 6 technical replicates per ECL were used. Data are presented as mean values ± SE. Significant differences within a row at $p < 0.05$ are indicated by different letters.

Cytokinins (pmol/g FW)	Induction treatment (°C)			
	23	40	50	60
iP	0.084 ± 0.008^{a}	0.046 ± 0.004^{b}	0.041 ± 0.003^{b}	0.064 ± 0.01^{b}
iPR	0.012 ± 0.005^{a}	0.009 ± 0.002^{a}	0.009 ± 0.002^{a}	0.01 ± 0.003^{a}
iPMP	0.387 ± 0.260^{a}	0.314 ± 0.136^{a}	0.303 ± 0.1^{a}	0.249 ±0.062^{a}
cZ	0.299 ± 0.106^{a}	0.223 ± 0.112^{a}	0.23 ± 0.06^{a}	0.237 ± 0.047^{a}
cZR	0.045 ± 0.003^{a}	0.029 ± 0.003^{b}	0.028 ± 0.003^{b}	0.036 ± 0.002^{ab}
tZR	0.0016 ± 1 x 10^{-4b}	0.002 ± 2 x 10^{-4b}	0.0022 ± 2 x 10^{-4ab}	0.0034 ± 2 x 10^{-4a}
DHZ	0.059 ± 0.008^{a}	0.037 ± 0.029 ^{a}	0.073 ± 0.046^{a}	0.097 ± 0.01^{a}
DHZR	0.007 ± 0.001^{a}	0.009 ± 0.003^{a}	0.008 ± 0.002^{a}	0.015 ± 0.01^{a}
Total CK bases[1]	0.484 ± 0.034^{a}	0.291 ± 0.069^{b}	0.367 ± 0.112^{ab}	0.449 ± 0.106^{a}
Total CK ribosides[2]	0.058 ± 0.011^{a}	0.048 ± 0.014^{a}	0.046 ± 0.012^{a}	0.059 ± 0.011^{a}
Total CK nucleotides[3]	0.241 ± 0.065^{a}	0.584 ± 0.302^{a}	0.367 ± 0.162^{a}	0.506 ± 0.314^{a}
Total iP[4]	0.479 ± 0.252^{a}	0.368 ± 0.142^{a}	0.353 ± 0.096^{a}	0.323 ± 0.066^{a}

[1]Total CK bases: iP, cZ, tZ, DHZ; [2]Total CK ribosides: iPR, cZR, tZR, DHZR; [3]Total CK nucleotides: iPMP, cZMP, tZMP, DHZMP; [4]Total iP: iP, iPR, iPMP.

Analysing the results by functional groups and considering the effect of the treatments, significant differences were found only for CK bases (cZ, tZ, DHZ, iP). No significant differences could be observed in the case of CK ribosides and CK nucleotides. The

concentration of total CK bases was significantly lower in EMs produced under 40°C treatment with respect to EMs originating from control treatment (23°C) or treatment at 60°C for 5 mins (Figure 5A, Table 4). The treatment at 50°C resulted in intermediate values (Figure 5A), however not significant compared to other treatments. Among the CK bases, significant differences were especially observed for iP with low concentrations observed in samples originating from the 50°C and 40°C treatments and higher levels observed for the control (23°C) and 60°C treatment (Figure 5B; Table 4). No significant differences were detected for other CK bases (cZ, tZ, DHZ) among temperature treatments but similar trends were observed. Both DHZ and cZ- type CKs were found at lower concentrations in EM samples produced under the 40°C induction treatment (Table 4). In the case of DHZ, the differences were on the verge of statistical significance (p = 0.079).

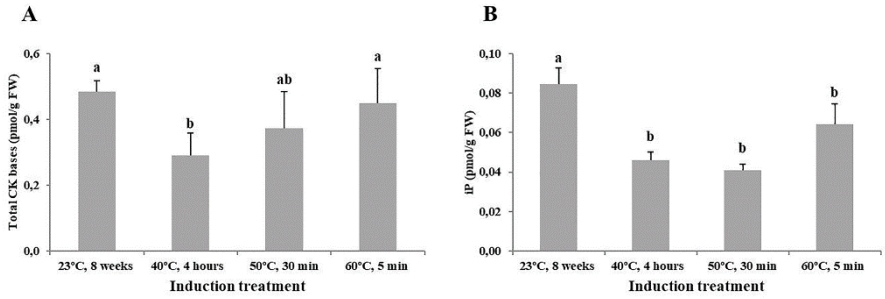

Figure 5. Effect of temperature treatment (23°C, 8 weeks; 40°C, 4 h; 50°C, 30 mins; 60°C, 5 mins) on the levels of total CK bases **(A)** and N^6-isopentenyladenine (iP) **(B)** in *P. radiata* EMs. Three biological replicates were used per treatment and data are presented as mean values ± SE. Significant differences at $p < 0.05$ are indicated by different letters.

Some significant differences were also found for CK ribosides (a transport form of CKs). Although no significant differences in total CK ribosides could be detected among treatments (Table 4), a heterogeneous behaviour was observed for the different riboside-types. Opposite patterns were observed for ribosides cZR and tZR. cZR followed similar trend as base forms (see Figure 5; Table 4), i.e. significant lower levels following the 40°C and 50°C treatments compared to control treatment (23°C). The concentration of this hormone was found at intermediate values for EMs produced under treatment

60°C (Figure 6A, Table 4). In contrast, tZR showed significantly higher concentration after treatment at 60°C compared to control (23°C) and 40°C treatments. The 50°C treatment resulted in intermediate values (Figure 6B; Table 4).

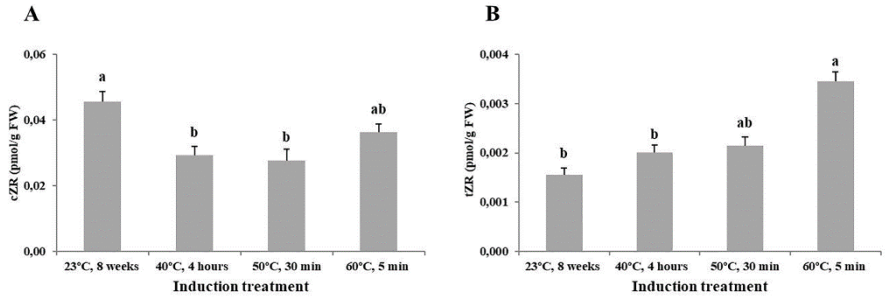

Figure 6. Effect of temperature treatment (23°C, 8 weeks; 40°C, 4 h; 50°C, 30 mins; 60°C, 5 mins) on the levels of cZR **(A)** and tZR **(B)** in *P. radiata* EMs. Three biological replicates were used per treatment and data are presented as mean values ± SE. Significant differences at $p < 0.05$ are indicated by different letters.

Finally, it should be mentioned that no differences were observed for iPMP, the most abundant hormone type in EMs. iPMP is the precursor of the active form iP which was shown to be affected by the temperature regime during induction (Figure 5B; Table 4).

4. DISCUSSION

This study provided experimental evidence confirming that the application of high temperatures during initiation of SE can result in altered behaviour of plants *ex vitro*, both at standard (growth rate) and drought conditions (survival, A_N, WUE). Moreover, different hormonal profiles at initial steps of the embryogenic process were observed. Unfortunately, these different hormonal profiles are unknown for the tested induction treatments in the case of the drought experiment except the control (23°C, 8 w).

As sessile organisms, plants are continuously and widely exposed to external stimuli such as diverse extreme weather conditions or pathogens. Stress is even exacerbated in trees because of their long lifespan. As a result, plants developed different survival strategies to deal with stress by modifying some of their morphological and physiological traits (Xia et al., 2015). Among these fine-tuned strategies, perhaps one of

the most sophisticated and promising ones is the so-called plant priming (Conrath et al., 2015).

At control conditions, plants coming from EMs initiated at 30°C for 4 weeks presented significantly higher growth rates compared to control treatment (23°C, 8 weeks), suggesting that long induction treatments at increased but quite moderate temperatures could establish some kind of "memory" in initiated embryogenic cells. This "memory" may persist throughout the SE process, triggering subsequent growth in the resulting plants, as already observed by Kvaalen & Johnsen (2008) in *Picea abies*. These authors reported increased leader shoot lengths during the second growth season when high temperatures were applied during SE. Several studies in conifers (spruces) (Johnsen et al., 2005; Webber et al., 2005) pointed out that different temperature regimes during both zygotic and somatic embryogenesis can affect the vegetative development of seedlings for years. In Norway spruce it has been shown that the temperature regime during embryogenesis is involved in the timing of bud set and thus cold acclimation. Therefore, the embryogenesis period could be crucial for plant priming.

The air temperature has been shown to positively influence growth and A_N in temperate or boreal trees (Way & Oren, 2010). As evidenced in Norway spruce, it could be possible that high temperatures during embryogenesis could act as a priming agent that prepares plants for a future scenario of higher temperatures, in which an improvement of the photosynthetic capacity is required by the increase in electron transport capacity and/or greater heat stability of Rubisco activase (Sage & Kubien, 2007).

Regarding the results obtained from the drought experiment, it is noticeable that Ψ_{pd} exhibited significant reductions at the end of the treatment, validating our experimental design. In the same way, all the other physiological parameters analysed decreased in line with $\Psi_{pd,}$ as previously postulated in conifers by other authors (Brodribb & Cochard, 2009). With such a water stress, the decrease by almost 3 times in growth rate (77.9 ± 13.9 for watered plants; 28.2 ± 2.9 for stressed plants) is similar to that observed in other conifer species (Turtola et al., 2003). Likewise, the strong decrease in g_s and the other gas-exchange parameters (A_N and E) over a narrow range of Ψ_{pd} has already been

reported in *Pinus radiata* and interpreted as an evidence of strongly isohydric stomatal response to water deficit (De Diego et al., 2012, 2015; Brodribb & McAdam, 2013). In agreement with those studies, the plants that seemed more sensible to drought stress reached Ψ_{pd} values of -2 MPa, which is considered the turgor lost point for this species (De Diego et al., 2012), whereas the most tolerant specimens kept around values of -1 MPa and did not usually present any apparent loss of turgor.

In spite of experimental conditions perfectly adapted to efficient drought test, no statistically significant differences were found for water-related parameters among treatments (Ψ_{pd} and RWC). Significant differences were only observed for 2 non-independent physiological traits, instant net photosynthesis (A_N) and intrinsic water use efficiency (WUE = A_N/E). Accordingly, both traits followed the same pattern: plants originating from the highest temperature induction treatment (50°C) with short exposure periods (5 min) exhibited a significant decrease. Other parameters such as E, g_s or growth rate followed the same trend (lowest values for the 50°C treatment) but were at the verge of statistical significance. Even though the differences detected for plants originating from the longer 30°C treatment (4 weeks) were not significant, a slight decrease in all parameters mentioned before was observed.

These results suggest that for similar water status, plants originating from high-temperature induction treatment (50°C, 5 min) tended to close stomata earlier, which allows a better maintenance of water status and avoid hydraulic failure (De Diego et al., 2012). Nevertheless, for extended drought periods carbon starvation can occur (Mcdowell et al., 2014). According to the carbon starvation hypothesis, when plants close stomata to prevent desiccation, photosynthetic carbon uptake diminishes to values near zero (Mcdowell et al., 2014). Continued demand for carbohydrates to maintain metabolism can deplete carbohydrate reserves, which are completely necessary to maintain both the molecular machinery required to face drought, such as the production of resin (Lewinsohn et al., 1993), but also some morphological adjustments such as fine root production (Villar-Salvador et al., 2004; Aaltonen et al., 2017). The mechanisms by which plants originating from control temperature treatment (23°C, 8 weeks) and to a

lesser extent moderate temperature treatment during induction (30°C, 4 weeks), can maintain favourable water status without early stomata closure could be multiple, starting from structural differences such as fine root and stomata density (Ewers et al., 2000; Mitton et al., 1998), or molecular changes such as the accumulation of compatible sugars, amino acids and polyamines (De Diego et al., 2013).

So, surprisingly the application of high temperatures during SE induction (either moderate for quite long period or high for a brief period), besides which are known to reduce water availability (García-Mendiguren et al., 2016a; Moncaleán et al., 2018), gave rise to plants with reduced capacity to face drought. There are several reports suggesting that increased tolerance to different kinds of stresses rely on similar metabolic adjustments, e.g. drought and freezing tolerance. In pine for example, protection against drought was accompanied by induction of superoxide dismutase (SOD) activity (Alonso et al., 2001), along with an increase in the expression of chaperones and late embryogenesis abundant proteins (Wang et al., 2003). These responses were also observed in other plants exposed to low temperatures (Rubio et al., 2002). Likewise, in Norway spruce, freezing tolerance is strictly correlated with drought tolerance, and this correlation is partially based on high SOD activities (Blödner et al., 2005). Other authors found out in *Quercus ilex* a significant increase in heat tolerance by drought exposure supporting that the mechanisms developed during acclimation to both stresses are strongly related, as both involve synthesis of heat shock proteins (Gimeno et al., 2009).

However, it has been reported that population differences in drought resistance are more related to the climate of origin (pedoclimatic adaptation and genetic background), while heat stress responses are governed by phenotypic plasticity and acclimation to environmental growing conditions (Marias et al., 2017). All this considered, deeper understanding of the molecular mechanisms involved in the altered behaviours observed among plants originating from different temperature regimes should be required.

To this purpose, a deep analysis of the CK profile of EMs produced under high temperature regimes was performed. Many studies have been published on conifer SE development during the last decades, but relatively little work has been carried out about the involvement of endogenous phytohormones during the process, and most of such studies are addressing different issues, i.e. the comparison of embryogenic and non-embryogenic calluses or genotypes/explants with different embryogenic ability (Bravo et al., 2017; Arrillaga et al., 2019). Even less information is available about the effect of stress on the hormonal profile over the course of SE, as most of the studies are carried out at plant level.

In this study most of the well documented isoprenoid CK forms and conjugates were observed, including bioactive bases, transport (CK riboside forms) and storage (CK N- and *O*- glucoside forms) forms, as well as CK nucleotides as biosynthetic precursors. However, no CK N-glucosides (7-G/9-G), the irreversible and inactive end products of cytokinin metabolism, could be detected, suggesting that the CK N-glucosyltransferase pathway, which takes part in numerous developmental processes such as growth of conifer buds (Zhang et al., 2003) or their organogenesis *in vitro* (Montalbán et al., 2013), is insignificant in SE, as already observed in other conifer studies such as Norway spruce (Vondrakova et al., 2018) or Douglas-fir (Gautier et al., 2019).

All the rest of CK forms observed (bases, transport and precursors) were at very low concentrations, which is in accordance with other studies executed in *Acca sellowiana* (Pescador et al., 2012) and *Picea abies* (Vondrakova et al., 2018) in which a drastic drop in the CK profile was observed during EM proliferation stage. In our experiments, the iP and cZ-types represented the major endogenous CKs in EMs. The highest amounts of cZ-types were in the active forms (cZ), while the most abundant form in the case of iP was the biosynthetic precursor iPMP. In spite of being considered CK derivatives with low biological activity in *Arabidopsis* (Nishiyama et al., 2011), cZ has been demonstrated to be the dominant form of CK in Se's of radiata pine (Moncaleán et al., 2018) and cotyledons of stone pine (Moncaleán et al., 2005). cZ is an abundant and active CK in most monocotyledonous species (Nishiyama et al., 2011) and plays an important role

during the development of seeds of eudicots (Tomaž & Marina, 2010). Regarding iP forms, studies carried out during early SE in the tree fern *Cyathea delgadii* showed greater concentrations of Z-type CKs compared to iPs (Grzyb et al., 2017). Nevertheless, results obtained from hormonal analysis performed during SE in cotton highlight the importance of iP during redifferentiation and embryogenesis induction (Zeng et al., 2007). Besides, in peach seeds, nucleotides and ribosides of the iP-type are predominant and are involved in embryo formation (Arnau et al., 1999).

Concerning the effect of temperature in the hormonal profile of EMs, several differences were observed among treatments for total CK bases and some CK forms such as iP, cZR and tZR. In the case of total CK bases, iP and cZR, a decreasing tendency was detected when applying higher temperature regimes than control (23°C, 8 weeks), especially for those applied for the longest periods of time (40°C-4 h and 50°C-30 mins). On the other hand, tZR levels showed the opposite behaviour, presenting the highest values at the highest temperature regime (60°C, 5 min), following an increasing tendency as temperature rose. These results support the idea that despite not being the best-studied hormone group for plant stress-responses, CKs actively participate in the transduction of signals (Argueso et al., 2009). These signals are triggered by various environmental stimuli, among which temperature plays a crucial role (Pavlů et al., 2018) potentially via fluxes of Ca^{2+} ions (Černý et al., 2014).

The differences observed in the hormonal profile could explain the varying behaviour observed throughout the whole SE under the same conditions reported in Castander-Olarieta et al. (2019), but also in previous studies when high temperatures and/or different agar concentrations were used. As observed in Moncaleán et al. (2018) and Fraga et al. (2016), high concentrations of cZR and active CKs in general are correlated with high production of mature embryos, which is in disagreement with the results obtained in the linked study Castander-Olarieta et al. (2019). In this case, the application of high temperatures led to a slight but not significant increase in the production of Se's, the same treatments that provoked a decrease in the amount of most CKs in the present work. However, the longest exposure treatments (50°C, 30 min) gave rise to a great

amount of barrel-shaped cotyledonary Se's, which usually present low germination and rooting rates, suggesting that CKs not only regulate the production of Se's but also influence their morphology. On the other hand, Moncaleán et al. (2018) showed that the highest success in the SE process coincided with low levels of iP types, as observed in our study.

At plant level, a decline in endogenous CK levels in reaction to stress has long been observed (Shashidhar et al., 1996), which is in accordance with the results obtained for EMs in this study, and also in previous ones (Moncaleán et al., 2018). CKs and ABA appear to have antagonistic roles, among others, in controlling stomatal function (Moncaleán et al., 2007; Kohli et al., 2013). Many studies have detected that heat stress induces a rapid but transient increase in active CK contents, followed by its significant depletion, suggesting that CKs could serve as first signal for thermomorphogenesis (Skalák et al., 2016). Afterwards, hormones classically related to stress such as ABA and SA seem to be the main agents involved in early impacts of stress in radiata pine (Escandón et al., 2016). As a result, CKs seem to exert a negative role on stress responses and a reduction in CK levels in short-term stress exposures has been demonstrated to improve drought and salt tolerance (Nishiyama et al., 2011; Bielach et al., 2017). Those plants usually present higher water contents, but not only because of a strict stomatal regulation, but also because of a better root system, since CKs are known to negatively regulate root growth and lateral root formation (Ramireddy et al., 2018).

However, for acclimation and recovery of plants, CKs seem to take active part by promoting a reduction in the oxidative damage and activating the stomata opening required to recover physiological functions and growth (Escandón et al., 2016). De Diego et al. (2015) also postulated that zeatin ribosides could act as protective molecules against drought. In fact, CKs trigger the accumulation of heat-shock proteins (Černý et al., 2011), and specifically, tZR has been proved to diminish membrane electrolyte leakage and activate the antioxidant system (Liu et al., 2002). In line with this information, the decrease in initiation and proliferation rates observed under high induction temperatures and long exposures in previous and linked studies (Castander-

Olarieta et al., 2019) could be influenced to a large extent by the general decrease detected in the CK content of EMs, since micromophological and ultrastructural analyses revealed the presence of oxidative damage in embryogenic cells. In the same way, an increase in the levels of tZR when applying 60°C for 5 mins could be the reason for the preservation of big, well organized embryogenic structures observed in Castander-Olarieta et al. (2019).

In parallel, García-Mendiguren et al. (2016b) showed that the stressful conditions during the initiation phase of radiata pine SE continued to influence the maturation phase by the presence of chaperones, heat-shock proteins and osmotically induced proteins in mature Se's. These results correlate with the increased levels of tZ riboside observed in EMs initiated under high temperatures, reinforcing its role as activator of the antioxidant system.

This study provides deeper information about the effect of temperature on SE at a physiological level, about a possible role of CKs in this process, and laid the foundation for a better understanding about the relationship between environmental conditions during SE and plant behaviour months later. However, further research is required at plant level to elucidate which are the molecular/physiological mechanisms involved in drought tolerance.

5. REFERENCES

Aaltonen, H., Linden, A., Heinonsalo, J., Biasi, C., and Pumpanen, J. (2017). Effects of prolonged drought stress on Scots pine seedling carbon allocation. *Tree Physiol.* 37, 418-427.

Allen, C.D., Macalady, A.K., Chenchouni, H., Bachelet, D., McDowell, N., Vennetier, M., et al. (2010). A global overview of drought and heat-induced tree mortality reveals emerging climate change risks for forests. *Forest Ecol. Manag.* 259, 660-684.

Alonso, R., Elvira, S., Castillo, F.J., and Gimeno, B.S. (2001). Interactive effects of ozone and drought stress on pigments and activities of antioxidative enzymes in *Pinus halepensis*. *Plant, Cell Environ.* 24, 905-916.

Argueso, C.T., Ferreira, F.J., and Kieber, J.J. (2009). Environmental perception avenues: The interaction of cytokinin and environmental response pathways. *Plant, Cell Environ.* 32, 1147-1160.

Arnau, J.A., Tadeo, F.R., Guerri, J., and Primo-Millo, E. (1999). Cytokinins in peach: Endogenous levels during early fruit development. *Plant Physiol. Biochem.* 37, 741-750.

Arrillaga, I., Morcillo, M., Zanón, I., Lario, F., Segura, J., and Sales, E. (2019). New approaches to optimize somatic embryogenesis in maritime pine. *Front. Plant Sci.* 10, 138.

Benjamini, Y., and Hochberg, Y. (1995). Controlling the false discovery rate: a practical and powerful approach to multiple testing. *J. R. Stat. Soc. B* 57, 289-300.

Bielach, A., Hrtyan, M., and Tognetti, V.B. (2017). Plants under stress: Involvement of auxin and cytokinin. *Int. J. Mol. Sci.* 18.

Blödner, C., Skroppa, T., Johnsen, Ø., and Polle, A. (2005). Freezing tolerance in two Norway spruce (*Picea abies* [L.] Karst.) progenies is physiologically correlated with drought tolerance. *J. Plant Physiol.* 162, 549-558.

Bravo, S., Bertín, A., Turner, A., Sepúlveda, F., Jopia, P., Parra, M.J., et al. (2017). Differences in DNA methylation, DNA structure and embryogenesis-related gene

expression between embryogenic and non-embryogenic lines of *Pinus radiata* D. don. *Plant Cell. Tiss. Org.* 130, 521-529.

Brodribb, T.J., and Cochard, H. (2009). Hydraulic failure defines the recovery and point of death in water-stressed conifers. *Plant Physiol.* 149, 575-584.

Brodribb, T.J., and McAdam, S.A.M. (2013). Abscisic ccid mediates a divergence in the drought response of two conifers. *Plant Physiol.* 162, 1370-1377.

Carneros, E., Toribio, M., and Celestino, C. (2017). Effect of ABA, the auxin antagonist PCIB and partial desiccation on stone pine somatic embryo maturation. *Plant Cell. Tiss. Org.* 131, 445-458.

Castander-Olarieta, A., Montalbán, I.A., De Medeiros Oliveira, E., Dell'Aversana, E., D'Amelia, L., Carillo, P., et al. (2019). Effect of thermal stress on tissue ultrastructure and metabolite profiles during initiation of radiata pine somatic embryogenesis. *Front. Plant Sci.* 9, 1-16.

Černý, M., Dyčka, F., Bobál'Ová, J., and Brzobohatý, B. (2011). Early cytokinin response proteins and phosphoproteins of *Arabidopsis thaliana* identified by proteome and phosphoproteome profiling. *J. Exp. Bot.* 62, 921-937.

Černý, M., Jedelský, P.L., Novák, J., Schlosser, A., and Brzobohatý, B. (2014). Cytokinin modulates proteomic, transcriptomic and growth responses to temperature shocks in *Arabidopsis*. *Plant, Cell Environ.* 37, 1641-1655.

Claeys, H., and Inzé, D. (2013). The agony of choice: How plants balance growth and survival under water-limiting conditions. *Plant Physiol.* 162, 1768-1779.

Claeys, H., Van Landeghem, S., Dubois, M., Maleux, K., and Inzé, D. (2014). What Is Stress? Dose-response effects in commonly used *in vitro* stress assays. *Plant Physiol.* 165, 519-527.

Conrath, U., Beckers, G.J.M., Langenbach, C.J.G., and Jaskiewicz, M.R. (2015). Priming for enhanced defense. *Annu. Rev. Phytopathol.* 53, 97-119.

Corcuera, L., Gil-Pelegrin, E., and Notivol, E. (2012). Aridity promotes differences in proline and phytohormone levels in *Pinus pinaster* populations from contrasting environments. *Trees - Struct. Funct.* 26, 799-808.

De Diego, N., Pérez-Alfocea, F., Cantero, E., Lacuesta, M., and Moncaleán, P. (2012). Physiological response to drought in radiata pine: Phytohormone implication at leaf level. *Tree Physiol.* 32, 435-449.

De Diego, N., Sampedro, M.C., Barrio, R.J., Saiz-Fernández, I., Moncaleán, P., and Lacuesta, M. (2013). Solute accumulation and elastic modulus changes in six radiata pine breeds exposed to drought. *Tree Physiol.* 33, 69-80.

De Diego, N., Saiz-Fernández, I., Rodríguez, J.L., Pérez-Alfocea, P., Sampedro, M.C., Barrio, R.J., et al. (2015). Metabolites and hormones are involved in the intraspecific variability of drought hardening in radiata pine. *J. Plant Physiol.* 188, 64-71.

Duliè, V., Zhang, Y., and Salathé, E.P. (2013). Changes in twentieth-century extreme temperature and precipitation over the western United States based on observations and regional climate model simulations. *J. Clim.* 26, 8556-8575.

Eliášová, K., Vondráková, Z., Malbeck, J., Trávníčková, A., Pešek, B., Vágner, M., et al. (2017). Histological and biochemical response of Norway spruce somatic embryos to UV-B irradiation. *Trees - Struct. Funct.* 31, 1279-1293.

Escandón, M., Cañal, M.J., Pascual, J., Pinto, G., Correia, B., Amaral, J., et al. (2016). Integrated physiological and hormonal profile of heat-induced thermotolerance in *Pinus radiata*. *Tree Physiol.* 36, 63-77.

Ewers, B.E., Oren, R., and Sperry, J.S. (2000). Influence of nutrient versus water supply on hydraulic architecture and water balance in *Pinus taeda*. *Plant, Cell Environ.* 23, 1055-1066.

Fehér, A., Pasternak, T.P., and Dudits, D. (2003). Transition of somatic plant cells to an embryogenic state. *Plant Cell. Tiss. Org.* 74, 201-228.

Fehér, A. (2015). Somatic embryogenesis - stress-induced remodeling of plant cell fate. *Biochim. Biophys. Acta - Gene Regul. Mech.* 1849, 385-402.

Feller, U., and Vaseva, I.I. (2014). Extreme climatic events: Impacts of drought and high temperature on physiological processes in agronomically important plants. *Front. Environ. Sci.* 2, 1-17.

Fraga, H.P.F., Vieira, L.N., Puttkammer, C.C., dos Santos, H.P., Garighan, J.A., and Guerra, M.P. (2016). Glutathione and abscisic acid supplementation influences somatic embryo maturation and hormone endogenous levels during somatic embryogenesis in *Podocarpus lambertii* Klotzsch ex Endl. *Plant Sci.* 253, 98-106.

García-Mendiguren, O., Montalbán, I.A., Goicoa, T., Ugarte, M.D., and Moncaleán, P. (2016a). Environmental conditions at the initial stages of *Pinus radiata* somatic embryogenesis affect the production of somatic embryos. *Trees - Struct. Funct.* 30, 949-958.

García-Mendiguren, O., Montalbán, I.A., Correia, S., Canhoto, J., and Moncaleán, P. (2016b). Different environmental conditions at initiation of radiata pine somatic embryogenesis determine the protein profile of somatic embryos. *Plant Biotech.* 33, 143-152.

García-Mendiguren, O., Montalbán, I.A., Goicoa, T., Ugarte, M.D., and Moncaleán, P. (2017). Are we able to modulate the response of somatic embryos of pines to drought stress?. *Acta Hortic.* 1155, 77-84.

Gautier, F., Label, P., Eliášová, K., Leplé, J.C., Motyka, V., Boizot, N., et al. (2019). Cytological, biochemical and molecular events of the embryogenic state in Douglas-fir (*Pseudotsuga menziesii* [Mirb.]). *Front. Plant Sci.* 10, 118.

Gimeno, T.E., Pas, B., Lemos-Filho, J.P., and Valladares, F. (2009). Plasticity and stress tolerance override local adaptation in the responses of Mediterranean holm oak seedlings to drought and cold. *Tree Physiol.* 29, 87-98.

Gosal, S.S., and Wani, S.H. (2018). "Cell and tissue culture approaches in relation to crop improvement" in Biotechnologies of Crop Improvement, eds. Gosal, S., Wani, S.H. (Springer, Cham, Switzerland), 1-15.

Grzyb, M., Kalandyk, A., Waligórski, P., and Mikuła, A. (2017). The content of endogenous hormones and sugars in the process of early somatic embryogenesis in the tree fern *Cyathea delgadii* Sternb. *Plant Cell. Tiss. Org.* 129, 387-397.

Jia, J., Zhou, J., Shi, W., Cao, X., Luo, J., Polle, A., et al. (2017). Comparative transcriptomic analysis reveals the roles of overlapping heat-/drought-responsive genes in poplars exposed to high temperature and drought. *Sci. Rep.* 7.

Johnsen, Ø., Fossdal, C.G., Nagy, N., MØlmann, J., Dæhlen, O.G., and SkrØppa, T. (2005). Climatic adaptation in *Picea abies* progenies is affected by the temperature during zygotic embryogenesis and seed maturation. *Plant, Cell Environ.* 28, 1090-1102.

Kang, N.Y., Cho, C., Kim, N.Y., and Kim, J. (2012). Cytokinin receptor-dependent and receptor-independent pathways in the dehydration response of *Arabidopsis thaliana*. *J. Plant Physiol.* 169, 1382-1391.

Kieber, J.J., and Schaller, G.E. (2018). Cytokinin signaling in plant development. *Development* 145, 1-7.

Kohli, A., Sreenivasulu, N., Lakshmanan, P., and Kumar, P.P. (2013). The phytohormone crosstalk paradigm takes center stage in understanding how plants respond to abiotic stresses. *Plant Cell Rep.* 32, 945-957.

Kvaalen, H., and Johnsen, Ø. (2008). Timing of bud set in *Picea abies* is regulated by a memory of temperature during zygotic and somatic embryogenesis. *New Phytol.* 177, 49-59.

Larkindale, J., and Knight, M.R. (2002). Protection against heat stress-induced oxidative damage in *Arabidopsis* involves calcium, abscisic acid, ethylene, and salicylic acid. *Plant Physiol*. 128, 682-695.

Le Gac, A.L., Lafon-Placette, C., Chauveau, D., Segura, V., Delaunay, A., Fichot, R., et al. (2018). Winter-dormant shoot apical meristem in poplar trees shows environmental epigenetic memory. *J. Exp. Bot.* 69, 4821-4837.

Lewinsohn, E., Gijzen, M., Muzika, R.M., Barton, K., and Croteau, R. (1993). Oleoresinosis in grand fir (*Abies grandis*) saplings and mature trees (modulation of this mound response by light and water stresses). *Plant Physiol.* 101, 1021-1028.

Liu, X., Huang, B., and Banowetz, G. (2002). Cytokinin effects on creeping bentgrass responses to heat stress: I. Shoot and root growth. *Crop Sci.* 42, 457-465.

Marias, D.E., Meinzer, F.C., Woodruff, D.R., and McCulloh, K.A. (2017). Thermotolerance and heat stress responses of Douglas-fir and ponderosa pine seedling populations from contrasting climates. *Tree Physiol.* 37, 301-315.

Mcdowell, N., Pockman, W.T., Allen, C.D., Breshears, D.D., Cobb, N., Kolb, T., et al. (2014). Mechanisms of plant survival and mortality during drought: Why do some plants survive while others succumb plants drought? *New Phytol.*178, 719-739.

Mitton, J.B., Grant, M.C., and Yoshino, A.M. (1998). Variation in allozymes and stomatal size in pinyon (*Pinus edulis*, *Pinaceae*), associated with soil moisture. *Am. J. Bot.* 85, 1262-1265.

Moncaleán, P., Cañal, M.J., Fernández, H., Fernández, B., and Rodríguez, A. (2003). Nutritional and gibberellic acid requirements in kiwifruit vitroponic cultures. *Vitr. Cell. Dev. Biol. - Plant* 39, 49-55.

Moncaleán, P., Alonso, P., Centeno, M.L., Cortizo, M., Rodríguez, A., Fernández, B., et al. (2005). Organogenic responses of *Pinus pinea* cotyledons to hormonal treatments: BA metabolism and cytokinin content. *Tree Physiology* 25, 1-9.

Moncaleán, P., Fernández, B., and Rodríguez, A. (2007). *Actinidia deliciosa* leaf stomatal characteristics in relation to benzyladenine incubation periods in micropropagated explants. *New Zeal. J. Crop Hort*. 35, 159-169.

Moncaleán, P., García-Mendiguren, O., Novák, O., Strnad, M., Goicoa, T., Ugarte, M.D., et al. (2018). Temperature and water availability during maturation affect the cytokinins and auxins profile of radiata pine somatic embryos. *Front. Plant Sci.* 9, 1-13.

Montalbán, I.A., De Diego, N., and Moncaleán, P. (2010). Bottlenecks in *Pinus radiata* somatic embryogenesis: Improving maturation and germination. *Trees - Struct. Funct.* 24, 1061-1071.

Montalbán, I.A., De Diego, N., and Moncaleán, P. (2011). Testing novel cytokinins for improved *in vitro* adventitious shoots formation and subsequent ex vitro performance in *Pinus radiata*. *Forestry* 84, 363-373.

Montalbán, I.A., de Diego, N., and Moncaleán, P. (2012). Enhancing initiation and proliferation in radiata pine (*Pinus radiata* D. Don) somatic embryogenesis through seed

family screening, zygotic embryo staging and media adjustments. *Acta Physiol. Plant.* 34, 451-460.

Montalbán, I.A., Novák, O., Rolčik, J., Strnad, M., and Moncaleán, P. (2013). Endogenous cytokinin and auxin profiles during *in vitro* organogenesis from vegetative buds of *Pinus radiata* adult trees. *Physiol. Plant.* 148, 214-231.

Montalbán, I.A., García-Mendiguren, O., Goicoa, T., Ugarte, M.D., and Moncaleán, P. (2015). Cold storage of initial plant material affects positively somatic embryogenesis in *Pinus radiata*. *New For.* 46, 309-317.

Montalbán, I.A., García-Mendiguren, O., and Moncaleán, P. (2016). "Somatic embryogenesis in *Pinus* spp." in *In vitro* embryogenesis in higher plants. Methods in molecular biology, eds. Germana, M., Lambardi, M. (Humana Press, New York), 405-415.

Montalbán, I.A., and Moncaleán, P. (2017). Long term conservation at -80ºC of *Pinus radiata* embryogenic cell lines: Recovery, maturation and germination. *Cryo-Letters* 38, 202-209.

Montalbán, I.A., and Moncaleán, P. (2018). Rooting of *Pinus radiata* somatic embryos: factors involved in the success of the process. *J. For. Res.*, 1-7.

Morel, A., Teyssier, C., Trontin, J.F., Eliášová, K., Pešek, B., Beaufour, M., et al. (2014). Early molecular events involved in *Pinus pinaster* Ait. somatic embryo development under reduced water availability: Transcriptomic and proteomic analyses. *Physiol. Plant.* 152, 184-201.

Muilu-Mäkelä, R., Vuosku, J., Hamberg, L., Latva-Mäenpää, H., Häggman, H., and Sarjala, T. (2015). Osmotic stress affects polyamine homeostasis and phenolic content in proembryogenic liquid cell cultures of Scots pine. *Plant Cell. Tiss. Org.* 122, 709-726.

Nishiyama, R., Watanabe, Y., Fujita, Y., Le, D.T., Kojima, M., Werner, T., et al. (2011). Analysis of cytokinin mutants and regulation of cytokinin metabolic genes reveals important regulatory roles of cytokinins in drought, salt and abscisic acid responses, and abscisic acid biosynthesis. *Plant Cell* 23, 2169-2183.

O'Brien, J.A., and Benková, E. (2013). Cytokinin cross-talking during biotic and abiotic stress responses. *Front. Plant Sci.* 4.

Ochatt, S.J. (2017). The role of stress on unravelling of somatic embryogenesis competence. *Acta Hortic*. 1155, 1-14.

Park, Y.S. (2002). Implementation of conifer somatic embryogenesis in clonal forestry: technical requirements and deployment considerations. *Ann. For. Sci.* 59, 651–656.

Pascual, J., Cañal, M.J., Correia, B., Escandón, M., Hasbún, R., Meijón, M., et al. (2014). "Can epigenetics help forest plants to adapt to climate change?" in Epigenetics in Plants of Agronomic Importance: Fundamentals and Applications (Springer, Cham, Switzerland), 125-146.

Pavlů, J., Novák, J., Koukalová, V., Luklová, M., Brzobohatý, B., and Černý, M. (2018). Cytokinin at the crossroads of abiotic stress signalling pathways. *Int. J. Mol. Sci.* 19, 1-36.

Pereira, C., Montalbán, I.A., García-Mendiguren, O., Goicoa, T., Ugarte, M.D., Correia, S., et al. (2016). *Pinus halepensis* somatic embryogenesis is affected by the physical and chemical conditions at the initial stages of the process. *J. For. Res.* 21, 143-150.

Pereira, C., Montalbán, I.A., Goicoa, T., Ugarte, M.D., Correia, S., Canhoto, J.M., et al. (2017). The effect of changing temperature and agar concentration at proliferation stage in the final success of Aleppo pine somatic embryogenesis. *For. Syst.* 26, 1-4.

Pescador, R., Kerbauy, G.B., de Ferreira, W.M., Purgatto, E., Suzuki, R.M., and Guerra, M.P. (2012). A hormonal misunderstanding in *Acca sellowiana* embryogenesis: Levels of zygotic embryogenesis do not match those of somatic embryogenesis. *Plant Growth Regul.* 68, 67-76.

Ramireddy, E., Hosseini, S.A., Eggert, K., Gillandt, S., Gnad, H., von Wirén, N., et al. (2018). Root engineering in barley: Increasing cytokinin degradation produces a larger root system, mineral enrichment in the shoot and improved drought tolerance. *Plant Physiol.* 177, 1078-1095.

Reza, S.H., Delhomme, N., Street, N.R., Ramachandran, P., Dalman, K., Nilsson, O., et al. (2018). Transcriptome analysis of embryonic domains in Norway spruce reveals potential regulators of suspensor cell death. *PLoS One* 13, 1-19.

Rittenberg, D., and Foster, L. (1940). A new procedure for quantitative analysis by isotope dilution, with application to the determination of amino acids and fatty acids. *J. Biol. Chem.* 133, 727-744

Rubio, M.C., Minchin, F.R., Webb, K.J., Arrese-Igor, C., Ramos, J., González, E.M., et al. (2002). Effects of water stress on antioxidant enzymes of leaves and nodules of transgenic alfalfa overexpressing superoxide dismutases. *Physiol. Plant.* 115, 531-540.

Sage, R.F., and Kubien, D.S. (2007). The temperature response of C3 and C4 photosynthesis. *Plant, Cell Environ.* 30, 1086-1106.

Sangwan, V., Örvar, B.L., Beyerly, J., Hirt, H., and Dhindsa Rajinder, S. (2002). Opposite changes in membrane fluidity mimic cold and heat stress activation of distinct plant MAP kinase pathways. *Plant J.* 31, 629-638.

Santa-Catarina, C., Silveira, V., Guerra, M.P., Steiner, N., Ferreira Macedo, A., Iochevet Segal Floh, E., and Wendt Dos Santos, A.L. (2012). The use of somatic embryogenesis for mass clonal propagation and biochemical and physiological studies in woody plants. *Curr. Top. Plant Biol*. 13, 103-119.

Scholander, P.F., Hammel, H.T., Bradstreet, E.D., and Hemmingsen, E.A. (1965). Sap pressure in vascular plants. *Science* 148, 339-346.

Shashidhar, V.R., Prasad, T.G., and Sudharshan, L. (1996). Hormone signals from roots to shoots of sunflower (*Helianthus annuus* L.). Moderate soil drying increases delivery of abscisic acid and depresses delivery of cytokinins in xylem sap. *Ann. Bot.* 78, 151-155.

Shinozaki, K., Yamaguchi-Shinozaki, K., and Seki, M. (2003). Regulatory network of gene expression in the drought and cold stress responses. *Curr. Opin. Plant Biol.* 6, 410-417.

Skalák, J., Cerný, M., Jedelský, P., Dobrá, J., Ge, E., Novák, J., et al. (2016). Stimulation of *ipt* overexpression as a tool to elucidate the role of cytokinins in high temperature responses of *Arabidopsis thaliana*. *J. Exp. Bot.* 67, 2861-2873.

Svačinová, J., Novák, O., Plačková, L., Lenobel, R., Holík, J., Strnad, M., et al. (2012). A new approach for cytokinin isolation from *Arabidopsis* tissues using miniaturized purification: pipette tip solid-phase extraction. *Plant Methods* 8, 1-14.

Tomaž, R., and Marina, D. (2010). Cytokinins and their function in developing seeds. *Acta Chim. Slov.* 57, 617-629.

Turtola, S., Manninen, AM., Rikala, R., and Kainulainen, P. (2003). Drought stress alters the concentration of wood terpenoids in scots pine and Norway spruce seedlings. *J. Chem. Ecol.* 29, 1981.

Vacca, R.A., Pinto, M.C.D., Valenti, D., Passarella, S., Marra, E., and Gara, L.D. (2004). Production of reactive oxygen species, alteration of cytosolic ascorbate peroxidase, and impairment of mitochondrial metabolism are early events in heat shock-induced programmed cell death in Tobacco Bright-Yellow 2 Cells. *Plant Physiol.* 134, 1100-1112.

Villar-Salvador, P., Planelles, R., Oliet, J., Peñuelas-Rubira, J.L., Jacobs, D.F., and González, M. (2004). Drought tolerance and transplanting performance of holm oak (*Quercus ilex*) seedlings after drought hardening in the nursery. *Tree Physiol.* 24, 1147-1155.

Vondrakova, Z., Dobrev, P.I., Pesek, B., Fischerova, L., Vagner, M., and Motyka, V. (2018). Profiles of endogenous phytohormones over the course of Norway spruce somatic embryogenesis. *Front. Plant Sci.* 9, 1-13.

Wahid, A., Gelani, S., Ashraf, M., and Foolad, M.R. (2007). Heat tolerance in plants: An overview. *Environ. Exp. Bot.* 61, 199-223.

Walter, C., Find, J.I., and Grace, L.J. (2005). "Somatic embryogenesis and genetic transformation in *Pinus radiata*" in Protocols for somatic embryogenesis in woody plants, eds. Jain, S.M., Gupta, P.K. (Springer, Dordrecht), 491-504.

Wang, W., Vinocur, B., and Altman, A. (2003). Plant responses to drought, salinity and extreme temperatures: Towards genetic engineering for stress tolerance. *Planta* 218, 1-14.

Wani, S.H., Kumar, V., Shriram, V., and Sah, S.K. (2016). Phytohormones and their metabolic engineering for abiotic stress tolerance in crop plants. *Crop J.* 4, 162-176.

Way, D.A., and Oren, R. (2010). Differential responses to changes in growth temperature between trees from different functional groups and biomes: a review and synthesis of data. *Tree Physiol.* 30, 669-688.

Webber, J., Ott, P., Owens, J., and Binder, W. (2005). Elevated temperature during reproductive development affects cone traits and progeny performance in *Picea glauca x engelmannii* complex. *Tree Physiol.* 25, 1219-1227.

Xia, X., Zhou, Y., Shi, K., Zhou, J., Foyer, C.H., and Yu, J. (2015). Interplay between reactive oxygen species and hormones in the control of plant development and stress tolerance. *J. Exp. Bot.* 66, 2839-2856.

Yakovlev, I.A., Fossdal, C.G., and Johnsen, Ø. (2010). MicroRNAs, the epigenetic memory and climatic adaptation in Norway spruce. *New Phytol.* 187, 1154-1169.

Yakovlev, I.A., Asante, D.K.A., Fossdal, C.G., Junttila, O., and Johnsen, T. (2011). Differential gene expression related to an epigenetic memory affecting climatic adaptation in Norway spruce. *Plant Sci.* 180, 132-139.

Zas, R., Cendán, C., and Sampedro, L. (2013). Mediation of seed provisioning in the transmission of environmental maternal effects in Maritime pine (*Pinus pinaster* Aiton). *Heredity* 111, 248-255.

Zeng, F., Zhang, X., Jin, S., Cheng, L., Liang, S., Hu, L., et al. (2007). Chromatin reorganization and endogenous auxin/cytokinin dynamic activity during somatic embryogenesis of cultured cotton cell. *Plant Cell. Tiss. Org.* 90, 63-70.

Zhang, H., Horgan, K.J., Reynolds, P.H.S., and Jameson, P.E. (2003). Cytokinins and bud morphology in *Pinus radiata*. *Physiol. Plant.* 117, 264-269.

Zhou, X., Zheng, R., Liu, G., Xu, Y., Zhou, Y., Laux, T., et al. (2017). Desiccation treatment and endogenous IAA levels are key factors influencing high frequency somatic embryogenesis in *Cunninghamia lanceolata* (Lamb.) hook. *Front. Plant Sci.* 8, 1-15.

CHAPTER 3

Quantification of endogenous aromatic cytokinins in *Pinus radiata* embryonal masses after application of heat stress during initiation of somatic embryogenesis

---

The content of this chapter corresponds to the published article "Castander-Olarieta, A., Pereira, C., Montalbán, I.A., Pěnčík, A., Petřík, I., Pavlović, I., Novák, O., Strnad, M, Moncaleán, P. (2020). Quantification of endogenous aromatic cytokinins in *Pinus radiata* embryonal masses after application of heat stress during initiation of somatic embryogenesis. *Trees – Structure & Function*".

1. INTRODUCTION

Cytokinins (CK) are one of the most important phytohormone groups controlling cell division, proliferation and differentiation in plants, and they are considered master regulators during plant growth and development (Wani et al., 2016). Despite not being traditionally classified as "stress-hormones", research carried out during the last decades has highlighted the importance of CK during numerous stress response, adaptation (Bielach et al., 2017) and hardening processes (De Diego et al., 2015).

Among abiotic stresses, drought and heat represent probably some of the most common constraints for plants. Apart of the widely studied function of CK during drought, CK may also take part in temperature sensing and heat signalling in *Arabidopsis* (Černý et al., 2014). They enhance heat stress tolerance (Prerostova et al., 2020) and recovery (Escandón et al., 2016), they regulate photosynthesis and the antioxidant and osmotic defence against heat in tobacco (Dobra et al., 2010; Lubovská et al., 2014) and could potentially be involved in long term physiological responses against heat in somatic embryogenesis (SE) of radiata pine (Moncaleán et al., 2018; Castander-Olarieta et al., 2020).

However, most of those experiments were centred on the study of isoprenoid CK. Little information is available about the role of endogenous aromatic CK in stress events. Natural aromatic CK are mainly constituted by N^6-benzyladenine (BA), kinetin (K), *meta*-Topolin (mT), *ortho*-Topolin (oT) and their derivatives, and differ both in terms of chemical structure and biological activity from their isoprenoid counterparts (Strnad, 1997). There are several reports suggesting that some aromatic CK such as kinetin (K) could mitigate heat and salinity stress (Chhabra et al., 2009; Ahanger et al., 2020), but most of the studies have evaluated their effect via external application, without their endogenous determination.

Therefore, in this study we have tried to elucidate if endogenous aromatic CK could be involved in heat stress responses in radiata pine. To this purpose, we have employed SE,

a useful biotechnological approach which has long been applied as a model to study different developmental and biochemical processes in plants.

2. MATERIALS AND METHODS

The selection of plant material and the hormone analysis followed the procedure described in Castander-Olarieta et al. (2020). Briefly, green cones collected from 4 genetically different open pollinated trees were surface-sterilized with 70% (v/v) ethanol, split into quarters and all the seeds were extracted and surface sterilized following Montalbán et al. (2012). Seed coats were removed and intact megagametophytes were excised out aseptically and placed horizontally onto EDM initiation medium (Walter et al., 2005) supplemented with 3.5 gL^{-1} gellan gum (Gelrite ®; Duchefa). At this point, the megagametophytes enclosing immature zygotic embryos were subjected to different temperature and incubation times based on results from previous studies (Moncaleán et al., 2018; Castander-Olarieta et al., 2019, 2020): 23°C (8 weeks, control), 40°C (4 h), 50°C (30 min) and 60°C (5 min). The culture medium was pre-warmed for 30 minutes before the start of the incubation period and at the end all the megagametophytes were kept at 23°C in darkness. Emerging embryonal masses (EM) were subcultured fortnightly to proliferation medium (same composition as initiation medium but 4.5 gL^{-1} gellan gum), and after 5 subculture periods, vigorously proliferating EM were frozen in liquid nitrogen and stored at -80°C until aromatic CK analysis.

Extraction, purification and quantification of endogenous aromatic CK was carried out from three established cell lines (ECL) per induction treatment, comprising a total of 12 different samples. The following 20 aromatic CK types were analysed: BA, N^6-benzyladenosine (BAR), N^6-benzyladenosine-5'monophosphate (BARMP), N^6-benzyladenine-7-glucoside (BA7G), N^6-benzyladenine-9-glucoside (BA9G), oT, *ortho*-Topolin riboside (oTR), *ortho*-Topolin-7-glucoside (oT7G), *ortho*-Topolin-9-glucoside (oT9G), mT, *meta*-Topolin riboside (mTR), *meta*-Topolin-7-glucoside (mT7G), *meta*-Topolin-9-glucoside (mT9G), *para*-Topolin (pT), *para*-Topolin riboside (pTR), *para*-

Topolin-7-glucoside (pT7G), *para*-Topolin-9-glucoside (pT9G), K, kinetin riboside (KR) and kinetin-9-glucoside (K9G).

Two replicates of 10 mg from each ECL were analysed following a slightly modified protocol described by Svačinová et al. (2012) using miniaturized purification (pipette tip solid-phase extraction). Samples were extracted in 1 ml of modified Bieleski with the addition of stable isotope-labelled internal standards (0.2 pmol for bases, ribosides and N9- and N7-glucosides; 0.5 pmol for CK nucleotides). After extraction, from each sample three technical replicates of 300 µl were transferred onto Stage Tips and purified using C18, SDB-RPS, and Cation-SR sorbents (Empore™). Eluates were evaporated to dryness and dissolved in 30 µl of mobile phase.

Mass analysis was carried out using an Acquity UPLC® System (Waters, Milford, MA, United States), and a triple-quadrupole mass spectrometer Xevo™ TQ-S MS (Waters MS Technologies, Manchester, United Kingdom). All mass spectrometry data were processed using the MassLynxTM software with TargetLynx™ program (version 4.2. Waters, Milford, MA, United States) and compounds were quantified by standard isotope dilution analysis.

The results from the hormone quantification were analysed using ANOVA. Tukey´s post-hoc test ($\alpha = 0.05$) was used for multiple comparisons. When required, the ECL was included in the model as a random effect to improve the fit and analyse the effect of treatments more accurately. When the analysis of variance did not fulfil the normality hypothesis a Kruskal-Wallis test was performed.

3. RESULTS AND DISCUSSION

Some ribosides (oTR, KR) and most of the N-glucosides (oT7G, oT9G, mT7G, mT9G, pT7G, pT9G, K9G) were under limit of detection. In contrast, the levels of BA were exceptionally high (Table 1). This fact reflected the presence of BA in the proliferation medium. Interestingly, the levels of K were relatively high (the third most abundant CK type), which correlates with recent research that highlights the role of K as an anti-

stress agent and inducer of programmed cell death (Żur et al., 2015). In fact, *in vitro* culture represents an unusual combination of stress factors, and programmed cell is an integral component of SE (Castander-Olarieta et al., 2019)

Although aromatic CK are likely to be present in many plant species and hydroxylated forms of BA occur naturally, in conifers they have only been detected in tissues cultivated in media containing BA (Cuesta et al., 2012; Montalbán et al., 2013). Particularly, during SE, despite the high concentration of aromatic CK during proliferation, no aromatic CK could be detected in BA-independent phases (Moncaleán et al., 2018; Vondrakova et al., 2019). These results suggest that the occurrence of aromatic CK has a strong dependency on exogenous BA, or it could be associated with early stages of SE.

Table 1. Endogenous aromatic cytokinins (pmol g^{-1} FW) in *P. radiata* EM initiated under different induction treatments (23°C, 8 weeks; 40°C, 4 h; 50°C, 30 min; 60°C, 5 min), followed by cultivation at control temperature of 23°C. Three ECLs per treatment, 2 replicates per ECL and 3 technical replicates per sample were used. Data are presented as mean values ± SE. Significant differences within a row at $p < 0.05$ are indicated by different letters.

Cytokinins (pmol/g FW)	Induction treatment (°C)			
	23	40	50	60
BA	285.25 ± 12.77^{a}	187.93 ± 18.5^{b}	122.71 ± 11.14^{c}	181.27 ± 14.39^{b}
BAR	1.13 ± 0.17^{ab}	2.37 ± 0.41^{a}	1.01 ± 0.06^{b}	1.1 ± 0.12^{b}
BARMP	3.86 ± 0.56^{b}	18.89 ± 4.82^{a}	5.87 ± 0.28^{ab}	6.91 ±1.2^{ab}
BA7G	0.011 ± 0.007^{a}	0.01 ± 0.002^{a}	0.007 ± 0.001^{b}	0.007 ± 0.001^{b}
BA9G	0.21 ± 0.03^{b}	0.69 ± 0.1^{a}	0.1 ± 0.023^{b}	0.14 ± 0.021^{b}
oT	0.26 ± 0.013^{a}	0.11 ± 0.007^{c}	0.09 ± 0.01^{c}	0.22 ± 0.034^{b}
mT	0.24 ± 0.022^{a}	0.23 ± 0.015^{a}	0.33 ± 0.1^{a}	0.27 ± 0.021^{a}
mTR	0.027 ± 0.002^{a}	0.029 ± 0.002^{a}	0.03 ± 0.003^{a}	0.03 ± 0.002^{a}
pT	0.075 ± 0.01^{b}	0.054 ± 0.008^{c}	0.05 ± 0.002^{c}	0.093 ± 0.011^{a}
pTR	0.023 ± 0.003^{b}	0.03 ± 0.003^{a}	0.019 ± 0.002^{b}	0.025 ± 0.003^{ab}
K	2.19 ± 0.26^{a}	2.16 ± 0.27^{a}	1.795 ± 0.3^{a}	2.86 ± 0.3^{a}

In the case of BA, the two N-glucoside forms could be detected. However, the amount of BA9G was between one and two orders of magnitude bigger than the amount of BA7G

(Table 1), suggesting that 9-glycosilation is the favoured deactivation pathway in *P. radiata,* as already observed in previous studies (Montalbán et al., 2013).

Despite this, the levels of N-glucosides were very low or no detectable for most of the CK types, which is consistent with previous studies in conifers (Vondrakova et al., 2018; Gautier et al., 2019; Castander-Olarieta et al., 2020). These data confirm that the CK N-glucosyltransferase pathway is almost insignificant during SE or not necessary under the described conditions, since an enhancement of N-glycosylation has been reported as a detoxification mechanism when plants are exposed to supra-optimal CK concentrations (Montalbán et al., 2013).

In line with this idea, the total levels of oT and pT where lower than those of mT (Table 1). Montalbán et al. (2013) observed that hydroxylation of BA at the *ortho*- and the *para*-position rather than in the *meta*-position could also serve as a regulation mechanism by the reduction of CK activity.

Analysing the results by functional groups, the most abundant forms were bases (active forms) in all aromatic CK detected, followed by ribosides (Table 1; Figure 1). In the case of BA, the concentration of bases was considerably higher than the rest of forms, indicating that the BA taken up by the embryogenic culture is metabolically quite stable, as already observed in SE of other conifer species (Gautier et al., 2019). Nonetheless, all the other functional groups could also be detected, being the precursors (BARMP) the second most abundant, in contrast to EM of Douglas-fir, where BAR was more abundant than BARMP (Gautier et al., 2019).

Considering the effect of temperature on the amount of aromatic CK, a significant decreasing tendency was observed for some free bases (BA, oT, pT), especially in EM originating from high temperatures and long exposures (40°C, 4 h; 50°C, 30 min) (Table 1, Figure 1). Fluctuating and slightly reduced aromatic CK contents were also reported in thermo-inhibited *Tagetes minuta* achenes (Stirk et al., 2012), and other stresses such as drought have also been demonstrated to reduce the endogenous content of some aromatic CK (Ghafari et al., 2020).

This tendency was also observed for some isoprenoid bases in EM of *P. radiata* generated under the same conditions in Castander-Olarieta et al. (2020) and coincides with the initiation and proliferation rates observed during SE in Castander-Olarieta et al. (2019). The highest levels of BA, which have been detected under induction treatment of 23°C (285.25 ± 12.77 pmol g^{-1} FW) seem to correlate with the high proliferation rates (%10.6 ± 2.121) observed under the same treatment in the above-mentioned study, while the lowest BA contents in 50°C treatment (122.71 ± 11.14 pmol g^{-1} FW) correlate with the lowest proliferation rates (%4.1 ± 1.26) observed under the same treatment. Both proliferation rates and BA levels for 40°C and 60°C treatments showed intermediate values. High levels of active free bases are known to be essential during cell proliferation (Moncaleán et al., 2005), and under certain stress conditions an increase of BA can trigger the synthesis of some osmoprotectants (Alvarez et al., 2008), whose function during stress has widely been documented (De Diego et al., 2015).

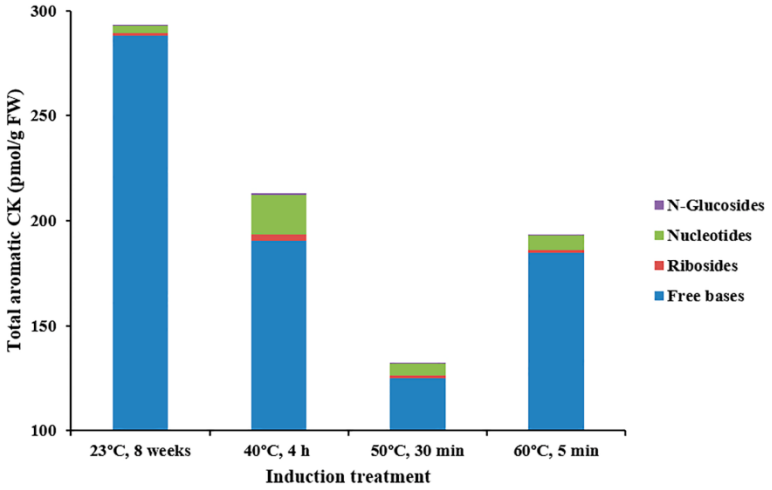

Figure 1. Concentration of total aromatic CK in EM of *P. radiata* originated from different temperature and incubation periods (23°C, 8 weeks; 40°C, 4h; 50°C, 30 min; 60°C, 5 min). The following aromatic CK derivatives were detected: free bases (BA, oT, mT, pT and K), ribosides (BAR, mTR, pTR), nucleotides (BAR5MP), and *N*-glucosides (BA7G, BA9G).

Although oT and pT are considered aromatic CK with low biological activity (Strnad, 1997), there is increasing evidence that they could be involved in different cellular and

biochemical processes, i.e. induction of cell differentiation and apoptosis in mammals (Ishii et al., 2003; Casati et al., 2011; Wang et al., 2019). The differences observed under high temperatures in this experiment support this idea (Table 1).

In parallel, 40°C treatment increased the levels of BAR, pTR, BARMP and BA9G (Table 1, Figure 1). An enhancement of the main deactivation pathway (BA9G) could correlate with the lower amounts of active BA bases observed at 40°C. Surprisingly, this effect was not observed under 50°C and 60°C treatments. A simultaneous increase in BARMP could seem quite contradictory because of its precursor nature. However, as reported in Moncaleán et al. (2005), BARMP plays a key role in BA homeostasis, and its accumulation could be the result of BA imbalances under stress. In fact, despite being not significant, the levels of BARMP were also increased in 50°C and 60°C treatments (Table 1; Figure 1). In any case, high levels of nucleotides and ribosides in expense of free bases have been related with low rates of cell proliferation and organogenic capacity in some pine species (Cuesta et al., 2012), which could also contribute to the low proliferation of EM observed in Castander-Olarieta et al. (2019) under high temperatures.

4. CONCLUSIONS

This study provides novel information about the possible involvement of endogenous aromatic CK during both SE and heat stress responses. The presence of aromatic CK during SE in radiata pine seems to be exogenous BA-dependent, or at least more relevant during early stages of SE. As SE in radiata pine can only be induced in the presence of exogenous BA, a choice of another conifer species that does not require any cytokinin for SE induction would be preferable for such a study to confirm the results obtained. Despite this fact, endogenous aromatic CK appear to be highly influenced by the temperature during induction and could strongly influence the success of the process, reinforcing their function as stress-mediators. Further research is required to confirm their activity in different plant species and developmental stages.

5. REFERENCES

Ahanger, M.A., Mir, R.A., Alyemeni, M.N., and Ahmad, P. (2020). Combined effects of brassinosteroid and kinetin mitigates salinity stress in tomato through the modulation of antioxidant and osmolyte metabolism. *Plant Physio.l Biochem*. 147, 31-42.

Alvarez, S., Marsh, E.L., Schroeder, S.G., and Schachtman, D.P. (2008). Metabolomic and proteomic changes in the xylem sap of maize under drought. *Plant Cell Environ.* 31, 325-340.

Bielach, A., Hrtyan, M., and Tognetti, V.B. (2017). Plants under stress: Involvement of auxin and cytokinin. *Int. J. Mol. Sci.* 18, 1427.

Casati, S., Ottria, R., Baldoli, E., Lopez, E., Maier, J.A.M., and Ciuffreda, P. (2011). Effects of cytokinins, cytokinin ribosides and their analogs on the viability of normal and neoplastic human cells. *Anticancer Res.* 31, 3401-3406.

Castander-Olarieta, A., Montalbán, I.A., De Medeiros Oliveira, E., Dell'Aversana, E., D'Amelia, L., Carillo, P., et al. (2019). Effect of thermal stress on tissue ultrastructure and metabolite profiles during initiation of radiata pine somatic embryogenesis. *Front. Plant Sci.* 9, 1-16.

Castander-Olarieta, A., Moncaleán, P., Pereira, C., Pěnčík, A., Petřík, I., Pavlović, I., et al. (2020) Cytokinins are involved in drought tolerance of *Pinus radiata* plants originating from embryonal masses induced at high temperatures. *Tree Physiol.* 1-15.

Černý, M., Jedelský, P.L., Novák, J., Schlosser, A., and Brzobohatý, B. (2014) Cytokinin modulates proteomic, transcriptomic and growth responses to temperature shocks in *Arabidopsis*. *Plant Cell Environ.* 37, 1641-1655.

Chhabra, M.L., Dhawan, A., Sangwan, N., Dhawan, K., and Singh, D. Phytohormones induced amelioration of high temperature stress in *Brassica juncea* (L.). Czern and Coss, Proceedings of 16th Australian Research Assembly on Brassicans, Ballarat, Australia, 10-14 September, 2009.

Cuesta, C., Novák, O., Ordás, R.J., Fernández, B., Strnad, M., Doležal, K., et al. (2012). Endogenous cytokinin profiles and their relationships to between-family differences

during adventitious caulogenesis in *Pinus pinea* cotyledons. *J. Plant Physiol.* 169, 1830-1837.

De Diego, N., Saiz-Fernández, I., Rodríguez, J.L., Pérez-Alfocea, P., Sampedro, M.C., Barrio, R.J., et al. (2015). Metabolites and hormones are involved in the intraspecific variability of drought hardening in radiata pine. *J. Plant Physiol.* 188, 64-71.

Dobra, J., Motyka, V., Dobrev, P., Malbeck, J., Prasil, I.T., Haisel., D., et al. (2010). Comparison of hormonal responses to heat, drought and combined stress in tobacco plants with elevated proline content. *J. Plant Physiol.* 167, 1360-1370.

Escandón, M., Cañal, M.J., Pascual, J., Pinto, G., Correia, B., Amaral, J., et al. (2016). Integrated physiological and hormonal profile of heat-induced thermotolerance in *Pinus radiata*. *Tree Physiol.* 36, 63-77.

Gautier, F., Label, P., Eliášová, K., Leplé, J.C., Motyka, V., Boizot, N., et al. (2019). Cytological, biochemical and molecular events of the embryogenic state in Douglas-fir (*Pseudotsuga menziesii* [Mirb.]). *Front. Plant Sci.* 10, 118.

Ghafari, H., Hassanpour, H., Jafari, M., and Besharat, S. (2020). Physiological, biochemical and gene-expressional responses to water deficit in apple subjected to partial root-zone drying (PRD). *Plant Physiol. Biochem.* 148, 333-346.

Ishii, Y., Sakai, S., and Honma, Y. (2003). Cytokinin-induced differentiation of human myeloid leukemia HL-60 cells is associated with the formation of nucleotides, but not with incorporation into DNA or RNA. *Biochim. Biophys. Acta* 1643, 11-24.

Lubovská, Z., Dobrá, J., Štorchová, H., Wilhelmová, N., and Vanková, R. (2014). Cytokinin oxidase/dehydrogenase overexpression modifies antioxidant defense against heat, drought and their combination in *Nicotiana tabacum* plants. *J. Plant Physiol.* 171, 1625-1633.

Moncaleán, P., Alonso, P., Centeno, M.L., Cortizo, M., Rodríguez, A., Fernández, B., et al. (2005). Organogenic responses of *Pinus pinea* cotyledons to hormonal treatments: BA metabolism and cytokinin content. *Tree Physiol.* 25, 1-9.

Moncaleán, P., García-Mendiguren, O., Novák, O., Strnad, M., Goicoa, T., Ugarte, M.D., et al. (2018). Temperature and water availability during maturation affect the cytokinins and auxins profile of radiata pine somatic embryos. *Front. Plant Sci.* 9, 1-13.

Montalbán, I.A., De Diego, N., and Moncaleán, .P (2012). Enhancing initiation and proliferation in radiata pine (*Pinus radiata* D. Don) somatic embryogenesis through seed family screening, zygotic embryo staging and media adjustments. *Acta Physiol. Plant.* 34, 451-460.

Montalbán, I.A., Novák, O., Rolčik, J., Strnad, M., and Moncaleán, P. (2013). Endogenous cytokinin and auxin profiles during in vitro organogenesis from vegetative buds of *Pinus radiata* adult trees. *Physiol. Plant.* 148, 214-231.

Prerostova, S., Dobrev, P.I., Kramna, B., Gaudinova, A., Knirsch, V., Spichal, L., et al. (2020). Heat acclimation and inhibition of cytokinin degradation positively affect heat stress tolerance of *Arabidopsis*. *Front. Plant Sci.* 11, 1-14.

Stirk, W.A., Novák, O., Žižková, E., Motyka, V., Strnad, M., and Van Staden, J. (2012). Comparison of endogenous cytokinins and cytokinin oxidase/dehydrogenase activity in germinating and thermoinhibited *Tagetes minuta* achenes. *J. Plant Physiol.* 169, 696-703.

Strnad, M. (1997). The aromatic cytokinins. *Physiol. Plant.* 101, 674-688.

Svačinová, J., Novák, O., Plačková, L., Lenobel, R., Holík, J., Strnad, M., et al. (2012). A new approach for cytokinin isolation from *Arabidopsis* tissues using miniaturized purification: pipette tip solid-phase extraction. *Plant Methods* 8, 1-14.

Vondrakova, Z., Dobrev, P.I., Pesek, B., Fischerova, L., Vagner, M., and Motyka, V. (2018). Profiles of endogenous phytohormones over the course of Norway spruce somatic embryogenesis. *Front. Plant Sci.* 9, 1-13.

Walter, C., Find, J.I., and Grace, L.J. (2005). "Somatic embryogenesis and genetic transformation in *Pinus radiata*" in Protocols for somatic embryogenesis in woody plants, eds. Jain, S.M., Gupta, P.K. (Springer, Dordrecht), 491-504.

Wang, L., Cheng, J., Lin, F., Liu, S.X., Pan, H., Li, M., et al. (2019). Ortho-topolin riboside induced differentiation through inhibition of STAT3 signaling in acute myeloid leukemia HL-60 cells. *Turkish J. Hematol.* 36, 162-168.

Wani, S.H., Kumar, V., Shriram, V., and Sah, S.K. (2016). Phytohormones and their metabolic engineering for abiotic stress tolerance in crop plants. *Crop J.* 4, 162-176.

Żur, I., Dubas, E., Krzewska, M., Waligórski, P., Dziurka, M., and Janowiak, F. (2015). Hormonal requirements for effective induction of microspore embryogenesis in triticale (× *Triticosecale* Wittm.) anther cultures. *Plant Cell Rep.* 34, 47-62.

CHAPTER 4

Proteome-wide analysis of heat-stress in *Pinus radiata* somatic embryos reveals a combined response of sugar metabolism and translational regulation mechanisms

---

The content of this chapter is under review in the journal "*Frontiers in Plant Science*"

1. INTRODUCTION

As sessile organisms, plants are continuously exposed to a great number of external stimuli and fluctuating stress factors, which are becoming progressively more common due to the on-going climate change situation. Derived from the current global warming trend, heat and drought are becoming a growing concern, as they provoke adverse effects on plant growth and development, significantly determining not only crop productivity but also the viability and survival of both natural ecosystems and planted forests (Allen et al., 2010, Shen et al., 2015).

Specifically, heat is responsible for alterations in membrane structures, DNA/RNA stability and cytoskeleton dynamics (Hasanuzzaman et al., 2013, Niu et al., 2018); heat disturbs primary metabolic pathways, leading to internal metabolic imbalances, which in turn can cause the accumulation of toxic reactive oxygen species (ROS). Changes in the redox homeostasis can result in protein denaturation and aggregation, altering the activity of essential enzymes (Paciolla et al., 2016).

In this regard, plants have evolved to rapidly detect and respond to all those factors by modifications and readjustments of the complex molecular machinery. The molecules forming this sophisticated network involve a great variety of metabolites, such as hormones, enzymes and other types of proteins (De Diego et al., 2012, 2013a, 2013b, 2015, Escandón et al., 2017, Taïbi et al., 2017). Besides, recent research has demonstrated that plants can store information from stressful conditions and respond in a more efficient way to future environmental constraints (Turgut-Kara et al., 2020). This "memory" is mediated by epigenetic mechanisms, which involve, among others, sustained alterations in gene expression, coupled with changes in hormonal profiles and accumulation of numerous signalling proteins and transcription factors (Galviz et al., 2020). In this sense, integration of "omics" approaches, which include epigenomics, transcriptomics, proteomics and metabolomics, may contribute to a better understanding of plant memory (Fleta-Soriano & Munné-Bosch, 2016).

Proteomics, which provides the missing link between the genome/transcriptome and the metabolome, allows the identification and quantification of stress-tolerance associated proteins and can be applied as a very useful tool to study stress tolerance in plants (Pinheiro et al., 2014). In the same way, the identification of stress-related proteins gives the possibility to use protein markers to improve selection of elite genotypes with high levels of tolerance to stress, conferring fitness advantages in a climate change scenario (Lippert et al., 2005).

Despite the fact that the diversity of proteins present in a cell is considerably smaller than the number of transcripts, and the methodological limitations traditionally encountered in proteomics for non-model species, this approach presents numerous advantages if compared to transcriptomics. Proteomics gives a more connected understanding of the phenotype because most biological functions in a cell are executed by proteins rather than by mRNAs, and changes in transcriptome are not always correlated with changes in the abundance of the corresponding protein species (Correia et al., 2016). Proteomics provides important information regarding post-transcriptional and post-translational regulation mechanisms and other factors such as mRNA localization and transport, translation rates, transcript and protein stability, and intercellular protein trafficking (Wang et al., 2013, Passamani et al., 2017). Besides, proteomic studies are very useful when working with non-model plant species because protein sequences are more conserved and allow their identification by comparison with orthologous proteins (García-Mendiguren et al., 2016a).

As a result, proteomics has become a necessary and complementary approach in the post-genomic era, and in recent years, high-throughput techniques have facilitated the study of proteomic responses in several plant species to many different abiotic stresses including cold (Yuan et al., 2019), heat (Escandón et al., 2017), drought (Taïbi et al., 2017), salinity (Passamani et al., 2017) or UV light (Pascual et al., 2017). Several studies in different plant species have identified some protein groups related to heat-stress responses, which include antioxidative enzymes, heat shock proteins (HSPs), proteins related to energy and carbohydrate metabolism, redox homeostasis, protein synthesis

and degradation, signal transduction and transcription factors (Escandón et al., 2017, Parankusam et al., 2017). The latest reports have also highlighted the importance of some nuclear proteins such as histones, methyl cycle enzymes or spliceosome elements during thermopriming and epigenetic-driven regulatory mechanisms (Lamelas et al., 2020).

Bearing all this information in mind and the hypothesis that somatic embryogenesis (SE) is a crucial process to establish an epigenetic memory and modulate the behaviour of somatic embryo-derived plants, as postulated by several authors (Kvaalen & Johnsen 2008, García-Mendiguren et al., 2017), in this work we have tried to combine both techniques, SE and proteomics, to study if the application of heat-stress during initial phases of SE in radiata pine (*Pinus radiata* D.Don) could determine the protein profile of somatic embryos (Se's) months later. This approach could give us useful information about the molecular mechanism underpinning stress responses during embryo formation, and shed light on how stress tolerance is built and maintained during the embryogenic process.

In previous studies we have reported that high temperatures can determine the morphology of embryonal masses (EMs) and Se's in *P. radiata* and *P. halepensis*, as well as their hormonal and metabolic profiles (Castander-Olarieta et al., 2019, 2020a, 2020b, Moncaleán et al., 2018, Pereira et al., 2020). Besides, those initial culture conditions can have long-lasting effects, modulating the development and drought stress resilience of somatic plants years later (Castander-Olarieta et al., 2020b). However, very few proteomic studies have been carried out in pine species addressing heat-stress, and, as far as we know, this is the first report carried out along SE applying such high temperatures.

To this purpose, we have applied a Short-GeLC-MS/MS approach in combination with the SWATH acquisition method (Anjo et al., 2015) which, when compared with the classically employed two-dimensional electrophoresis systems (2-DE), substantially reduces the amount of sample handling and lightens the data analysis process without compromising the protein identification efficiency. Furthermore, this strategy enables

the detection of challenging insoluble transmembrane proteins and has great potential when working with non-sequenced species (Heringer et al., 2018).

Finally, in order to have a broader perspective and confirm our results, a high-performance liquid chromatography (HPLC) analysis has been carried out to find whether specific changes in the proteome could have resulted in modifications of several metabolic pathways, i.e., sugar metabolism, which is known to have a key role in stress-response mechanisms (De Diego et al., 2013a).

2. MATERIALS AND METHODS

2.1. Plant material and heat stress experiment

Green female cones of *Pinus radiata* from five genetically different mother trees in a seed orchard established by Neiker in Deba (Spain, latitude: 43°16′59"N, longitude: 2°17′59"W, altitude: 50 m), were collected in June 2018 and processed according to Montalbán et al. (2012). Seeds were sterilized following the aforementioned protocol and megagametophytes enclosing immature zygotic embryos were carefully extracted and placed horizontally onto Petri dishes containing Embryo Development Medium (EDM, Walter et al., 2005), supplemented with 3.5 g L^{-1} gellan gum (Gelrite®, Duchefa, Haarlem, The Netherlands). At this point, intact megagametophytes were subjected to different incubation conditions for different time periods (Cond1 = 23°C, 8 weeks, Cond2 = 40°C, 4 h, Cond3 = 60°C, 5 min). In all cases, the Petri dishes were prewarmed to the desirable temperature prior to the cultivation of the megagametophytes. Eight megagametophytes were used per Petri dish and ten Petri dishes per treatment, comprising a total of 1200 megagametophytes, including all treatments and mother trees. After the treatments, all the samples were kept at 23°C in darkness and the following steps of SE (proliferation and maturation) were carried out at standard conditions as reported in Montalbán & Moncaleán (2018).

After 8 weeks on initiation medium, initiation rates were calculated and growing EMs were separated from the megagametophytes and subcultured to a fresh EDM initiation

medium. After 14 days, EMs were subcultured onto the same medium but 4.5 g L^{-1} gellan gum every 2 weeks until maturation. Following four periods of subculturing, actively growing EMs were recorded as established cell lines (ECL), and the percentage of proliferating lines respect to the EMs initiated was calculated.

Maturation was performed using six replicates (Petri dishes) per ECL and 10 ECLs per treatment. After 12 weeks, maturation success was evaluated, the number of mature and well-formed Se's per gram of embryogenic tissue was calculated and 100 mg of Se's per ECL were frozen in liquid nitrogen for both protein and soluble sugar analyses.

2.2. Protein and metabolite extraction and protein sample preparation

Protein and metabolite extractions from mature Se's were performed following the combined protocol described by Valledor et al. (2014). Briefly, 800 µl of cold extraction buffer (methanol:chloroform:water 2.5:1:0.5, v:v:v) were added to 100 mg of liquid nitrogen grinded Se's. Five ECLs were used per temperature condition. Then, samples were centrifuged at 20,000 g for 6 min at 4°C.

The supernatant, containing metabolites, was transferred to a new microcentrifuge tube and 800 µl of phase separation mix (chroloform:water 1:1) were added. After centrifugation (10,000 g, 5 min, room temperature), the upper aqueous phase was transferred again to a new tube for an extra fractionating step with 300 µl of phase separation mix. Finally, the upper layer containing polar metabolites was saved to new tubes and stored at -80°C until HPLC analysis.

Pellets containing proteins and nuclei acids were washed with 1 ml of 0.75% (v/v) β-mercaptoethanol in 100% methanol, centrifuged (20,000 g, 6 min, 4°C) and the supernatant discarded. The washing step was repeated once. Pellets were then air dried and dissolved in 400 µl of pellet solubilisation buffer [PSB; 7 M guanidine HCl, 2% (v/v) Tween-20, 4% (v/v) Triton-×100, 50 mM Tris, pH 7.5, 1% (v/v) β-mercaptoethanol] for incubation at 37°C in a thermal shaker for 20 min. Then, samples were centrifuged (14000 g, 3 min) and the supernatants were transferred to silica columns to bind DNA

(Zymo Research, Irvin, California, USA). After 1 min of incubation, columns were centrifuged (10,000 g, 1 min) and the flowthrough was mixed with 300 µl of acetonitrile. The mix was transferred to a new silica column, incubated for 1 min, and centrifuged at 10,000 g for 1 min. The flowthrough was transferred to a new tube and 550 µl of phenol and 600 µL of water were added. Samples were mixed, centrifuged (10,000 g, 5 min) and the upper phenolic phase was transferred to a new tube that contained 600 µl PWB [0.7 M sucrose, 50 mM Tris-HCl pH 7.5, 50 mM EDTA, 0.5% β-mercaptoethanol, 0.5% (v/v) Plant Protease Inhibitor Cocktail from Sigma, St. Louis, Missouri, USA]. After vortexing and centrifugation (10,000 g, 5 min, room temperature), upper phenolic phase was transferred to a new tube and proteins were precipitated overnight at -20°C by the addition of 1.5 ml of 0.1 M ammonium acetate, 0.5% β-mercaptoethanol in methanol. Samples were then centrifuged at 10,000 g for 15 min at 4°C, the supernatant removed, and pellets were washed with cold acetone three times. Finally, proteins were precipitated by centrifugation (10,000 g, 15 min) and pellets were air dried and re-suspended in 100 µl of solubilisation buffer [7M urea, 2M thiourea, 2% (w/v) CHAPS, 1% (w/v) DTT].

As a preparatory step prior to LC-MS analysis, protein extracts (50 µl) were re-precipitated with 4 volumes of cold acetone (250 µl) for 30 min at -80°C. Samples were centrifuged at 20,000 g, refrigerated at 4°C for about 20 min and the pellet was re-suspended in 50 µl of 1× Laemmli Sample Buffer. The total protein concentration was measured for each sample using the Pierce 660 nm Protein Assay kit (Thermo Scientific™, Waltham, Massachusetts, USA). For data-dependent acquisition (DDA) experiments, replicates from each treatment were pooled into three different samples (Cond1 = 23°C, 8 weeks; Cond2 = 40°C, 4 h; Cond3 = 60°C, 5 min) before sample processing and for data-independent acquisition (DIA) each sample was processed individually. Protein content from each sample (adjusted based on the protein quantification values obtained previously) was separated by SDS-PAGE for about 17 min at 110 V (Short-GeLC Approach, Anjo et al., 2015) and stained with Coomassie Brilliant Blue G-250. For DDA experiments, each lane was divided into 5 gel pieces and for DIA experiments into 3 gel pieces for further individual processing. After destaining with a

50 mM ammonium bicarbonate and 30% acetonitrile solution, gel bands were incubated overnight with trypsin for protein digestion and peptides were extracted from the gel using 3 solutions containing different percentages of acetonitrile (30, 50, and 98%) with 1% formic acid. The organic solvent was evaporated using a vacuum-concentrator and peptides were re-suspended in 30 µl of a solution containing 2% acetonitrile and 0.1% formic acid. Each sample was sonicated using a cup-horn (Ultrasonic processor, 750W) for about 2 min, 40% amplitude, and pulses of 1 sec ON/OFF. Ten µl of each sample were analysed by LC-MS/MS, either for DIA or DDA experiments.

2.3. Protein and soluble sugar analysis

Protein samples were analysed on a NanoLC™ 425 System coupled to a Triple TOF™ 6600 mass spectrometer (Sciex, Framingham, Massachusetts, USA). The ionization source was the OptiFlow® Turbo V Ion Source equipped with the SteadySpray™ Low Micro Electrode (1-10µL). The chromatographic separation was performed on a Triart C18 Capillary Column 1/32" (12 nm, S-3µm, 150 x 0.3 mm, YMC) and using a Triart C18 Capillary Guard Column (0.5 × 5 mm, 3 µm, 12nm, YMC) at 50°C. The flow rate was set to 5 µl min^{-1} and mobile phases A and B were 5% DMSO plus 0.1% formic acid in water and 5% DMSO plus 0.1% formic acid in acetonitrile, respectively. The LC program was performed as followed: 5 – 35% of B (0 - 40 min), 35 – 90% of B (40 – 41 min), 90% of B (41-45 min), 90 - 5% of B (45 – 46 min), and 5% of B (46 – 50 min). The ionization source was operated in the positive mode set to an ion spray voltage of 4500 V, 10 psi for nebulizer gas 1 (GS1), 15 psi for nebulizer gas 2 (GS2), 25 psi for the curtain gas (CUR), and source temperature (TEM) at 100°C. For DDA experiments, the mass spectrometer was set to scanning full spectra (m/z 350-1250) for 250 ms, followed by up to 100 MS/MS scans (m/z 100 – 1500). Candidate ions with a charge state between +1 and +5 and counts above a minimum threshold of 10 counts per second were isolated for fragmentation and one MS/MS spectrum was collected before adding those ions to the exclusion list for 15 s (mass spectrometer operated by Analyst® TF 1.7, Sciex). The rolling collision was used with a collision energy spread of 5. For SWATH experiments, the mass spectrometer was operated in a looped product ion mode and specifically

tuned to a set of 90 overlapping windows, covering the precursor mass range of 350-1250 m/z. A 50 ms survey scan (350-1250 m/z) was acquired at the beginning of each cycle, and SWATH-MS/MS spectra were collected from 100-1800 m/z for 35 ms resulting in a cycle time of 3.2 s.

For soluble sugar quantification, 200 µl of metabolite samples obtained in section 2.2 were totally dried on a Speedvac to remove the methanol from the extraction buffer and re-suspended in 100 µl distilled water. Soluble sugar and sugar alcohol analysis was performed by HPLC using an Agilent 1260 Infinity II coupled to refractive index detector (RID) (Agilent Technologies, Santa Clara, USA). A Hi-Plex Ca column (7.7 x 300 mm, 8 µm) was used for separation of fructose, glucose, sucrose, mannitol and sorbitol. The mobile phase was pure water and the samples were injected in the column at a flow rate of 0.2 ml min^{-1} at 80°C for 40 min. Sugar concentrations were determined from internal calibration curves constructed with the corresponding commercial standards. The concentrations obtained from the HPLC analysis were conveniently adjusted taking into account the initial concentration step (2 times), and results were expressed as µmol g FW^{-1}.

2.4. Data analysis

Ion-Library construction (DDA information)

A specific ion-library of the precursor masses and fragment ions was created by combining all files from the DDA experiments in one protein identification search using the ProteinPilot™ software (v5.0, Sciex®). The paragon method parameters were the following: searched against the reviewed Viridiplantae database (Swissprot) downloaded on 1st April from UniProtKB (www.uniprot.org; The UniProt Consortium, 2019), cysteine alkylation by acrylamide, digestion by trypsin, and gel-based ID. An independent False Discovery Rate (FDR) analysis, using the target-decoy approach provided by Protein Pilot™, was used to assess the quality of identifications.

Relative quantification of proteins (SWATH-MS)

SWATH data processing was performed using SWATH™ processing plug-in for PeakView™ (v2.0.01, Sciex®). Protein relative quantification was performed in all samples using the information from the protein identification search. Quantification results were obtained for peptides with less than 1% of FDR, by the sum of up to 5 fragments/peptide and selecting the peptides presenting a coefficient of variation (CV) smaller than 50%. Each peptide was normalized for the total sum of areas for the respective sample. Protein relative quantities were obtained by the sum of the normalized values for up to 15 peptides protein^{-1} and a correlation analysis between samples was performed to assure that all samples from the same condition showed the same behaviour.

2.5. Statistical analysis

The effect of each treatment on the initiation and proliferation rates was evaluated performing a logistic regression and the corresponding analysis of deviance. The mother tree was introduced into the model as a block variable to reduce variability and the Tukey's post-hoc test ($\alpha = 0.05$) was used for multiple comparisons. In the case of the number of Se's per gram of ET, the usual analysis of variance (ANOVA) did not fulfil the normality hypothesis, and thus, a linear mixed effects model was considered, including the ECL as a random effect with different variance parameters for each treatment level to correct for heteroscedasticity.

For the analysis of the protein results, two different approaches were employed, combining multivariate and univariate analyses. First, we performed a partial least square-discriminant analysis (PLS-DA) using the MetaboAnalyst web-based platform (www.metaboanalyst.ca; Pang et al., 2020) to find out the separation between the three conditions and simultaneously identify the most significant top protein features able to classify the three groups based on variable influence on projections (VIP) values. Those proteins were then clustered based on their biological function according to the FunRich software and the Plants database from UniProtdatabase (https://www.uniprot.org/help/plants). In parallel, as cross-validation, a Kruskal-Wallis test was performed to select the proteins which were statistically different between the

3 conditions. The Dunn's test of Multiple Comparisons, with Benjamini-Hochberg *p*-value adjustment, was performed to determine in which comparisons statistical differences were observed. Finally, proteins overlapping between the Kruskal-Wallis test significant proteins and PLS-DA VIP list were selected and a cluster analysis was performed to them using the MetaboAnalyst web-based platform in order to investigate their relation and relative abundance by generating heatmap and correlation matrix plots. For the heatmap hierarchical clustering the Euclidean distance and the Complete algorithm were used and for the correlation matrix the Pearson's correlation test was applied.

To assess the effect of the treatments on the levels of each sugar, an ANOVA was conducted followed by multiple comparisons based on Tukey's post hoc test ($\alpha = 0.05$). When the ANOVA did not fulfil the normality hypothesis the Kruskal-Wallis test was performed.

3. RESULTS

3.1. Effect of temperature treatments on somatic embryogenesis

Analysing the effect of each treatment on the different steps of SE (initiation, proliferation, maturation), statistically significant differences were only observed during initiation ($p < 0.05$). Initiation rates were significantly lower at 40°C for 4 h, whereas treatments at 23°C for 8 weeks and 60°C for 5 min presented similar values (Table 1). Regarding proliferation, no differences could be observed among treatments. The three treatments showed similar proliferation rates, being the ones obtained at 60°C for 5 minutes slightly higher than the other two (Table 1). Maturation rates were beyond 90% for the three treatments, so temperature did not reduce the maturation capacity of EMs. In the same way, no significant differences were detected for the number of Se's produced per gram of embryogenic tissue. Nonetheless, the application of high temperatures slightly increased the formation of mature Se's, especially at 40°C for 4 h treatment (Table 1).

3.2. Relative quantification of proteins

Proteomic analysis allowed the identification of 1200 proteins from the reviewed Viridiplantae database. After data processing and the application of the abovementioned filters, 758 proteins were used for quantitative analyses. The correlation analysis performed demonstrated that samples were highly correlated between them, with correlation values above 0.72 (data not shown).

Table 1. Embryonal mass initiation (%) and proliferation rates (%), and number of somatic embryos per gram of embryogenic tissue from *P. radiata* megagametophytes cultured under different temperature conditions. Data are presented as mean values ± SE. Significant differences at $p < 0.05$ are indicated by different letters.

Treatment	Initiation %	Proliferation %	Se's g^{-1} ET
23°C, 8 weeks	44 ± 2.95[a]	31.82 ± 2.09[a]	121.87 ± 45.72[a]
40°C, 4 h	30.5 ± 3.08[b]	30.33 ± 3.01[a]	170.83 ± 53.86[a]
60°C, 5 min	43.5 ± 2.99[a]	36.21 ± 2.54[a]	129.4 ± 41.71[a]

For visualization of sample groups and to reduce the complexity of the results, a PLS-DA analysis was performed, a supervised model that uses multivariate techniques to extract via linear combinations of original variables that can predict class membership giving the largest predicted indicator variable. The three conditions employed in this experiment were clearly distinguished and separated by the loading plots of the first and second components of PLS-DA pairwise comparison models (Figure 1). These two components accounted for almost the 33% of the total variance. The first component potentially gathered variability related to heat-stress responses, while the biological function of the second component remained unclear due to an excess of variability.

The proteins presenting VIP values greater than 1 were considered the best classifiers, the ones contributing the most to the separation of the three conditions and thus, the ones involved in heat-stress responses. This selection included 262 proteins (Supplementary Figure 1), which were subjected to a gene ontology enrichment analysis to extract information about their mayor biological function. This analysis revealed that

the selected proteins belonged to numerous pathways, covering a great number of cellular processes, from primary to secondary metabolism (Figure 2). However, three biological functions were considerably more represented than the other ones, which included proteins involved in direct stress response and adaptation processes, proteins constituents of the translation machinery, translation regulation and proteome reorganization, and proteins involved in carbohydrate metabolism. Other pathways such as amino acid or lipid metabolisms were also represented, although to a lesser extent, and a great proportion of functions related to the life cycle of proteins were detected (folding, catalysis, transport), accounting for almost the 20% of the total enrichment analysis. At the transcriptome level, some proteins involved in gene expression regulation and RNA processing/metabolism also seemed to be involved in the response to heat, together with signal receptors and proteins constituents of signalling cascades. Finally, a small group of proteins taking part in cell division, response to abscisic acid and methylation processes were also selected by the PLS-DA analysis.

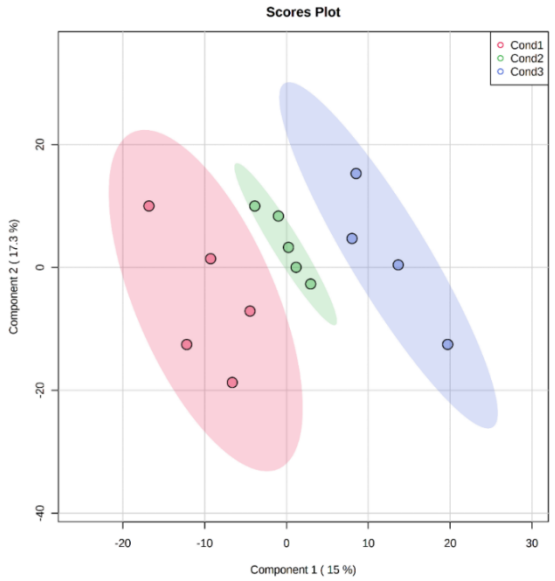

Figure 1. Bi-dimensional representation of the scores for the PLS-DA analysis using the 758 quantified proteins extracted from somatic embryos originating from embryonal masses initiated under three different conditions (Cond1 = 23°C, 8 weeks, Cond2 = 40°C, 4 h, Cond3 = 60°C, 5 min). Data normalization was performed using the AutoScale method and the scores of the two first components are represented showing the ovals at 95% confidence interval.

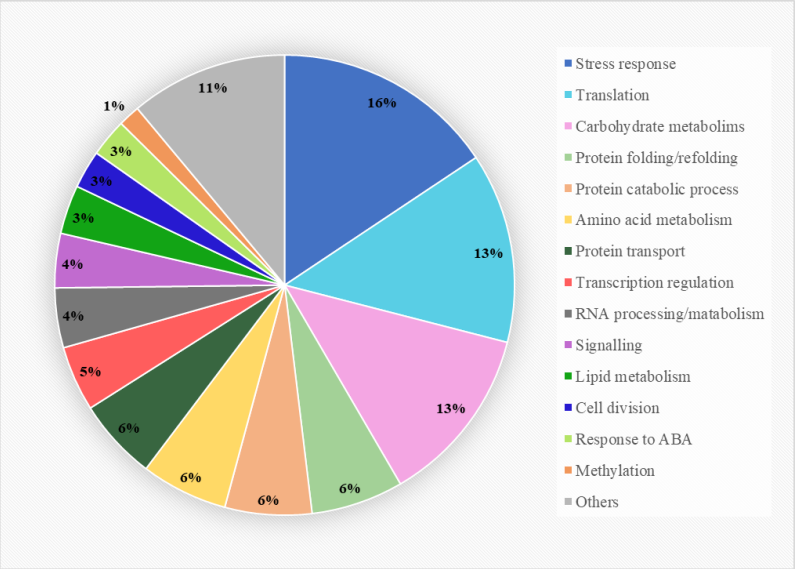

Figure 2. Gene ontology enrichment analysis of the 262 proteins selected from the PLS-DA analysis presenting VIP values greater than 1. The biological function clustering was performed using the FunRich software and the Plants database from UniProtdatabase.

The univariate statistical analysis revealed that 64 proteins were differentially accumulated ($p < 0.05$) between the three conditions (Supplementary Table 1). Comparing these proteins with the 262 proteins selected from the PLS-DA analysis we observed that 54 proteins were common between both statistical approaches and were considered the top significant proteins after heat-stress response in our samples (Supplementary Figure 2). The complete list of these proteins, their accession number, the fold-change between conditions, and the results from both statistical analyses are shown in Tables 2 and 3.

In order to better visualise the relation between proteins, a cluster analysis was performed with the selected 54 top significant proteins by generating a heatmap (Figure 3) and a correlation matrix (Supplementary Figure 3). These analyses showed two clearly differenced groups of proteins based on their relative abundance between conditions. One of the groups presented an abundance increasing tendency from the control condition of 23°C (Cond1) to the highest temperature condition of 60°C (Cond3). The condition of 40°C for 4 hours (Cond2) showed an intermediate behaviour. As

observed in the correlation matrix, all the proteins from this group were closely interrelated, presenting high positive correlation coefficients. This protein group included a great variety of proteins, among which some of them were specific of the group: HSPs and chaperones (small heat shock protein, DnaJ protein homolog ANJ1, DnaJ protein homolog) and proteins involved in ion and small molecules transport (outer plastidial membrane protein porin, mitochondrial outer membrane protein porin 2, mitochondrial outer membrane protein porin 5, sugar transporter ESL1). Some proteins related to the synthesis of specific sugars and sugar alcohols were also over-accumulated under high temperatures, such as UDP-glucuronic acid decarboxylase 4 and inositol 3-phosphate synthase isozyme 3.

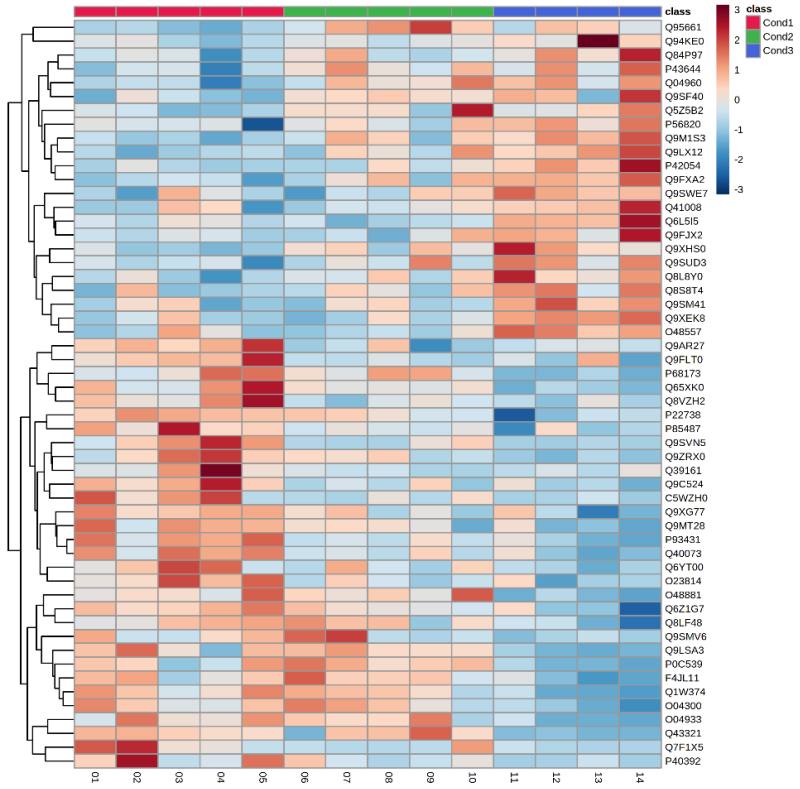

Figure 3. Hierarchical clustering heatmap using the 54 proteins selected from the combination of Kruskal-Wallis test and the PLS-DA analysis in somatic embryos of *P. radiata* originating from high temperature conditions (Con1 = 23°C, 8 weeks, Cond2 = 40°C, 4 h, Cond3 = 60°C, 5 min). Hierarchical clustering was performed at the protein (rows) using Euclidean distance and Complete for the clustering algorithm.

Table 2. Top significant proteins selected from the combination of univariate statistical analysis (Kruskal-Wallis test) and multivariate PLS-DA analysis ($p < 0.05$ and VIP > 1) in somatic embryos of *P. radiata* originating from embryonal masses induced under high temperature conditions (Cond1 = 23°C, 8 weeks, Cond2 = 40°C, 4 h, Cond3 = 60°C, 5 min). Fold changes are presented as the ratio between one condition and the other.

		Fold Change			Kruskal-Wallis	PLS-DA
Description	**Accession**	**Cond2/ Cond1**	**Cond3/ Cond1**	**Cond3/ Cond2**	***p*-value**	**VIP**
60S ribosomal protein L3-2	P22738	0.84	0.55	0.65	0.005	2.43
Small heat shock protein, chloroplastic	Q95661	2.68	1.94	0.72	0.007	1.38
Methionine--tRNA ligase, cytoplasmic	Q9SVN5	0.35	0.12	0.34	0.009	2.22
Outer plastidial membrane protein porin	P42054	1.1	1.58	1.43	0.01	2.25
Mitochondrial outer membrane protein porin 2	Q6L5I5	0.91	1.38	1.51	0.011	1.9
DnaJ protein homolog	Q04960	1.42	1.51	1.06	0.013	2.17
Unknown protein 3 (Fragment)	P85487	0.66	0.47	0.71	0.013	2.12
40S ribosomal protein S12	Q9XHS0	1.39	1.76	1.27	0.015	2.28
Thiamine biosynthetic bifunctional enzyme BTH1, chloroplastic	O48881	1.03	0.71	0.69	0.016	1.86
Translationally-controlled tumor protein homolog	Q9ZRX0	0.85	0.68	0.8	0.017	2.21
Ketol-acid reductoisomerase, chloroplastic	Q65XK0	0.74	0.4	0.53	0.017	2.22
Ribulose bisphosphate carboxylase/oxygenase activase, chloroplastic	P93431	0.71	0.58	0.82	0.018	2.42
Actin-2	P0C539	1.3	0.4	0.31	0.018	1.51
Probable fructokinase-6, chloroplastic	Q9C524	0.7	0.65	0.93	0.018	2.08
Ferredoxin--nitrite reductase, chloroplastic	Q39161	0.59	0.64	1.09	0.018	1.51
60S ribosomal protein L23	Q9XEK8	0.98	1.37	1.4	0.018	2.11
Adenosylhomocysteinase	P68173	0.93	0.22	0.24	0.018	1.98
Pyruvate dehydrogenase E1 component subunit beta-1	Q6Z1G7	0.89	0.69	0.78	0.02	2.27
Ribulose bisphosphate carboxylase/oxygenase activase A	Q40073	0.68	0.52	0.77	0.02	2.35
Sugar transporter ESL1	Q94KE0	1.19	1.77	1.49	0.021	1.85
Casein kinase II subunit alpha-2	Q9AR27	0.63	0.71	1.13	0.021	1.67
Protein translation factor SUI1 homolog	Q9SM41	1.02	1.23	1.21	0.021	1.96
Probable RNA-binding protein ARP1	Q9M1S3	1.36	1.74	1.28	0.022	2.38
Polyadenylate-binding protein 8	Q9FXA2	1.24	1.57	1.27	0.022	2.37
Aminopeptidase M1	Q8VZH2	0.56	0.5	0.89	0.025	1.97
Phosphomannomutase	Q1W374	0.95	0.65	0.68	0.026	2.23

Table 3. Continuation of Table 2. Top significant proteins selected from the combination of univariate statistical analysis (Kruskal-Wallis test) and multivariate PLS-DA analysis ($p < 0.05$ and VIP > 1) in somatic embryos of *P. radiata* originating from embryonal masses induced under high temperature conditions (Cond1 = 23°C, 8 weeks, Cond2 = 40°C, 4 h, Cond3 = 60°C, 5 min). Fold changes are presented as the ratio between one condition and the other.

		Fold Change			Kruskal-Wallis	PLS-DA
Description	**Accession**	**Cond2/ Cond1**	**Cond3/ Cond1**	**Cond3/ Cond2**	***p*-value**	**VIP**
Probable UDP-arabinopyranose mutase 1	O04300	1.02	0.54	0.53	0.026	1.9
60S ribosomal protein L30-3	Q9LSA3	1.02	0.76	0.75	0.026	1.8
Inosine triphosphate pyrophosphatase	C5WZH0	0.84	0.8	0.95	0.026	2.11
4-coumarate--CoA ligase-like 5	Q7F1X5	0.38	0.14	0.37	0.026	1.76
60S ribosomal protein L17	O48557	0.94	1.4	1.49	0.027	1.83
Probable sucrose-phosphate synthase 2	O04933	0.96	0.53	0.56	0.027	2.05
40S ribosomal protein S2-1	Q8L8Y0	1.15	1.36	1.18	0.028	2.21
60S ribosomal protein L4-1	Q9SF40	2.93	3.55	1.21	0.03	1.85
Eukaryotic translation initiation factor 3 subunit D	P56820	1.2	1.46	1.22	0.032	1.97
Proteasome subunit alpha type-6	Q9XG77	0.88	0.81	0.91	0.032	1.98
Protein argonaute 1D	Q5Z5B2	1.67	1.66	0.99	0.032	1.48
Threonine synthase, chloroplastic	Q9MT28	0.87	0.77	0.89	0.033	2.1
Probable inositol 3-phosphate synthase isozyme 3	Q9LX12	1.97	3.2	1.62	0.034	2.29
Proteasome subunit alpha type-7-A	Q6YT00	0.81	0.64	0.79	0.034	2.01
Protein EXPORTIN 1A	Q9SMV6	1.09	0.43	0.39	0.035	1.25
Ras-related protein RIC1	P40392	0.59	0.36	0.6	0.037	1.82
V-type proton ATPase subunit E	Q9SWE7	1.02	1.25	1.22	0.038	1.71
3-ketoacyl-CoA thiolase 1, peroxisomal	Q8LF48	0.98	0.72	0.74	0.038	1.87
Importin subunit alpha-2	F4JL11	1.05	0.76	0.72	0.039	1.66
Acetyl-coenzyme A carboxylase carboxyl transferase subunit alpha, chloroplastic	Q41008	1.06	1.46	1.37	0.039	1.83
Enolase	Q43321	0.93	0.04	0.05	0.039	2.1
Probable phospholipid hydroperoxide glutathione peroxidase	O23814	0.69	0.62	0.89	0.04	2.07
Mitochondrial outer membrane protein porin 5	Q84P97	1.09	1.28	1.17	0.042	1.94
DnaJ protein homolog ANJ1	P43644	1.29	1.34	1.04	0.046	1.87
60S ribosomal protein L26-2	Q9FJX2	1.02	1.36	1.33	0.046	1.86
Ribonuclease TUDOR 2	Q9FLT0	0.67	0.69	1.03	0.047	1.76
Cytochrome c oxidase subunit 6b-3	Q9SUD3	1.19	1.47	1.24	0.048	2.04
UDP-glucuronic acid decarboxylase 4	Q8S8T4	1.1	1.31	1.19	0.048	2.02

Following the same pattern, a great number of structural constituents of ribosomes and translation regulation factors were detected (40S ribosomal protein S12, 60S ribosomal protein L23, 60S ribosomal protein L17, 40S ribosomal protein S2-1, 60S ribosomal protein L4-1, 60S ribosomal protein L26-2, protein translation factor SUI1 homolog, polyadenylate-binding protein 8, eukaryotic translation initiation factor 3 subunit D). Finally, it is also remarkable the observed higher amount of proteins involved in the posttranscriptional regulation of RNA metabolism at high temperatures, such as RNA-binding protein ARP1 and protein ARGONAUTE 1D, and of one protein that takes part in the fatty acid biosynthetic process (acetyl-coenzyme A carboxylase carboxyl transferase subunit alpha). Besides, some of these proteins presented high fold changes between control (Cond1) and treatments (Cond2 and Cond3), such as small heat shock protein, 60 S ribosomal protein L4-1 and inositol 3-phosphate synthase isozyme 3 (Table 2, Table 3).

On the contrary, the other subgroup of proteins showed reduced abundance levels under high temperature conditions, especially at 60°C for 5 min (Figure 3), and was negatively correlated with the first group of proteins (Supplementary Figure 3). This cluster was composed to a vast extent by central metabolism enzymes, covering diverse pathways such as, glycolysis, citric acid cycle, fatty acid beta-oxidation or Calvin cycle (pyruvate dehydrogenase E1 component subunit beta-1, enolase, ribulose bisphosphate carboxylase/oxygenase activase A, ribulose bisphosphate carboxylase/oxygenase activase, 3-ketoacyl-CoA thiolase 1), and some proteins involved in the synthesis of specific sugars such as fructokinase-6, sucrose-phosphate synthase 2, UDP-arabinopyranose mutase and phosphomannomutase. Proteins involved in oxidative-stress defence were clearly down-expressed (thiamine biosynthetic bifunctional enzyme BTH1, 4-coumarate--CoA ligase-like 5, phospholipid hydroperoxide glutathione peroxidase, EXPORTIN 1A), together with those implicated in amino acid synthesis and protein catalysis (threonine synthase, ketol-acid reductoisomerase, proteasome subunit alpha type-6, proteasome subunit alpha type-7-A, aminopeptidase M1). Other proteins found at lower concentrations at high temperatures included structural constituents of the cytoskeleton (actin-2, translationally-controlled tumor protein homolog), some

proteins related with translation (60S ribosomal protein L3-2, 60S ribosomal protein L30-3, methionine--tRNA ligase), post-transcriptional gene regulation and epigenetic mechanisms (ribonuclease TUDOR 2, adenosylhomocysteinase), nitrogen metabolism (ferredoxin--nitrite reductase), cellular receptors for nuclear import (importin subunit alpha-2) or electron transport proteins (cytochrome c oxidase subunit 6b-3). It is noticeable that some of them presented high fold changes: enolase, methionine--tRNA ligase, adenosylhomocysteinase, and 4-coumarate--CoA ligase-like 5 (Table 2, Table 3).

3.3. Soluble sugar content quantification

The HPLC approach revealed the presence of three (fructose, glucose, sucrose) of the five sugar and sugar alcohols analysed. Sorbitol and mannitol could not be detected in Se's using this technique. All sugars presented similar concentrations, although the levels of sucrose and fructose were slightly higher than those of glucose (Table 4). Taking into account the effect of the treatments, no significant differences were observed. However, the levels of sucrose were on the verge of statistical significance (p = 0.078), showing a decreasing tendency at high temperatures, especially at 60°C for 5 minutes treatment (%23 decrease with respect to control treatment of 23°C). This pattern was not appreciable for the rest of sugars detected, although the lowest levels were also observed at 60°C for 5 min treatment (Table 4).

Table 4. Effect of temperature treatment (23°C, 8 weeks, 40°C, 4 h, 60°C, 5 min) on the levels of the following sugars and sugar alcohols in somatic embryos of *P. radiata*: fructose, glucose and sucrose. Data are presented as mean values ± SE. Significant differences among treatments at $p < 0.05$ are indicated by letters.

Treatment	Fructose	Glucose	Sucrose
23°C, 8 weeks	70.88 ± 1.95[a]	46.77 ± 5.03[a]	72.98 ± 5.34[a]
40°C, 4 h	74.57 ± 3.31[a]	46.75 ± 5.64[a]	67.41 ± 5.88[a]
60°C, 5 min	66.12 ± 6.55[a]	40.76 ± 6.26[a]	56.19 ± 3.52[a]

4. DISCUSSION

Recent advances in "omics" technologies have enabled the identification, systematic analysis and interconnection of some of the different transcriptional, translational, metabolic and signalling pathways governing plant response to numerous biotic and abiotic stress factors, including heat. In this sense, although gene expression analyses have provided useful information about the molecular mechanisms underlying heat-stress response and thermotolerance, proteomics offers a more accurate image of the current cell status, by accounting for alternative splicing or post-translational modifications that usually result in poor transcript/protein correlations (Becker et al., 2003). Besides, protein metabolic processes are very susceptible to environmental temperatures, and thus, proteomics has become a very useful approach when studying this type of stresses (Yuan et al., 2019). Consequently, in this work we have tried to study the proteome of Se's to obtain insights about the effect of heat-stress at early stages of radiata pine SE and elucidate how that effect can modulate the success of different stages of the process.

Following the same tendency observed in previous studies (Castander-Olarieta et al., 2019), in this work the combination of high temperatures and long exposure time-periods (40°C, 4 h) provoked a considerable decrease of around 13% in the initiation success of EMs. This could be attributed to oxidative damage and structural imbalances at cellular and tissue level (Castander-Olarieta et al., 2019). In agreement with this work is also the pattern observed at maturation stage. Although not significant, probably due to the recurrent high variability observed among genotypes in terms of maturation productivity, the number of Se's slightly increased under high temperatures, reinforcing the role of temperature as an activator of embryo development (Castander-Olarieta et al., 2019).

On the other hand, no differences were observed at the proliferation stage. Castander-Olarieta et al. (2019) reported that the detrimental effects of the application of high temperatures during initiation could also be observed after several subculture periods during proliferation. Results obtained at this stage seem quite ambiguous, as other

authors reported higher proliferation rates when EMs were induced under stressful conditions (Fehér, 2015, García-Mendiguren et al., 2016b). This fact could be attributed to the type and dose of the applied stress and the capacity of EMs to overcome the consequences of stress.

Multivariate statistical analysis of the proteomic results revealed a large amount of proteins differentially responding to the three temperature conditions even several months later at Se's stage. This fact could explain the altered behaviours described during the different stages of SE in this study and previous ones. These proteins covered a broad spectrum of biological and molecular functions, but three groups were clearly more represented, including proteins involved in stress responses, proteome readjustment and carbohydrate metabolism. In spite of being at lower levels, proteins taking part in other interesting metabolic pathways were also detected, such as amino acid and lipid synthesis, transcription regulation, RNA metabolism and methylation. These results are in agreement with other studies carried out in radiata pine plantlets subjected to different stress conditions (Escandón et al., 2017, Pascual et al., 2017, Lamelas et al., 2020).

Further statistical analyses combining multivariate with univariate approaches highlighted the importance of 54 proteins as the top significant ones contributing to the separation between the three conditions. Among these proteins, it is noticeable the higher presence of HSPs and molecular chaperones in Se's originating from EMs induced at high temperatures. HSPs are an extremely heterogeneous group of proteins produced by most eukaryotic cells. They are up-regulated under supra-optimal high temperatures (Yuan et al., 2019, Jiang et al., 2020) and prevent proteins from being denatured by assisting in protein folding and processing. In that way, proteins can maintain a proper stability and function under unfavourable conditions (Hasanuzzaman et al., 2013, Krishnan et al., 2020).

Many studies have observed that these types of molecules are essential for heat-tolerance (Meiri & Breiman, 2009, Perez et al., 2009). In fact, while other stress responsive proteins such as ROS detoxifying enzymes have been described as important

mediators in basal thermo-tolerance and early response processes, HSPs and chaperones appear to be required for both basal and acquired thermo-tolerance (Bokszczanin & Fragkostefanakis, 2013), even contributing to plant acclimation (Escandón et al., 2017). Reinforcing this idea, there are several examples of transgenic plants constitutively expressing HSPs that without a previous heat treatment exhibit an enhanced thermo-tolerance (Lee et al., 1995, Malik et al., 1999). As a result, the delayed and sustained accumulation of this type of proteins in Se's of radiata pine could suggest that some kind of "memory" machinery in being triggered, leading to a consequent acquired thermo-tolerance. It would be interesting to confirm if this protein profile is maintained throughout the SE process, influencing the *ex vitro* performance of the generated plants, as observed at the physiological level under control and drought stress conditions in Castander-Olarieta et al. (2020b). Besides, the accumulation of HSPs has also been observed under other abiotic stress conditions, including drought (Kosová et al., 2011, Taïbi et al., 2017), which could provide simultaneous protection against more than one environmental constraint. Increased tolerance to different kind of stresses based on the activation of similar metabolic pathways has already been reported, for example, during drought and cold (Shinozaki et al., 2003).

Chaperones and HSPs seem to be closely related with many other proteins in cells, such as, stress responsive, proteome remodelling or posttranscriptional regulation elements. Escandón et al. (2017) observed that mitochondrial electron transport proteins were connected to small HSPs under heat-stress conditions. In our work, in spite of being negatively correlated to HSPs, a cytochrome oxidase was also influenced by temperature conditions. Other authors have also highlighted the responsiveness of these proteins under heat in chickpea or tomato pollen (Parankusam et al., 2017, Keller et al., 2018).

In the same way, the proteome analysis revealed that the translasome machinery, including ribosomal proteins and translation regulation factors, together with proteins involved in protein catalysis and homeostasis such as different proteasome subunits, had a relevant role during heat-stress response, as already described in other studies (Wang et al., 2018, Li et al., 2019). Although varying patterns were observed under the

different temperature conditions, most of the ribosomal proteins and all the translation regulation factors followed an accumulation tendency when heat was applied, while all the proteins involved in protein degradation were down-represented. In fact, one of the proteins presenting the highest fold-changes was the 60S ribosomal protein L4-1, which was detected at higher concentrations at both 40°C and 60°C treatments. This protein has been found to be temperature sensitive, increasing considerably its expression under cold (Schlaen et al., 2015). As a result, we can state that heat provokes a deep reorganization of the proteome, by a strict regulation of translation and an altered ribosome composition that could result in a selective mRNA translation to better cope with adverse conditions.

Besides, the relative abundance and differential expression of the aforementioned proteins seem to have further implications in different plant developmental processes via interconnections with phytohormones and other signalling molecules. For example, the function of some ribosomal proteins has been proved to be linked with cytokinin molecular circuits (Černý et al., 2013). Interestingly, the application of the same high temperature conditions at initiation of *P. radiata* and *P. halepensis* SE provoked changes in the cytokinin profile of EMs (Castander-Olarieta et al., 2020a, 2020b, Pereira et al., 2020). It would be of special interest for future studies to confirm if those changes are maintained in Se's and study their relationship with the translasome machinery.

Apart from that, protein homeostasis seems to have special relevance during conifer SE, as indicated by the differential expression of specific proteasome subunits and translation elongation factors during EM proliferation and Se's development in numerous conifer species (Trontin et al., 2016). Specifically, at maturation stage the synthesis of major storage proteins of the globulin and albumin families and proteins involved in acquisition of desiccation tolerance (late embryogenesis abundant proteins) appear to be of great relevance, even determining the germination capacity of Se's (Klimaszewska et al., 2004; Businge et al., 2013). Furthermore, Lippert et al. (2005) proposed the proteasome complex as a molecular marker of embryo development. Consequently, the different proteasome and translation regulation factors profiles

observed in this study could be associated with the enhanced capacity of EMs subjected to heat-stress to produce Se's and with the different morphologies observed in Castander-Olarieta et al. (2019) among Se's originating from different temperature treatments.

In the same way, investigations focused on the function of thermoprotection mediated by HSPs have demonstrated that these proteins can work in association with functional stress granules and processing bodies (Miroshnichenko et al., 2005). Stress granules and processing bodies are dense aggregations in the cytosol composed of proteins and RNAs that appear when the cell is under stress. They have long been proposed to protect RNAs from harmful conditions, inhibiting the degradation of mRNAs involved in stress adaptation and acting as positive regulators of mRNA decapping during stress (Jang et al., 2020). Besides, recent research has demonstrated that stress granules seem to be important sites of post-transcriptional gene regulation (Gutierrez-Beltran et al., 2015). Interestingly, in this study the ribonuclease TUDOR 2, which is essential for the integrity and function of stress granules and processing bodies, was differentially expressed under high temperatures, confirming the role of stress granules during stress conditions and reinforcing the interconnection of HSPs and the posttranscriptional regulation machinery.

Other proteins involved in posttranscriptional regulation of gene expression have also been designed as top significant in this study. This is the case of protein ARGONAUTE 1D, which was found at higher concentrations under high temperature conditions, positively correlating with HSPs. Similar responses have also been observed in other plant model systems (Zhang et al., 2012). These types of proteins bind to short RNAs such as microRNAs (miRNAs) or short interfering RNAs (siRNAs), and repress the translation of mRNAs which are complementary to them. These gene expression regulatory mechanisms have been reported to be key players during the formation of temperature-dependent epigenetic memory in Norway spruce (Yakovlev & Fossdal, 2017).

Adenosylhomocysteinase, another protein related to epigenetic regulation, showed a decreasing pattern in Se's from high temperatures, especially at 60°C for 5 min. It controls methylation through regulation of the intracellular concentration of adenosylhomocysteine, a competitive inhibitor of S-adenosyl-L-methionine-dependent methyl transferase reactions. These data suggest that heat-stress might have derived in hypomethylation of Se's. Similar results were obtained by Lamelas et al. (2020), indicating that DNA methylation, together with posttranscriptional regulation mechanisms may be involved in the maintenance of acquired thermotolerance, providing signs of the establishment of an epigenetic memory. It would be interesting to perform further analyses to confirm this hypothesis and study its evolution along the whole SE process to see if the altered behaviour of the resulting somatic plants in Castander-Olarieta et al. (2020b) could be attributed to this fact. Besides, regulation of DNA methylation seems to be determinant during SE in *Pinus* spp. (Klubicová et al., 2017).

Heat also induced changes in the metabolism of Se's. The levels of acetyl-coenzyme A carboxylase carboxyl transferase subunit alpha, an enzyme that takes part in a sub-pathway of the fatty acid biosynthetic process, was clearly accumulated at high temperatures. Heat-stress increases membrane fluidity and as a result plants need to alter fatty acid composition of lipids to compensate for those changes (Escandón et al., 2017).

On the other hand, the glycolytic pathway, as well as the citric acid cycle and β-oxidation of fatty acids appeared to be less active in samples originating from high temperatures, as the proteins pyruvate dehydrogenase E1 component subunit beta-1, enolase and 3-ketoacyl-CoA thiolase 1 were found at lower levels. Parankusam et al. (2017) and Wang et al. (2018) also observed the same pattern when applying heat to chickpea and radish plants, respectively. A decrease in carbon catabolism has also been detected under favourable maturation conditions in *P. pinaster* EMs, leading to high quality embryos (Morel et al., 2014). However, other reports in *Picea glauca* and some broad-leaf woody

plants highlight the importance of high enolase activity as a marker of embryogenic character and normal embryo development (Lippert et al., 2005, Correia et al., 2012).

In the same way, the levels of enzymes involved in the synthesis of starch and sucrose (fructokinase-6 and sucrose-phosphate synthase 2) were reduced under high temperatures, as confirmed by the HPLC analysis for sucrose. Despite this fact, the levels of sucrose were considerably higher in all samples if compared with those from EMs in previous studies (Castander-Olarieta et al., 2019). The increase of sucrose during the formation of Se's has long been documented as a symbol of acquisition of desiccation tolerance (Businge et al., 2013).

The simultaneous decrease of the glycolytic activity and of the synthesis of disaccharides and polysaccharides would result in the accumulation of free soluble monosaccharides like glucose or fructose. However, this was not observed at the HPLC analysis, and thus, we could assume that these molecules might be serving as precursors for the synthesis of other specific compounds. In fact, inositol 3-phosphate synthase isozyme 3, the key enzyme for the synthesis of myo-inositol from glucose, was notably accumulated under high temperatures, as already observed in other plant species (Khurana et al., 2012). This molecule has been described to act as a compatible solute, maintaining plant cell turgor and stabilizing membranes and proteins (Bokszczanin & Fragkostefanakis, 2013). Nonetheless, the levels of mannitol and sorbitol, molecules previously identified as important osmolytes under heat and drought (Alhaithloul, 2019; Ivanov et al., 2019), were not detectable in radiata pine Se's using HPLC.

Likewise, the differential expression of phosphomannomutase, UDP-arabinopyranose mutase and UDP-glucuronic acid decarboxylase 4 also suggests a drift from glycolysis and starch accumulation towards the synthesis of cell-wall non-cellulosic polysaccharides. Specifically, UDP-glucuronic acid takes part in the synthesis of D-xylose, a constituent component of cell-wall polymers whose concentration has been demonstrated to change under heat-stress (Lima et al., 2013).

In this study two enzymes involved in the activation of rubisco, the first major carbon fixation protein of the Calvin cycle, were detected as being down-expressed at high temperatures. Numerous studies have reported a decrease of photosynthesis and rubisco activity under high temperatures (Parankusam et al., 2017, Li et al., 2019). The presence of these molecules results somewhat surprising as completely white pre-germinating Se's were used in this experiment. Consequently, it remains unclear whether their differential expression could influence the subsequent steps of the process. However, this is not the first work highlighting the presence of enzymes related to the carbon assimilation machinery in both zygotic and somatic embryos (Masmoudi et al., 1999; Niemenak et al., 2015).

In correlation with these enzymes we found a huge amount of proteins involved in oxidative stress response processes and in the synthesis of certain amino acids. All of them showed a decreasing tendency in Se's originating from high temperature conditions, probably conditioned by the decreased in central metabolism activity, the reduced availability of carbon skeletons and a simultaneous reduction of nitrogen assimilation (lower levels of ferredoxin--nitrite reductase). These proteins included an enzyme responsible of the synthesis of thiamine (thiamine biosynthetic bifunctional enzyme BTH1), which provides oxidative stress resistance via regulation of glucose metabolism (Kartal & Palabiyik, 2019), and 4-coumarate--CoA ligase-like 5, involved in the flavonoid and phenylpropanoid biosynthesis pathway, whose accumulation is essential for the prevention of oxidative damage (Eliášová et al., 2017). Phospholipid hydroperoxide glutathione peroxidase, which protects cells and enzymes from oxidative damage by catalysing the reduction of hydrogen peroxide, lipid peroxides and organic hydroperoxide, by glutathione (Yant et al., 2003), was also included in this group. Similar results were obtained for EXPORTIN 1A, a protein involved in heat-induced oxidative stress basal resistance (Wu et al., 2010), and threonine synthase, whose product, threonine, is the precursor of isoleucine (Johsi et al., 2010), other amino acid whose enzyme was down-expressed (ketol-acid reductoisomerase). Previous studies carried out in our laboratory (Castander-Olarieta et al., 2019) reported the accumulation of phenolic compounds and branched chain amino acids (isoleucine) in EMs at first

subculture after heat application, in opposition to the results from this study in Se's months later. As a result, we can assume that the response to oxidative stress is more relevant during short-term heat exposures, as observed by Escandón et al. (2017), rather than during acclimatization or acquired tolerance.

Finally, it is noticeable that several transmembrane transport proteins (porins) and sugar transporters were found at higher levels under high temperatures. Several authors have remarked the importance of these proteins during osmotic stress adaptation and thermal sensing (Brumós et al., 2009; Yakovlev et al., 2016). Based on the positive correlation of these proteins and the increased levels of specific compatible solutes such as myo-inositol, we can hypothesize that a synergistic response is taking place for an enhanced and controlled transport of osmolytes in Se's originating from heat stress conditions.

This study provides novel information about the long-term effect of heat-stress on radiata pine SE at the proteome level. Results indicated a complex and selective reorganization of the proteome, combined with the possible activation of certain epigenetic and posttranscriptional regulation mechanisms, as well as the accumulation of HSPs and chaperones and a drift in the carbohydrate metabolism towards the synthesis of fatty acids, specific compatible solutes and cell-wall remodelling carbohydrates. These results suggest that the application of stress during initial steps of the SE process could provoke delayed effects in embryogenic cells leading to changes in the subsequent stages up to plant level.

5. REFERENCES

Alhaithloul, H.A.S. (2019). Impact of combined heat and drought stress on the potential growth responses of the desert grass *Artemisia sieberi alba*: Relation to biochemical and molecular adaptation. *Plants* 8.

Allen, C.D., Macalady, A.K., Chenchouni, H., Bachelet, D., McDowell, N., Vennetier, M., et al. (2010). A global overview of drought and heat-induced tree mortality reveals emerging climate change risks for forests. *Forest Ecol. Manag.* 259, 660-684.

Anjo, S.I., Santa, C., and Manadas, B. (2015). Short GeLC-SWATH: a fast and reliable quantitative approach for proteomic screenings. *Proteomics* 15, 757-762.

Becker, J.D., Boavida, L.C., Carneiro, J., Haury, M., and Feijo, J.A. (2003). Transcriptional profiling of *Arabidopsis* tissues reveals the unique characteristics of the pollen transcriptome. *Plant Physiol.* 133, 713-725.

Bokszczanin, K.L., and Fragkostefanakis, S. (2013). Perspectives on deciphering mechanisms underlying plant heat stress response and thermotolerance. *Front. Plant Sci.* 4, 1-20.

Brumós, J., Colmenero-Flores, J.M., Conesa, A., Izquierdo, P., Sánchez, G., Iglesias, D.J., et al. (2009). Membrane transporters and carbon metabolism implicated in chloride homeostasis differentiate salt stress responses in tolerant and sensitive *Citrus* rootstocks. *Funct. Integr. Genomics* 9, 293.

Businge, E., Bygdell, J., Wingsle, G., Moritz, T., and Egertsdotter, U. (2013). The effect of carbohydrates and osmoticum on storage reserve accumulation and germination of Norway spruce somatic embryos. *Physiol. Plant.* 149, 273-285.

Castander-Olarieta, A., Montalbán, I.A., De Medeiros Oliveira, E., Dell'Aversana, E., D'Amelia, L., Carillo, P., et al. (2019). Effect of thermal stress on tissue ultrastructure and metabolite profiles during initiation of radiata pine somatic embryogenesis. *Front. Plant Sci.* 9, 1-16.

Castander-Olarieta, A., Moncaleán, P., Pereira, C., Pěnčík, A., Petřík, I., Pavlović, I., et al. (2020a). Cytokinins are involved in drought tolerance of *Pinus radiata* plants originating from embryonal masses induced at high temperatures. *Tree Physiol.* 1-15.

Castander-Olarieta, A., Pereira, C., Montalbán, I.A., Pěnčík, A., Petřík, I., Pavlović, I., et al. (2020b). Quantification of endogenous aromatic cytokinins in *Pinus radiata* embryonal masses after application of heat stress during initiation of somatic embryogenesis. Trees.

Černý, M., Kuklová, A., Hoehenwarter, W., Fragner, L., Novák, O., Rotková, G., et al. (2013). Proteome and metabolome profiling of cytokinin action in *Arabidopsis* identifying both distinct and similar responses to cytokinin down- and up-regulation. *J. Exp. Bot.* 64, 4193-4206.

Correia, S., Vinhas, R., Manadas, B., Lourenço, A.S., Veríssimo, P., and Canhoto, J.M. (2012). Comparative proteomic analysis of auxin-induced embryogenic and nonembryogenic tissues of the solanaceous tree *Cyphomandra betacea* (tamarillo). *J. Proteome Res.* 11, 1666-1675.

Correia, S.I., Alves, A.C., Veríssimo, P., and Canhoto, J.M. (2016). "Somatic embryogenesis in broad-leaf woody plants: what we can learn from proteomics", in *In Vitro* Embryogenesis in Higher Plants, eds. Germana, M., Lambardi, M. (Humana Press, New York), 117-129.

De Diego, N., Pérez-Alfocea, F., Cantero, E., Lacuesta, M., and Moncaleán, P. (2012). Physiological response to drought in radiata pine: phytohormone implication at leaf level. *Tree Physiol.* 32, 435-449.

De Diego, N., Sampedro, M.C., Barrio, R.J., Saiz-Fernández, I., Moncaleán, P., and Lacuesta, M. (2013a). Solute accumulation and elastic modulus changes in six radiata pine breeds exposed to drought. *Tree Physiol.* 33, 69-80.

De Diego, N., Rodríguez, J.L., Dodd, I.C., Pérez-Alfocea, F., Moncaleán, P., and Lacuesta, M. (2013b). Immunolocalization of IAA and ABA in roots and needles of radiata pine (*Pinus radiata*) during drought and rewatering. *Tree Physiol*. 33, 537-549.

De Diego, N., Saiz-Fernández, I., Rodríguez, J.L., Pérez-Alfocea, P., Sampedro, M.C., Barrio, R.J., et al. (2015). Metabolites and hormones are involved in the intraspecific variability of drought hardening in radiata pine. *J. Plant Physiol.* 188, 64-71.

Eliášová, K., Vondráková, Z., Malbeck, J., Trávníčková, A., Pešek, B., Vágner, M., et al. (2017). Histological and biochemical response of Norway spruce somatic embryos to UV-B irradiation. *Trees - Struct. Funct.* 31, 1279-1293.

Escandón, M., Valledor, L., Pascual, J., Pinto, G., Cañal, M.J., and Meijón, M. (2017). System-wide analysis of short-term response to high temperature in *Pinus radiata*. *J. Exp. Bot.* 68, 3629-3641.

Fehér, A. (2015). Somatic embryogenesis - stress-induced remodeling of plant cell fate. Biochim. Biophys. *Acta - Gene Regul. Mech.* 1849, 385-402.

Fleta-Soriano, E., and Munné-Bosch, S. (2016). Stress memory and the inevitable effects of drought: a physiological perspective. *Front Plant Sci.* 15, 7-143.

Galviz, Y.C.F., Ribeiro, R.V., and Souza, G.M. (2020). Yes, plants do have memory. *Theor. Exp. Plant Physiol.* 32, 195-202.

García-Mendiguren, O., Montalbán, I.A., Correia, S., Canhoto, J., and Moncaleán, P. (2016a). Different environmental conditions at initiation of radiata pine somatic embryogenesis determine the protein profile of somatic embryos. *Plant Biotechnol.* 33, 143-152.

García-Mendiguren, O., Montalbán, I.A., Goicoa, T., Ugarte, M.D., and Moncaleán, P. (2016b). Environmental conditions at the initial stages of *Pinus radiata* somatic embryogenesis affect the production of somatic embryos. *Trees - Struct. Funct.* 30, 949-958.

García-Mendiguren, O., Montalbán, I.A., Goicoa, T., Ugarte, M.D., and Moncaleán, P. (2017). Are we able to modulate the response of somatic embryos of pines to drought stress? *Act. Hortic.* 1155, 77-84.

Gutierrez-Beltran, E., Moschou, P.N., Smertenko, A.P., and Bozhkov, P. V. (2015). Tudor staphylococcal nuclease links formation of stress granules and processing bodies with mRNA catabolism in *Arabidopsis*. *Plant Cell* 27, 926-943.

Hasanuzzaman, M., Nahar, K., Alam, M.M., Roychowdhury, R., and Fujita, M. (2013). Physiological, biochemical, and molecular mechanisms of heat stress tolerance in plants. *Int. J. Mol. Sci.* 14, 9643-9684.

Heringer, A.S., Santa-Catarina, C., and Silveira, V. (2018). Insights from proteomic studies into plant somatic embryogenesis. *Proteomics* 18, 1700265.

Ivanov, Y.V., Kartashov, A.V., Zlobin, I.E., Sarvin, B., Stavrianidi, A.N., and Kuznetsov, V.V. (2019). Water deficit-dependent changes in non-structural carbohydrate profiles, growth and mortality of pine and spruce seedlings in hydroculture. *Environ. Exp. Bot.* 157, 151-160.

Jang, G.J., Jang, J.C., and Wu, S.H. (2020). Dynamics and functions of stress granules and processing bodies in plants. *Plants* 9, 1122.

Jiang, C., Bi, Y., Mo, J., Zhang, R., Qu, M., Feng, S., et al. (2020). Proteome and transcriptome reveal the involvement of heat shock proteins and antioxidant system in thermotolerance of *Clematis florida*. *Sci. Rep.* 10, 1-13.

Kartal, B., and Palabiyik, B. (2019). Thiamine leads to oxidative stress resistance via regulation of the glucose metabolism. *Cell Mol. Biol.* 65, 73-77.

Keller, M., Simm, S., Bokszczanin, K.L., Bostan, H., Bovy, A., Chaturvedi, P., et al. (2018). The coupling of transcriptome and proteome adaptation during development and heat stress response of tomato pollen. *BMC Genomics* 19, 1-20.

Klimaszewska, K., Morency, F., Jones-Overton, C., and Cookeb, J. (2004). Accumulation pattern and identification of seed storage proteins in zygotic embryos of *Pinus strobus* and in somatic embryos from different maturation treatments. *Physiol. Plant.* 121, 682-690.

Klubicová, K., Uvácková, L., Danchenko, M., Nemecek, P., Skultéty, L., Salaj, J., et al. (2017). Insights into the early stage of *Pinus nigra* Arn. somatic embryogenesis using discovery proteomics. *J. Proteomics* 169, 99-111.

Krishnan, H.B., Kim, W.S., Oehrle, N.W., Smith, J.R., and Gillman, J.D. (2020). Effect of heat stress on seed protein composition and ultrastructure of protein storage vacuoles in the cotyledonary parenchyma cells of soybean genotypes that are either tolerant or sensitive to elevated temperatures. *Int. J. Mol. Sci.* 21, 1-16.

Khurana, N., Chauhan, H., and Khurana, P. (2012). Expression analysis of a heat-inducible, Myo-inositol-1-phosphate synthase (MIPS) gene from wheat and the alternatively spliced variants of rice and *Arabidopsis*. *Plant. Cell. Rep.* 31, 237-251.

Kosová, K., Vítámvás, P., Prášil, I.T., and Renaut, J. (2011). Plant proteome changes under abiotic stress - Contribution of proteomics studies to understanding plant stress response. *J. Proteom.* 74, 1301-1322.

Kvaalen, H., and Johnsen, Ø. (2008). Timing of bud set in *Picea abies* is regulated by a memory of temperature during zygotic and somatic embryogenesis. *New Phytol.* 177, 49-59.

Lamelas, L., Valledor, L., Escandón, M., Pinto, G., Cañal, M.J., and Meijón, M. (2020). Integrative analysis of the nuclear proteome in *Pinus radiata* reveals thermopriming coupled to epigenetic regulation. *J. Exp. Bot.* 71, 2040-2057.

Lee, J.H., Hubel, A., and Schoffl, F. (1995). Derepression of the activity of genetically engineered heat shock factor causes constitutive synthesis of heat shock proteins and increased thermotolerance in transgenic *Arabidopsis*. *Plant J.* 8, 603-612.

Li, S., Yu, J., Li, Y., Zhang, H., Bao, X., Bian, J., et al. (2019). Heat-responsive proteomics of a heat-sensitive spinach variety. *Int. J. Mol. Sci.* 20, 1-21.

Lima, R.B., Dos Santos, T.B., Vieira, L.G.E., Ferrarese, M.D.L.L., Ferrarese-Filho, O., Donatti, L., et al. (2013). Heat stress causes alterations in the cell-wall polymers and anatomy of coffee leaves (*Coffea arabica* L.). *Carbohydr. Polym.* 93, 135-143.

Lippert, D., Jun, Z., Ralph, S., Ellis, D.E., Gilbert, M., Olafson, R., et al. (2005) Proteome analysis of early somatic embryogenesis in *Picea glauca*. *Proteomics* 5, 461-473.

Malik, M.K., Slovin, J.P., Hwang, C.H., and Zimmerman, J.L. (1999). Modified expression of a carrot small heat shock protein gene, Hsp17.7, results in increased or decreased thermotolerance. *Plant J.* 20, 89-99.

Masmoudi, R., Rival, A., Nato, A., Lavergne, D., Drira, N., and Ducreux, G. (1999). Carbon metabolism in *in vitro* cultures of date palm: the role of carboxylases (PEPC and RubisCO). *Plant Cell Tissue Organ Cult.* 57, 139-143.

Meiri, D., and Breiman, A. (2009). *Arabidopsis* ROF1 (FKBP62) modulates thermotolerance by interacting with HSP90.1 and affecting the accumulation of HsfA2-regulated sHSPs. *Plant J.* 59, 387-399.

Miroshnichenko, S., Tripp, J., Zur Nieden, U., Neumann, D., Conrad, U., and Manteuffel, R. (2005). Immunomodulation of function of small heat shock proteins prevents their assembly into heat stress granules and results in cell death at sublethal temperatures. *Plant J.* 41, 269-281.

Moncaleán, P., García-Mendiguren, O., Novák, O., Strnad, M., Goicoa, T., Ugarte, M.D., et al. (2018). Temperature and water availability during maturation affect the cytokinins and auxins profile of radiata rine somatic embryos. *Front. Plant Sci.* 9, 1-13.

Montalbán, I.A., and Moncaleán, P. (2018). "*Pinus radiata* (D. Don) somatic embryogenesis" in Step Wise Protocols for Somatic Embryogenesis of Important Woody Plants, eds. Jain, S., Gupta, P. (Springer, Cham, Switzerland), 1-11.

Montalbán, I.A., De Diego, N., and Moncaleán, P. (2012). Enhancing initiation and proliferation in radiata pine (*Pinus radiata* D. Don) somatic embryogenesis through seed family screening, zygotic embryo staging and media adjustments. *Acta Physiol. Plant.* 34, 451-460.

Morel, A., Teyssier, C., Trontin, J.F., Pešek, B., Eliášová, K., Beaufour, M., et al. (2014). Early molecular events involved in *Pinus pinaster* Ait. somatic embryo development under reduced water availability: transcriptomic and proteomic analysis. *Physiol. Plant.* 152, 184-201.

Niemenak, N., Kaiser, E., Maximova, S.N., Laremore, T., and Guiltinan, M.J. (2015). Proteome analysis during pod, zygotic and somatic embryo maturation of *Theobroma cacao*. J. *Plant Physiol.* 180, 49-60.

Paciolla, C., Paradiso, A., and de Pinto, M.C. (2016). "Cellular redox homeostasis as central modulator in plant stress response" in Redox State as a Central Regulator of Plant-Cell Stress Responses, eds. Gupta, D., Palma, J., Corpas, F. (Springer International Publishing), 1-23.

Pang, Z., Chong, J., Li, S., and Xia, J. (2020). MetaboAnalystR 3.0: toward an optimized workflow for global metabolomics. *Metabolites* 10, 186.

Parankusam, S., Bhatnagar-Mathur, P., and Sharma, K.K. (2017). Heat responsive proteome changes reveal molecular mechanisms underlying heat tolerance in chickpea. *Environ. Exp. Bot.* 141, 132-144.

Pascual, J., Canal, M.J., Escandon, M., Meijon, M., Weckwerth, W., and Valledor, L. (2017). Integrated physiological, proteomic, and metabolomic analysis of ultra violet (UV) stress responses and adaptation mechanisms in *Pinus radiata*. Mol. Cell. *Proteomics* 16, 485-501.

Passamani, L.Z., Barbosa, R.R., Reis, R.S., Heringer, A.S., Rangel, P.L., Santa-Catarina, C., et al. (2017). Salt stress induces changes in the proteomic profile of micropropagated sugarcane shoots. *PLoS One* 12, 1-21.

Pereira, C., Castander-Olarieta, A., Montalbán, I.A., Pěnčík, A., Petřík, I., Pavlović, I., et al. (2020). Embryonal masses induced at high temperatures in Aleppo pine: Cytokinin profile and cytological characterization. *Forests* 11, 807.

Perez, D.E., Hoyer, J.S., Johnson, A.I., Moody, Z.R., Lopez, J., and Kaplinsky, N.J. (2009). BOBBER1 is a noncanonical *Arabidopsis* small heat shock protein required for both development and thermotolerance. *Plant Physiol.* 151, 241-252.

Pinheiro, C., Guerra-Guimarães, L., David, T.S., and Vieira, A. (2014). Proteomics: State of the art to study Mediterranean woody species under stress. *Environ. Exp. Bot.* 103, 117-127.

Niu, Y., and Xiang, Y. (2018). An Overview of biomembrane functions in plant responses to high-temperature stress. *Front. Plant Sci.* 9, 915.

Schlaen, R.G., Mancini, E., Sanchez, S.E., Perez-Santángelo, S., Rugnone, M.L., Simpson, C.G., et al. (2015). The spliceosome assembly factor GEMIN2 attenuates the effects of temperature on alternative splicing and circadian rhythms. *Proc. Natl. Acad. Sci. U. S. A.* 112, 9382-9387.

Shen, H., Zhong, X., Zhao, F., Wang, Y., Yan, B., Li, Q., et al. (2015). Overexpression of receptor-like kinase ERECTA improves thermotolerance in rice and tomato. *Nat. Biotechnol.* 33, 996-1003.

Shinozaki, K., Yamaguchi-Shinozaki, K., and Seki, M. (2003). Regulatory network of gene expression in the drought and cold stress-responses. *Curr. Opin. Plant Biol.* 6, 410-417.

Taïbi, K., del Campo, A.D., Aguado, A., and Mulet, J.M. (2015). The effect of genotype by environment interaction, phenotypic plasticity and adaptation on *Pinus halepensis* reforestation establishment under expected climate drifts. *Ecol. Eng.* 84, 218-228.

The UniProt Consortium. (2019). UniProt: a worldwide hub of protein knowledge. *Nucleic Acids Res.* 47, 506-515.

Trontin, J.F., Klimaszewska, K., Morel, A., Hargreaves, C., and Lelu-Walter, M.A. (2016). "Molecular aspects of conifer zygotic and somatic embryo development: A review of genome-wide approaches and recent insights" in *In Vitro* Embryogenesis in Higher Plants, eds. Germana, M., Lambardi, M. (Humana Press, New York), 167-207.

Turgut-Kara, N., Arikan, B., and Celik, H. (2020). Epigenetic memory and priming in plants. *Genetica* 148, 47-54.

Valledor, L., Escandón, M., Meijón, M., Nukarinen, E., Cañal, M.J., and Weckwerth, W. (2014). A universal protocol for the combined isolation of metabolites, DNA, long RNAs, small RNAs, and proteins from plants and microorganisms. *Plant J.* 79, 173-180.

Walter, C., Find, J.I., and Grace, L.J. (2005). "Somatic embryogenesis and genetic transformation in *Pinus radiata*" in Protocols for somatic embryogenesis in woody plants, eds. Jain, S.M., Gupta, P.K. (Springer, Dordrecht), 491-504.

Wang, X., Liu, Z., Niu, L., and Fu, B. (2013). Long-term effects of simulated acid rain stress on a staple forest plant, *Pinus massoniana* Lamb: a proteomic analysis. *Trees* 27, 297-309.

Wang, R., Mei, Y., Xu, L., Zhu, X., Wang, Y., Guo, J., et al. (2018). Differential proteomic analysis reveals sequential heat stress-responsive regulatory network in radish (*Raphanus sativus* L.) taproot. *Planta* 247, 1109-1122.

Wu, S.J., Wang, L.C., Yeh, C.H., Lu, C.A., and Wu, S.J. (2010). Isolation and characterization of the *Arabidopsis* heat-intolerant 2 (hit2) mutant reveal the essential role of the nuclear export receptor EXPORTIN1A (XPO1A) in plant heat tolerance. *New Phytol.* 186, 833-842.

Yakovlev, I.A., Carneros, E., Lee, Y., Olsen, J.E., and Fossdal, C.G. (2016). Transcriptional profiling of epigenetic regulators in somatic embryos during temperature induced formation of an epigenetic memory in Norway spruce. *Planta* 5, 1237-1249.

Yakovlev, I.A., and Fossdal, C.G. (2017). In silico analysis of small RNAs suggest roles for novel and conserved miRNAs in the formation of epigenetic memory in somatic embryos of Norway spruce. *Front. Physiol.* 8.

Yant, L.J., Ran, Q., Rao, L., Van Remmen, H., Shibatani, T., Belter, J.G., et al. (2003). The selenoprotein GPX4 is essential for mouse development and protects from radiation and oxidative damage insults. *Free Radic Biol Med.* 34, 496-502.

Yuan, L., Wang, J., Xie, S., Zhao, M., Nie, L., Zheng, Y., et al. (2019). Comparative proteomics indicates that redox homeostasis is involved in high-and low-temperature stress tolerance in a novel wucai (*Brassica campestris* L.) genotype. *Int. J. Mol. Sci.* 20.

Zhang, T., Zhao, X., Wang, W., Pan, Y., Huang, L., Liu, X., et al. (2012). Comparative transcriptome profiling of chilling stress responsiveness in two contrasting rice genotypes. *PLoS One* 7.

6. SUPPLEMENTARY MATERIAL

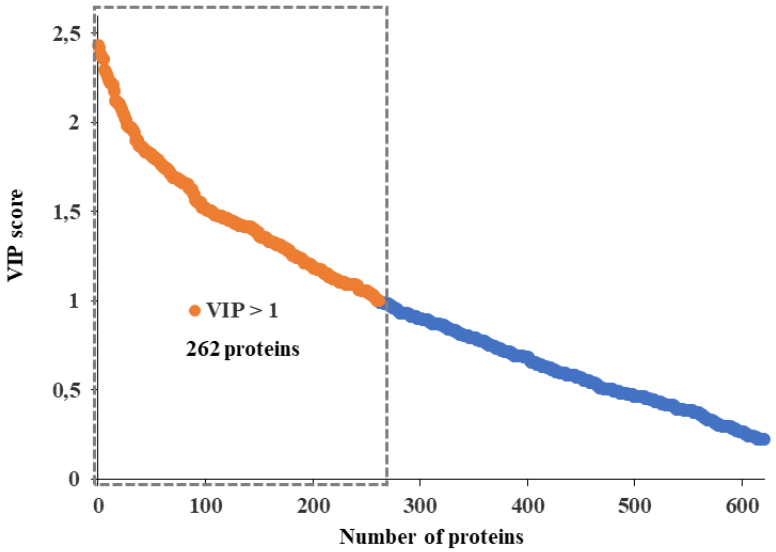

Supplementary Figure 1. Graphical representation of the results from the PLS-DA analysis showing that 262 proteins out of 758 presented VIP vales higher than 1. These proteins were considered the best classifiers and selected for further analyses.

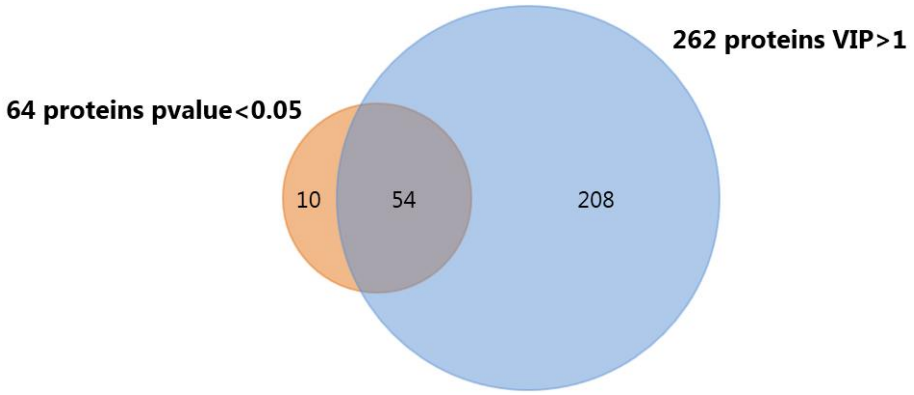

Supplementary Figure 2. Venn-diagram showing that 54 proteins were common between the 64 with $p < 0.05$ from the univariate analysis and the 262 resulted from the PLS-DA analysis with VIP > 1.

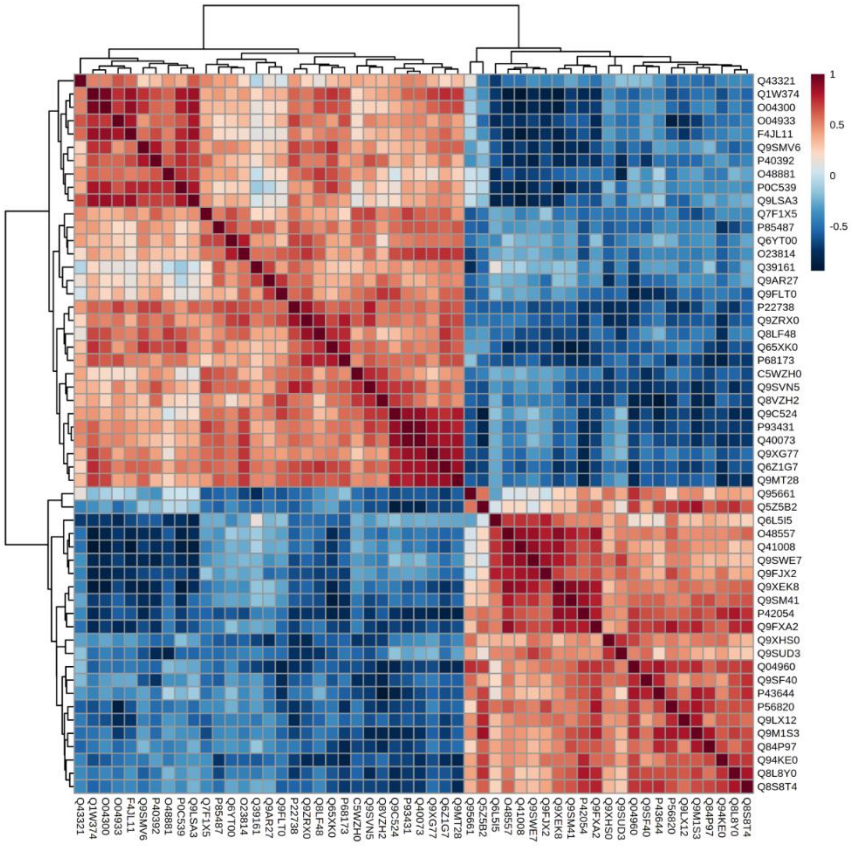

Supplementary Figure 3. Heatmap of the Spearman correlation coefficients of the 54 proteins selected by the combination of the Kruskal-wallis test ($p < 0.05$) and the PLS-DA analysis (VIP > 1) in somatic embryos of *P. radiata* originating from embryonal masses induced under high temperature conditions (Con1 = 23°C, 8 weeks, Cond2 = 40°C, 4 h, Cond3 = 60°C, 5 min). Red colour shows positive correlation whereas blue colour represents negative correlation among the selected proteins.

Supplementary Table 1. Proteins differentially accumulated in *P. radiata* somatic embryos obtained from embryonal masses induced under high temperature conditions (Con1 = 23°C, 8 weeks, Cond2 = 40°C, 4 h, Cond3 = 60°C, 5 min) according to the Kruskal-Wallis test ($p < 0.05$). Fold changes are presented as the ratio between one condition and the other.

		Fold Change			Kruskal-Wallis
Description	**Accession**	**Cond2/Cond1**	**Cond3/Cond1**	**Cond3/Cond2**	***p*-value**
60S ribosomal protein L3-2	P22738	0.84	0.55	0.65	0.005
Small heat shock protein, chloroplastic	Q95661	2.68	1.94	0.72	0.007
Mitochondrial outer membrane protein porin 2	Q6L5I5	0.86	1.37	1.60	0.010
Outer plastidial membrane protein porin	P42054	1.10	1.58	1.43	0.010

Multiple organellar RNA editing factor 8, chloroplastic/mitochondrial	Q9LKA5	1.34	1.06	0.79	0.010
DnaJ protein homolog	Q04960	1.42	1.51	1.06	0.013
Unknown protein 3 (Fragment)	P85487	0.66	0.47	0.71	0.013
Actin-2	P0C539	1.28	0.28	0.22	0.013
Malate dehydrogenase 1, cytoplasmic	P93819	0.73	1.02	1.39	0.016
Thiamine biosynthetic bifunctional enzyme BTH1, chloroplastic	O48881	1.03	0.71	0.69	0.016
Ketol-acid reductoisomerase	Q65XK0	0.75	0.39	0.52	0.016
Translationally-controlled tumor protein homolog	Q9ZRX0	0.85	0.68	0.80	0.017
Ribulose bisphosphate carboxylase/oxygenase activase	P93431	0.71	0.58	0.82	0.018
Probable fructokinase-6, chloroplastic	Q9C524	0.70	0.65	0.93	0.018
Ferredoxin--nitrite reductase	Q39161	0.59	0.64	1.09	0.018
60S ribosomal protein L23	Q9XEK8	0.98	1.37	1.40	0.018
Peroxisomal fatty acid beta-oxidation multifunctional protein	Q8W1L6	0.60	0.88	1.46	0.019
Pyruvate dehydrogenase E1 component subunit beta-1, mitochondrial	Q6Z1G7	0.89	0.69	0.78	0.020
Probable transcription factor PosF21	Q04088	0.61	0.51	0.83	0.020
Ribulose bisphosphate carboxylase/oxygenase activase A	Q40073	0.68	0.52	0.77	0.020
Sugar transporter ESL1	Q94KE0	1.19	1.77	1.49	0.021
Casein kinase II subunit alpha-2	Q9AR27	0.63	0.71	1.13	0.021
Protein translation factor SUI1 homolog	Q9SM41	1.02	1.23	1.21	0.021
Probable RNA-binding protein ARP1	Q9M1S3	1.36	1.74	1.28	0.022
Polyadenylate-binding protein 8	Q9FXA2	1.24	1.57	1.27	0.022
Aminopeptidase M1	Q8VZH2	0.56	0.50	0.89	0.025
Peptide methionine sulfoxide reductase A4, chloroplastic	Q336R9	0.71	1.20	1.69	0.025
60S ribosomal protein L30-3	Q9LSA3	1.02	0.76	0.75	0.026
Probable UDP-arabinopyranose mutase 1	O04300	1.02	0.54	0.53	0.026
Phosphomannomutase	Q1W374	0.95	0.65	0.68	0.026
Inosine triphosphate pyrophosphatase	C5WZH0	0.84	0.80	0.95	0.026
60S ribosomal protein L17	O48557	0.94	1.40	1.49	0.027
Probable sucrose-phosphate synthase 2	O04933	0.96	0.53	0.56	0.027
40S ribosomal protein S2-1	Q8L8Y0	1.15	1.36	1.18	0.028
60S ribosomal protein L4-1	Q9SF40	2.93	3.55	1.21	0.030
Serine carboxypeptidase 3	P21529	1.36	0.83	0.61	0.031
DEAD-box ATP-dependent RNA helicase 7	Q39189	0.84	1.99	2.37	0.031
Eukaryotic translation initiation factor 3 subunit D	P56820	1.20	1.46	1.22	0.032
Proteasome subunit alpha type-6	Q9XG77	0.88	0.81	0.91	0.032
Protein argonaute 1D	Q5Z5B2	1.67	1.66	0.99	0.032

Threonine synthase, chloroplastic	Q9MT28	0.87	0.77	0.89	0.033
Probable inositol 3-phosphate synthase isozyme 3	Q9LX12	1.97	3.20	1.62	0.034
Proteasome subunit alpha type-7-A	Q6YT00	0.86	0.79	0.92	0.036
Ras-related protein RIC1	P40392	0.59	0.36	0.60	0.037
V-type proton ATPase subunit E	Q9SWE7	1.02	1.25	1.22	0.038
Chaperone protein dnaJ A6	Q0JB88	1.25	1.07	0.86	0.038
3-ketoacyl-CoA thiolase 1, peroxisomal	Q8LF48	0.98	0.72	0.74	0.038
Importin subunit alpha-2	F4JL11	1.05	0.76	0.72	0.039
60S ribosomal protein L13a	O65055	0.74	0.95	1.28	0.039
Acetyl-coenzyme A carboxylase carboxyl transferase subunit alpha, chloroplastic	Q41008	1.06	1.46	1.37	0.039
40S ribosomal protein S12	Q9XHS0	1.06	1.37	1.29	0.039
Enolase	Q43321	0.93	0.04	0.05	0.039
Probable phospholipid hydroperoxide glutathione peroxidase	O23814	0.69	0.62	0.89	0.040
Cysteine proteinase inhibitor A	Q10992	0.80	1.06	1.32	0.040
Mitochondrial outer membrane protein porin 5	Q84P97	1.09	1.28	1.17	0.042
Aminomethyltransferase, mitochondrial	P54260	0.70	1.00	1.42	0.046
60S ribosomal protein L26-2	Q9FJX2	1.02	1.36	1.33	0.046
DnaJ protein homolog ANJ1	P43644	1.29	1.34	1.04	0.046
Ribonuclease TUDOR 2	Q9FLT0	0.67	0.69	1.03	0.047
Fumarate hydratase 1, mitochondrial	P93033	0.80	0.80	0.99	0.047
UDP-glucuronic acid decarboxylase 4	Q8S8T4	1.11	1.32	1.19	0.048
60S ribosomal protein L12	O50003	0.89	1.06	1.19	0.048
Cytochrome c oxidase subunit 6b-3	Q9SUD3	1.19	1.47	1.24	0.048
Uncharacterized protein At2g24330	Q9ZQ34	1.83	1.38	0.75	0.049

CHAPTER 5

Induction of radiata pine somatic embryogenesis at high temperatures provokes a long-term decrease in DNA methylation/hydroxymethylation and differential expression of stress-related genes

---

The content of this chapter corresponds to the published article "Castander-Olarieta, A., Pereira, C., Sales, E., Meijón, M., Arrillaga, I., Cañal, M.J., Goicoa, T., Ugarte, M.D., Moncaleán, P., Montalbán, I.A. (2020). Induction of radiata pine somatic embryogenesis at high temperatures provokes a long-term decrease in DNA methylation/hydroxymethylation and differential expression of stress-related genes. *Plants* 9, 1762."

1. INTRODUCTION

Epigenetic mechanisms refer to all the mitotically and/or meiotically heritable changes in patterns of gene expression that occur without alterations in DNA sequence (Iwasaki & Paszkowski, 2014). The regulation of gene expression is tightly influenced by the accessibility of genes for the transcriptional machinery, and the packaging grade of chromatin is fundamental during these processes (Bravo et al., 2017). Multiple mechanisms have been found to define the distinct chromatin states and accessibility of regulatory elements. Among them, covalent modifications (acetylation, methylation, phosphorylation, ubiquitination and sumoylation) of histone proteins tails, addition of histone variants, the position and spacing of nucleosomes and cytosine methylation of the DNA are the main targets of current epigenetic studies (Lämke & Bäurle, 2017). Besides, non-coding RNAs, including small RNAs, are currently gaining special interest as novel epigenetic regulators influencing the distribution of epigenetic marks and the expression of specific genes at both transcriptional ad post-transcriptional levels (Yakovlev & Fossdal, 2017).

DNA methylation is the most studied epigenetic mark due to its occurrence in plants and mammals, its stability and its role in gene regulation and genome structure maintenance through transposon silencing (Amaral et al., 2020). Methylation is site specific and usually occurs in the fifth carbon position of cytosines in the following sequences: CG, CHG and CHH (where H = A, T or C) (Kumar et al., 2013). Although DNA methylation has frequently been linked with gene expression repression, its specific location in, for example, CG gene body sequences, has most often been associated with transcriptional activity (Dubin et al., 2015).

The recent progress in genome-wide analysis of epigenetic marks has demonstrated that these mechanisms are essential for the adaptation of plants to changing environments and stress conditions through phenotypic plasticity (Boyko & Kovalchuk, 2008). This adaptive response is based on the ability to produce different phenotypes in response to different environments, and results of especial relevance in the case of non-mobile and

long-living organisms like trees under the current climate change situation (Perrone & Martinelli, 2020). In this sense, variations of DNA methylation levels have been documented under different stress conditions including heat (Tittel-Elmer et al., 2010; Li et al., 2016).

Most of the epigenetic marks activated under stress events are reverted when the environmental constrain is no longer present. However, plants can maintain part of those marks developing the capacity to remember the stress episode (stress priming) and establishing an epigenetic memory that leads to both temporary or sustained structural, genetic and biochemical modifications that prepare plants to respond more efficiently to future stress exposures (Show et al., 2018). Furthermore, in some cases a crosstalk among different stimuli can occur, leading to multiple stress memory acquisition (cross-priming) (Blödner et al., 2005).

There are multiple examples in nature that support this phenomenon. Vernalization, in which cold exposure of winter annual plants synchronizes flowering to the optimal season, is a clear example (Bouché et al., 2017). Memory of pathogen attack, formerly referred to as systemic acquired resistance, is well documented (Conrath et al., 2015; Kumar et al., 2020, Morcillo et al., 2020), and the chemical priming of seeds to enhance stress tolerance and pathogen resistance of young plants after germination is a usual agronomic practice (Lämke & Bäurle, 2017). Some of the best-known examples of epigenetic memory in forest tree species are found in Norway spruce, for which the environmental conditions during both zygotic and somatic embryogenesis (SE) seem to modulate the timing of bud set and bud burst of plants years later (Kvaalen & Johnsen, 2008). In the case of poplar trees, differences in DNA methylation of stress-responsive genes and hormonal pathways have been observed in winter-dormant shoot apical meristems after drought events during the vegetative period (Le Gac et al., 2018).

In addition to the common methylation of cytosine, in recent years other modifications of cytosine at the same position, such as the oxidized form 5-hydroxymethylcytosine (5hmC), have gained special attention because of their role as demethylation intermediates and transcriptional regulators during many cellular and developmental

processes in mammals and fungi (Shi et al., 2017). Although the presence of 5hmC in plants is still ambiguous, increasing evidence supports its non-casual enzymatic origin (Moricová et al., 2013), and its specific and conserved location in several plant genomes, potentially contributing to plant development and homeostasis control (Wang et al., 2015). Besides, the latest studies have revealed non-negligible quantities of this molecule in the DNA of a conifer species (Yakovlev et al., 2019).

In previous studies we have observed that the application of high temperatures during initiation of *Pinus radiata* and *Pinus halepensis* SE modulates not only the success of the different stages of the process, but also the morphology and biochemical status (hormones, metabolites) of embryonal masses (EMs) and somatic embryos (Se's) (Castander-Olarieta et al., 2019, 2020a, 2020b; Pereira et al., 2020). Moreover, those changes can have long-lasting effects determining the *ex vitro* behaviour of somatic plants years later at both control and stress conditions (Castander-Olarieta et al., 2020a).

As a result, in this study we have tried to evaluate if all those changes can be attributed to the establishment of an epigenetic memory based on specific modifications of cytosine residues by heat. To this aim, high liquid chromatography (HPLC) coupled to mass spectrometry has been employed, which allows a sensible and precise identification of the different nucleotides, including 5mhC, and requires little amount of genomic DNA starting material (Fernández et al., 2017). In parallel, the differential expression of putative stress-related genes throughout the SE process has been analysed to assess if the observed epigenetic changes have provoked modifications at the transcriptome level.

2. MATERIALS AND METHODS

2.1. Plant material and heat stress experiment

Seeds of *P. radiata* were extracted from green female cones collected in June 2018 from five genetically different open-pollinated trees, and surface sterilized following Montalbán et al. (2012). Megagametophytes enclosing immature zygotic embryos were

excised out aseptically and placed horizontally onto Petri dishes containing Embryo Development Medium (EDM, Walter et al., 2005), supplemented with 3.5 g L^{-1} gellan gum (Gelrite®, Duchefa, Haarlem, The Netherlands). At this point, explants were subjected to different temperature and incubation time periods: 23°C, 8 weeks; 40°C, 4 h; 60°C, 5 min. The culture medium was pre-warmed for 30 min before the start of the experiment and at the end all the megagametophytes were kept at 23°C in darkness. Eight megagametophytes were used per Petri dish and ten Petri dishes per treatment, comprising a total of 1200 megagametophytes, including all mother trees.

After 8 weeks on the same medium, emerging EMs bigger than 3-5 mm in diameter were separated from the megagametophytes and subcultured to fresh EDM medium. After 14 days, a small part from each EMs was frozen in liquid nitrogen and stored at -80°C for subsequent molecular analyses (T1). The other part was transferred to medium of the same composition but 4.5 g L^{-1} gellan gum fortnightly until maturation 4 weeks later. At this point, actively proliferating EMs were selected and half of the embryogenic tissue was frozen in liquid nitrogen as explained before (T2). The other part was subjected to maturation as described in Montalbán & Moncaleán (2018). Six replicates (Petri dishes) per ECL and 10 ECLs per treatment were used. After 12 weeks, 100 mg of mature and well-formed Se's were frozen in liquid nitrogen (T3).

The remaining Se's were placed with root caps pointing downwards on Petri dishes with half-strength macronutrients LP medium (1/2 LP, Quoirin & Lepoivre 1977 modified by AitkenChristie et al., 1988) supplemented with 2 g L^{-1} activated charcoal and 9 g L^{-1} gellan gum (Difco® Agar granulated, Becton Dickinson, Franklin Lakes, New Jersey, USA) at an angle of approximately 60°. For the first 7 days Petri dishes were placed under dim light (10 μmol m^{-2} s^{-1}) and then maintained for 5 weeks under 16-h photoperiod at 100 μmol m^{-2} s^{-1} provided by cool white fluorescent tubes (TFL 58 W/33; Philips, Amsterdam, The Netherlands). Successfully germinated seedlings were subcultured to glass jars (diameter 59 and height 66 mm, Sigma-Aldrich, St. Louis, Missouri, USA) with medium of the same composition.

After 6 weeks, part of the seedlings that had developed a proper root system and new non-cotyledonary needles were entirely frozen in liquid nitrogen (T4) and the rest transferred *ex vitro* to 43 cm^3 pots containing blond peat moss (Pindstrup, Ryomgård, Denmark): vermiculite (8:2, v/v) in a greenhouse under controlled conditions as described in Castander-Olarieta et al. (2020a). Growing saplings with more than 5 cm height were transplanted to bigger pots with new substrate of the same composition but adding 3 g L^{-1} Osmocote® Topdress fertilizer (Everris, Geldermalsen, The Netherlands) and watered regularly for one year. Then, needles form the apical area of the somatic plants were frozen in liquid nitrogen (T5) and stored at -80°C until DNA and RNA extractions. At this point plants presented similar phenotypic traits (colour and length of needles, number of shoots, etc) and no differences in the mean height was observed among plants originating from different temperature treatments (23 °C: 32.3 ± 3 cm; 40 °C: 32.2 ± 2.5 cm; 60 °C: 31.5 ± 1.3 cm).

2.2. Global DNA methylation (GDM)/hydroxymethylation analysis

Genomic DNA was extracted from samples collected at T2 and T5 (proliferating EMs and needles of one-year-old somatic plants growing in the greenhouse, respectively). For T2 samples five ECLs were used per treatment and 15 mg of lyophilized tissue was used as starting material, while for T5 samples three ECLs per treatment and two clones per ECL were used (a total of six samples per treatment). As starting material 100 mg of fresh tissue grounded in liquid nitrogen to a fine powder was employed. All samples were extracted in 800 µl preheated (60°C) buffer containing 2% CTAB, 1.4 M NaCl, 20 mM EDTA, 100 mM Tris-HCl, 2% PVP (w/v), 8 mM ascorbic acid and 5 mM DIECA, supplemented with 89 mM β-mercaptoethanol. Samples were incubated at 65°C for 30 min (gently shaking each 10 min), followed by the addition of 500 µl chloroform/isomylalcohol (24:1, v/v). After vortexing and centrifugation at 10,000 rpm for 5 min, the aqueous phase was transferred to a new tube and RNA was digested by the addition of 10 µl of RNase A (50 mg/mL, Sigma-Aldrich) at 37ºC for 1 h. Phase separation by chloroform/isoamylalcohol was repeated once and then DNA was precipitated by the addition of 600 µl cold isopropanol (-20°C) and centrifugation at 11,000 rpm for 10 min at 4°C. DNA pellet was washed with 1 ml ethanol 50%,

centrifuged at 14,000 rpm for 5 min, and the supernatant discarded. Pellets were air-dried and DNA was resuspended in 50 µl ultra-pure water. Quantification was carried out using a Nanodrop™ 2000 (Thermo Fisher Scientific, Waltham, Massachusetts, USA).

Genomic DNA was hydrolysed as follows: ten microlitres of DNA containing approximately 1 µg DNA were denaturalised at 100°C for 2 min and digested by the addition of 1.13 µl sodium acetate 50 mM and zinc chloride 40 mM solution and 2.5 µl nuclease P1 (2.5 U, Sigma-Aldrich). Samples were incubated at 37°C overnight. Then 2.5 µl Tris buffer (0.5 M, pH 8.3) and 1 µl alkaline phosphatase (0.3 U, Sigma) were added and incubated at 37°C for 2 h and 30 min. After the addition of 40 µl ultra-pure water and precipitation with 200 µl pure ethanol (-20°C) plus centrifugation at 15,000 for 15 min (4°C), supernatants were transferred to low-binding tubes and evaporated using a vacuum-concentrator. Finally, digested free nucleotides were resuspended in 100 µl ultra-pure water.

Methylation and hidroxymethylation levels were analysed on a 1200 Series HPLC system coupled to a 6410 Triple Quad mass spectrometer from Agilent Technologies (Santa Clara, USA). The chromatographic separation was performed on a Zorbax SB-C18 column (2.1 × 100 mm, 3.5 µm, Agilent Technologies). The mobile phase was 11% methanol and 0.1% formic acid in water and 5 µl of samples were injected in the column at a flow rate of 0.1 mL min^{-1}. The electrospray ionization source (ESI) was operated in the positive ion multiple reaction monitoring mode (MRM) set to an ion spray voltage of 3,500 V, 40 psi for nebulizer and source temperature at 350°C. The intensity of specific MH^+ → fragment ion transitions were recorded (5mC m/z 242 → 126, 5hmC m/z 258 → 142 and C m/z 228 → 112). Identification of cytosine, 5mC and 5hmC were assessed by injection of commercial standards (5-Methylcytosine & 5-Hydroxymethylcytosine DNA Standard Set, Zymo Research, Irvine, California, USA) under the same LC-ESI-MS/ MS-MRM conditions. The measured percentage of 5mC and 5hmC in each experimental sample was calculated from the MRM peak area divided by the combined peak areas for 5mC plus 5hmC plus cytosine (total cytosine pool). In the case of 5hmC, its percentage with respect to the total modified cytosine pool was also calculated.

2.3. RNA extraction

Extraction of total RNA from samples at T1 (EMs after first subculture) and T4 (*in vitro* seedling) was performed using the RNeasy Plant Mini Quit (Qiagen, Venlo, The Netherlands) with slight modifications depending on the type of sample. For T1 samples, three pools of 300 mg from different ECLs were employed for each temperature treatment. In this case samples were grinded directly in the lysis buffer with a plastic piston. For T4 samples, 3 ECLs per treatment and 100 mg of fresh material per sample were employed. To eliminate any residual genomic DNA, RNA samples were treated with Recombinant DNase I (RNase-free, Takara Bio, Shiga, Japan) according to the manufacturer's protocol. The quantity of isolated RNA both before and after DNase treatment was measured using a Nanodrop™ 2000. RNA integrity and potential DNA contamination were assessed by agar gel electrophoresis.

RNA extractions from T2 (proliferating EMs) and T3 (Se's) samples were performed using five ECLs per treatment and following the combined protocol described by Valledor et al. (2014) with modifications. This protocol was used because it enables the simultaneous extraction of proteins, metabolites and RNA. The results from proteins and metabolites extraction will be discussed in further experiments. 0.8 ml and 2 ml of cold extraction buffer were added to 100 mg of grinded T3 samples and 500 mg of grinded T2 samples, respectively. Then, samples were centrifuged, the supernatant discarded, and pellets were washed with 1 ml and 2 ml of 0.75% (v/v) β-mercaptoethanol in 100% methanol (for T2 and T3 samples, respectively). After another centrifugation step, the supernatant was discarded, and the washing step was repeated once. Pellets were then air dried and dissolved in 1 ml of pellet solubilization buffer for incubation at 37°C in a thermal shaker for 20 min. Then, samples were centrifuged, and the supernatants were transferred to silica columns to bind DNA. After 1 min of incubation, columns were centrifuged and the flowthrough was mixed with 300 µl and 600 µl of acetonitrile for each sample type. The mix was transferred to a new silica column, incubated for 1 min, and centrifuged. Columns with bound RNA were washed as described in Valledor et al. (2014), with an on-column digestion of DNA after the first washing (DNase I Set, Zymo

Research), and eluted twice, first with 50 µl and then with 75 µl of RNase free-water for maximum yield.

For samples at T5, the previously described protocols were not effective and thus, a different protocol was used. 100 mg of liquid nitrogen grinded samples (three ECLs per treatment and two clones per ECL) were added to 2 ml tubes containing pre-heated (65°C) extraction buffer (100 mM Tris, 30 mM EDTA, 2 M NaCl, 3% CTAB, 2% PVP-40, 2% PVPP, 4% β-mercaptoethanol). After vortexing, samples were incubated at 65°C for 5 min and 800 µl of chloroform/isoamylalcohol (24:1, v/v) were added. Samples were vigorously mixed, incubated on ice for 2 min and centrifuged at 11,000 rpm for 10 min at 4°C. The aqueous phase was saved and precipitated for 1 h at 4°C by the addition of ¼ (v/v) LiCl (10M). Then, samples were centrifuged at 11,000 for 30 min at 4°C and the supernatant was discarded. Pellets were washed with 500 µl cold ethanol (70%), centrifuged for 5 min at 4°C, air dried for 15 min and resuspended in 45 µl RNase free-water. After digestion of DNA using DNase I Set (Zymo Research), 600 µl of water and 700 µl of chloroform/isoamylalcohol (24:1, v/v) were added. The following steps (precipitation, washing…) were carried out as previously described and finally, RNA pellets were resuspended in 50 µl of RNAse free-water.

2.4. Expression pattern of stress-related genes

The expression level of 6 genes related to thermal (Escandón et al., 2017) and drought stress (Qin et al., 2014) was determined by qRT-PCR from the RNA extracted at different stages of SE (T1, T2, T3, T4, T5). The genes analysed were the following: *50S RIBOSOMAL_L6_CHP* (*50SR*), *SUPEROXIDE DISMUTASE [Cu-Zn]* (*SOD*), *TRANSCRIPTION FACTOR APFI* (*APFI*), *HSP20 FAMILY PROTEIN* (*HSP20*), *ADH_SF_ZN_TYPE* (*ADH*) and *DEHYDRATION INDUCED PROTEIN* (*DI19*). cDNA was synthetized from 1000 ng of RNA using the PrimeScript RT Reagent Kit (Takara) and random hexamers as primers following the manufacturer's instructions. Relative gene expression was measured by qPCR (StepOne Plus, Thermo Fisher Scientific). Three technical replicates were analysed per sample using *ACTIN* (*ACT*) as endogenous control. Primer efficiencies were estimated by template dilutions and the equation $E = 10^{(-1/slope)}$, which gave values

always greater than 1.81. Reactions were carried out in 20 µl containing 1 µg of cDNA, 0.3 µM of each primer and the SYBR green master mix (Takara Bio, Shiga, Japan). The PCR conditions were: initial denaturation at 95°C for 20 s, followed by 40 cycles of 95°C for 3 s and 60°C for 30 s. The relative transcript levels were normalized using ACT, and the relative expression of each gene (R) was calculated on the basis of ΔC_t values (Livak & Schmittgen, 2001) using the following formula: $R = 2^{-\Delta Ct}$. Then, the fold change between expression values obtained at control treatment of 23°C and treatments at 40°C and 60°C was calculated in logarithmic scale. Gene specific primers for all genes were as described by Escandón et al. (2017) and Alvarez et al. (2016).

2.5. Statistical analysis

To assess the effect of the treatments on both methylation/hydroxymethylation levels and gene expression values, a usual analysis of variance (ANOVA) was conducted. A Tukey´s post-hoc test ($\alpha = 0.05$) was used for multiple comparisons. When required, the ECL was included in the model as a random effect to improve the fit and analyse the effect of treatments more accurately by accounting for heteroscedasticity in the data. When the analysis of variance did not fulfil the normality hypothesis a Kruskal-Wallis test was performed.

3. RESULTS

3.1. Global DNA methylation/hydroxymethylation analysis

Global DNA methylation analysis in T2 samples (proliferating EMs) revealed high levels of 5-methylcytosine (5mC) in all treatments (around 40%), but no significant differences among them. However, the differences observed were on the verge of statistical significance ($p = 0.0934$), being the treatment at 60°C for 5 min the one presenting the lowest global methylation values. These levels in the other two treatments, including control temperature of 23°C, were slightly higher, being the 40°C for 4 h treatment the one presenting the highest difference (3.03%) with respect to the treatment with the lowest values (60°C for 5 min) (Table 1).

Although 5hmC was undetectable in most of the T2 samples, a fact that made impossible the comparison among treatments, in the sample presenting the highest total cytosine pool very low levels of 5hmC could be detected (0.004%; data not shown). As a result, we can assume that this molecule was present in the rest of the samples but its levels were under limit of detection due to a lower content of total cytosine residues.

Regarding the results from T5 samples, the observed GDM rates were similar to those from EMs (around 40%), but in this case statistically significant differences were observed among treatments. The pattern was similar to the one observed previously; the levels of 5mC were considerably lower at treatment 60°C for 5 min (almost 3% if compared with the other two treatments), but in this case both control treatment at 23°C and treatment at 40°C for 4 h showed very similar GDM rates (Table 1).

Table 1. Methylation and hydroxymethylation rates of *Pinus radiata* proliferating embryonal masses collected at T2 and needles of one-year-old somatic plants (T5) originating from megagametophytes cultured under different temperature treatments (23°C, 8 weeks; 40°C, 4 h; 60°C, 5 min). Data are presented as mean values ± SE. Significant differences among treatments at $p < 0.05$ are indicated by different letters.

T2		T5			
Treatment	**5mC %**	**Treatment**	**5mC %**	**5hmC %**	**5hmC/5mC × 100**
23° C, 8 weeks	39.28 ± 1.06[a]	23° C, 8 weeks	40.45 ± 0.53[a]	0.0175 ± 0.0024[a]	0.044 ± 0.0071[a]
40° C, 4 h	40.85 ± 0.36[a]	40° C, 4 h	40.39 ± 0.22[a]	0.0103 ± 0.0005[b]	0.026 ± 0.0012[b]
60° C, 5 min	37.82 ± 1.06[a]	60° C, 5 min	37.64 ± 0.33[b]	0.0101 ± 0.0003[b]	0.027 ± 0.0009[b]

In opposition to the results obtained from proliferating EMs, in one-year-old somatic plant needles the levels of 5hmC were detectable in almost all the samples analysed (83.3%). Despite being considerable low rates, the values observed were more than twice as high as those from EMs. Considering the effects of temperature, significant differences were observed among treatments. Hydroxymethylation rates were appreciably lower in both groups of samples originating from EMs subjected to heat-stress. In this case, the levels of both treatments (40°C, 4 h and 60°C, 5 min) showed very similar values. The same pattern was detected when analysing the percentage of hydroxylated cytosine forms with respect to the total amount of modified cytosine bases (5hmC/5mC × 100). On this subject, both treatments at high temperatures were the

ones with the lowest 5hmC rates, and the values between them were also very similar (Table 1).

3.2. Expression pattern of stress-related genes

The relative expression analysis of genes involved in heat and drought stress responses revealed that the application of high temperatures during induction of SE in radiata pine resulted in the differential expression of certain genes with respect to the control treatment of 23°C throughout the entire process and in somatic plants more than one year later. The results also showed that in most of the cases the differential expression of the genes changed along the different stages of SE, not following a defined pattern.

For samples at T1, significant differences were found for three of the six genes analysed: *APFI*, *HSP20* and *50SR* (Figure 1; T1). The most evident changes were observed for *HSP20*. In both 40°C and 60°C treatments, the relative expression of this gene was considerably lower than in control temperature of 23°C, presenting high fold change values. The same pattern was observed for 50SR (lower expression at both 40°C and 60°C treatments), but with lower fold changes. In the case of the transcription factor APFI however, the differences were only significant for the 40°C treatment, and its expression was just slightly lower than that of the control treatment.

Samples at T2 showed differential expression of *APFI*, *DI19* and *ADH* (Figure 1; T2). As in T1, the gene *APFI* presented small significant differences, but at this stage its expression increased in EMs originating from the treatment at 60°C for 5 min, while no differences were observed in those from the 40°C treatment. *ADH* and *DI19* showed a decreasing pattern, with significant differences at both high temperature treatments for *ADH* and only at 40°C for *DI19*. It is also noticeable that despite not being significant, the expression of *HSP20* at this stage was also lower at high temperatures, especially at 60°C for 5 min. In any case, fold changes were lower if compared with T1.

In mature Se's (T3), genes *50SR* and *SOD* presented lower expression values at high temperatures than at control conditions (Figure 1; T3). Regarding *50SR*, the expression pattern was similar to the one observed at T1, with significant differences in both

treatments, while in the case of *SOD* significant differences were only detected at 60°C. As in T2, fold changes were low for all the analysed genes.

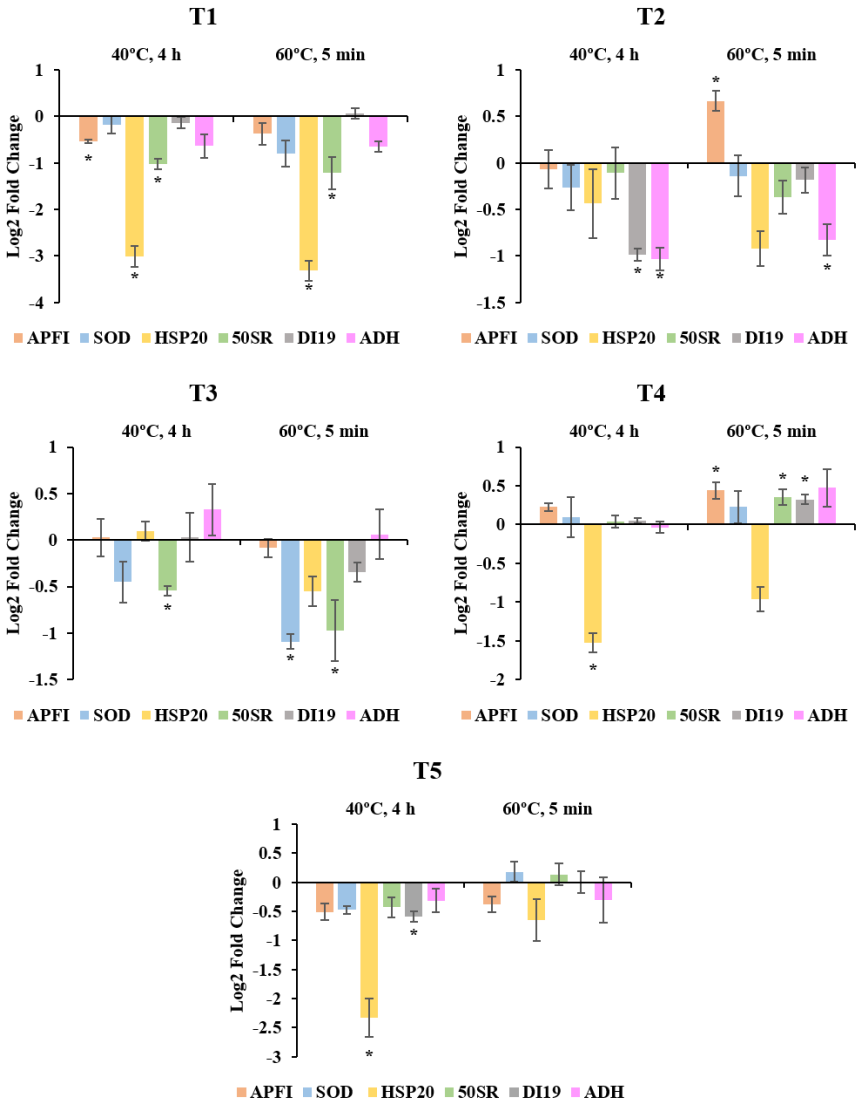

Figure 1. Fold-relative gene expression of six stress-related genes (*APFI*, *SOD*, *HSP20*, *50SR*, *DI19* and *ADH*) along the different stages of *Pinus radiata* somatic embryogenesis (T1, T2, T3, T4 and T5) between samples originating from different temperature conditions during induction (23°C, 8 weeks; 40°C, 4 h; 60°C, 5 min). Data are presented as mean values ± SE. * Denotes significant differences at $p < 0.05$ among high temperature treatments with respect to the control temperature of 23°C.

At T4, *HSP20* presented the most noticeable results. Although both treatments at high temperatures showed a decreasing tendency, only the expression levels at 40°C for 4 h were statistically significant. Certain genes were up-regulated in 60°C treatment (*APFI*, *50SR* and *DI19*), but their fold changes were very low (Log2 Fold change < 0.5). With the exception of *HSP20*, the relative expression of the rest of the genes was very similar between control conditions and high temperatures (Figure 1; T4).

Very similar results were obtained at T5, but with an enhanced response of *HSP20*. As in *in vitro* plantlets, the expression of this gene was notably down-regulated in needles of one-year-old somatic plantlets at 40°C. In this case, the fold change was higher, reaching values similar to those from T1. At 60°C treatment however, the differences observed for *HSP20* were low and not significant. Following with this treatment, it is worth mentioning that the increase observed for *APFI*, *50SR* and *DI19* at T4 were no longer present at this stage, while at 40°C treatment *DI19* showed slightly lower significant values (Figure 1; T5).

4. DISCUSSION

Epigenetics has been demonstrated to be essential for long-lifespan organisms with complex life-cycles like forest tree species, regulating many developmental and stress-response processes. During the annual cycle, for example, different developmental transitions like bud set in autumn and bud burst in spring are governed by changes in DNA methylation patterns (Santamaría et al., 2009). Besides, these epigenetic alterations and the establishment of epigenetic marks strongly contribute to the development of phenotypic plasticity and environmental stress memory through the differential expression of specific genes and the regulation of transposable elements mobility (Amaral et al., 2020). Despite this fact, only limited studies have been implemented with trees and we still lack information about the multiple regulatory layers connecting epigenetic variations, gene expression and phenotypic traits in trees.

The combination of natural or artificially-induced epigenetic diversity exploitation and selection of epigenetic marks could provide fitness advantage to clonal trees with

limited genetic diversity under the on-going climate change situation, highlighting the potential role of epigenetics in tree improvement and breeding (Show et al., 2018). In this regard, embryo development and seed maturation seem to be crucial periods for the formation of stable epigenetic modifications (Yakovlev et al., 2016). This could be used as a valuable tool during clonal propagation systems (i.e., SE) to produce epigenetic variants by the application of controlled stresses early in the life of the plant (García-Mendiguren et al., 2017).

Following this idea, the GDM analysis carried out in this study during radiata pine SE revealed that proliferating EMs were highly methylated (> 37% in all treatments) if compared with several studies carried out in EMs of *P. radiata* and other *Pinus* species. Bravo et al. (2017) observed GDM rates lower than 5% in similar-aged EMs of radiata pine and results in *Pinus nigra* underlined that the formation of bipolar structures in EMs can only be obtained when 5mC levels are not higher than 18% (Noceda et al., 2009). Nonetheless, micromorphological analyses carried out in our laboratory confirmed the presence of polarised structures presenting different developmental and organizational stages under similar culture conditions in radiata pine (Castander-Olarieta et al., 2019).

Induction of SE and cell dedifferentiation is usually accompanied by a drastic hypomethylation of DNA, enabling the expression of key genes involved in SE such as WUS and BBM (De la Peña et al., 2015). Besides, embryogenic potential is usually correlated with low 5mC levels, as observed in many studies with both angiosperms and gymnosperms where embryogenic cell lines (ECLs) able to develop the whole embryogenic program and produce plants showed lower DNA methylation rates than non-embryogenic calli (Miguel & Marum, 2011; Corredoira et al., 2017).

However, some studies suggest that the GDM rate of EMs could be species and developmental stage specific. In two *Acca sellowiana* accessions, Fraga et al. (2012) reported levels of DNA methylation ranging from 22.6% to 44.3% during 30 days of culture. Teyssier et al. (2013) observed methylation rates of 45.8% in EMs of a hybrid larch (*Larix × eurolepsis*) and showed that when those EMs were subjected to

maturation, methylation drastically increased up to 61.5% in the first week, followed by a decrease to 53.4% in mature cotyledolary Se's. Likewise, during microspore SE in *Brassica napus* a decrease in DNA methylation occurs, while during embryo differentiation GDM increases (Solís et al., 2012). Several authors even highlighted the association between increased methylation levels during Se's differentiation, high cell division rates, and activation of embryogenic gene expression program (Che et al., 2006). As a result, the methylations rates observed in radiata pine EMs in this study could be associated with the specific developmental stage at which they were collected.

The results obtained in needles of one-year-old somatic plants are in agreement with previous studies carried out in radiata pine trees (Fraga et al., 2002a, 2002b). These authors observed specific methylation rates associated with aging and phase-change in this species, and reported GDM of around 30% in basal portions of juvenile radiata pine tree needles, while those rates increased up to almost 60% in the apical areas. In the current experiment full needles were analysed, so the methylation rates detected correlate with those studies. Interestingly, GDM levels in needles were similar to those observed in EMs. It would be interesting to study the evolution of GDM after the first subculture of EMs, to confirm whether methylation increases progressively with each subculture period, and also to observe what happens during Se's formation and plant conversion.

Regarding the effect of temperature on GDM levels during induction of SE, significant differences were detected among treatments at plant level. Although not significant, in EMs the 60°C for 5 min treatment provoked a decrease in the content of 5mC, while moderate temperatures and long-exposures slightly increased those levels. In *ex vitro* plants those effects were more evident. The pattern observed in EMs was attenuated at the highest temperature (60°C), presenting a significant GDM decrease of around 3% when compared to the other treatments. In *Arabidopsis*, Berdasco et al. (2008) reported that a chemically-induced 3% decrease in DNA methylation led to the differential expression of 1794 transcripts.

Although many studies have underlined the responsiveness of the methylome to heat, changes of DNA methylation under this stress seem not to follow a consistent trend if observed the published data, since different species and cell types appear to respond in different ways. Exposure of *Arabidopsis* plants to heat resulted in increased GDM (Boyko et al., 2010). The same trend was observed in Norway spruce seedling originating from a warm embryonic environment (Johnsen et al., 2005). Alakärppä et al. (2018) also observed differences in the content of 5mC of Scots pine embryos from contrasting habitats. On the other hand, in cotton anthers and oilseed rape cultured microspores, heat led to hypomethylation of the DNA (Min et al., 2014; Li et al., 2016).

Although preliminary, these results could be connected with the developmental and drought resilience changes observed among somatic plants originating from different induction temperature treatments in a previous study (Castander-Olarieta et al., 2020a). There, we observed that differences temperature pulses at this stage provoked variations in the growth rates of plants years later in the greenhouse. In this regard, Browne et al. (2020) showed that the application of the demethylating agent 5-Azacytidine led to a reduction in the growth rate of oak seedlings. In addition, some other studies are highlighting the interconnection of the methylation status of plants and their capacity to cope with stress, i.e, drought (Sow et al., 2020). As a result, further analyses addressing the specific distribution of methylated regions are required to confirm our hypothesis and shed light on the molecular mechanisms leading to those phenotypic variations.

The use of HPLC coupled to mass spectrometry in this study enabled the identification of 5hmC in both EMs and somatic plant needles of radiata pine, although at very low concentrations. It is noticeable however, that radiata pine genome is 23 billion base pairs, eight times the size of the human genome. Consequently, even if the percentage of 5hmC is not so high, the amount of hydroxylated cytosines could be relevant in terms of total number. As far as we know, this is the first report confirming the presence of this oxidised form of 5mC in pines, and the second in conifers (Yakovlev et al., 2019). In fact,

Alakärppä et al. (2018) reported no traces of this molecule in zygotic embryos and megagametophytes of Scots pine using a CG-MS method.

Despite being considered the sixth nucleobase in DNA and its demonstrated functionality in mammals (Shi et al., 2017), researchers are still doubtful about its existence and biological function in plants. As a matter of fact, 5hmC has been found at very low quantities in plant genomes. This, together with the existence of DNA glycosylases in plants that can cleavage 5mC directly from the genome (Jang et al., 2014) and the lack of enzymatic homologues in plants for the mammal readers and writers of 5hmC (TET/UHRF2) (Nystedt et al., 2013) suggest that 5hmC may be the end product of DNA damage, being involved in passive demethylations processes (Shi et al., 2017). However, some studies defend its enzymatic origin (Moricová et al., 2013; Yakovlev et al., 2019) and due to its high abundance in transposable elements located in heterochromatin regions (Wang et al., 2015) and during specific developmental stages (Moricová et al., 2013), it may be involved in heterochromatin formation and maintenance of genome stability together with 5mC (Valinluck et al., 2004).

Supporting this idea, we found different concentrations of 5hmC in EMs and needles of one-year-old somatic plants. The hydroxymethylation levels in EMs were considerably lower than in needles, being almost undetectable in most of the samples. However, methylation levels were similar in both tissue types. Accordingly, in human cells, Nestor et al. (2012) found that the content of 5hmC is highly variable and does not necessarily correlate with the content of 5mC. In line with these findings, we also observed decreased levels of 5hmC in needles of somatic plant originating from high temperatures. Although methylation rates presented the same tendency at 60°C treatment, at 40°C changes in methylation did not correlate with those of 5hmC. There are not studies addressing the role of 5hmC under stress conditions in plants, but based on these results we can hypothesize that this modification of cytosine may take part in numerous cell processes, including stress responses, not only as a passive intermediate of demethylation but also as a potential epigenetic mark in plants.

Together with changes in methylation and hydroxymethylation rates, the present study confirmed the differential expression of several stress-related genes along the phases of SE in radiata pine. Even though a clear pattern was not maintained throughout the process, some points were worth noting. As a general trend, the gene coding for a heat shock protein (*HSP20*) was down-regulated at high temperatures in most of the developmental stages analysed, presenting the highest fold changes at early stages in EMs and at plant level. Heat shock proteins (HSP) are essential during exposure to heat stress by preventing proteins from denaturation, and their sustained accumulation enhances thermo-tolerance (Bokszczanin & Fragkostefanakis, 2013). Responsiveness under other stress conditions like drought has also been documented (Taïbi et al., 2017).

The long term down-regulation of HSP at high temperatures in this study may correlate with the decreased drought-resilience observed in previous studies in plants originating from high temperatures (Castander-Olarieta et al., 2020a). In fact, although the expression of genes encoding HSP tend to increase under heat conditions, several authors have reported that selective autophagy mediates the specific degradation of HSP at later stages of thermo-recovery phase, compromising the long-term acquired HSP memory (Sedaghatmehr et a., 2019; Venkatesh et al., 2020).

Alternatively, other authors have postulated that all types of HSP may not be involved in regulation of heat acclimation and have reported unique transcription patterns for several HSP homologs (Ujino-Ihara, 2020). Furthermore, many studies have reported poor transcript/proteins correlations. For instance, in heat-primed azalea plants recover to control temperature, transcripts of HSP decreased rapidly in a short time, while proteins maintained a sustained accumulation for a long period, therefore conferring resistance to subsequent stress events (Wang et al., 2020). As a result, it would be of special interest to combine the results from this experiment with proteomic analyses to confirm our hypothesis.

In proliferating EMs and Se's, transcripts encoding enzymes involved in oxidative stress (*ADH* and *SOD*) were found at lower concentrations. Although these enzymes are required to detoxify compounds resulting from heat-stress at short-term exposures,

their accumulation during long-term acquired tolerance or acclimation seem not to be significant (Escandón et al., 2017). The same pattern was observed for the ribosomic protein *50SR* in EMs at initiation and in Se's. During Se's formation, protein homeostasis and synthesis of reserve proteins are of special relevance (Businge et al., 2013). Consequently, alterations in the levels of proteins involved in translation like *50SR* could have important effects for the success of the process, even determining the morphology of Se's, as observed in previous studies (Castander-Olarieta et al., 2019). Besides, the biological function of this *50SR* has also been linked to cytokinins (Černý et al., 2013), and its down-regulation as a consequence of high temperatures could be an explanation for the decrease of most of the cytokinin types analysed in Castander-Olarieta et al. (2020a, 2020b) under the same temperature conditions.

In spite of being previously categorised as an excellent candidate biomarker under heat-stress in radiata pine, and the demonstrated relevance of transcriptional control during thermotolerance (Escandón et al., 2017), the transcription factor *APFI* did not show a clear pattern in our study and its gene expression differences presented very low fold changes. It is noticeable that Escandón et al. (2017) only observed its protein accumulation at early stress-response stages. Similar results were obtained for *DI19*. *DI19* family of proteins are a novel type of Cys2/His2 zinc-finger proteins and their overexpression results in drought-sensitive phenotypes in *Arabidopsis* (Quin et al., 2014). However, some studies suggest that post-translational modifications of these proteins may be important for regulating their function (Rodriguez Milla et al., 2006), and thus, further research is required to assess whether the observed transcript profile changes are reflected in the phenotype.

In conclusion, this study confirmed that high temperatures at early stages of radiata pine SE can provoke long-term changes in the methylation status of the resulting somatic plants, revealing the formation of a stable epigenetic memory. We also detected for the first time in a pine species the presence of 5hmC, and observed that its concentration can fluctuate according to the tissue type or to environmental factors like temperature. All these alterations could be related with the sustained differential expression of

several stress-related genes along the whole embryogenic process, with a special emphasis on the role of HSP.

5. REFERENCES

Aitken-Christie, J., Singh, A.P., and Davies, H. (1988) "Multiplication of meristematic tissue: a new tissue culture system for radiata pine" in Genetic manipulation ofwoody plants, eds. Hanover, J.W., Keathley, D.E. (Plenum Press, New York and London), 413-432.

Alakärppä, E., Salo, H.M., Valledor, L., Cañal, M.J., Häggman, H., and Vuosku, J. (2018). Natural variation of DNA methylation and gene expression may determine local adaptations of Scots pine populations. *J. Exp. Bot*. 69, 5293-5305.

Alvarez, C., Valledor, L., Sáez, P., Hasbún, R., Sánchez-Olate, M., Cañal, M.J., et al. (2016). Changes in gene expression in needles and stems of *Pinus radiata* rootstock plants of different ontogenic age. *Am. J. Plant Sci.* 7, 1205-1216.

Amaral, J., Ribeyre, Z., Vigneaud, J., Sow, M.D., Fichot, R., Messier, C., et al. (2020). Advances and promises of epigenetics for forest trees. *Forests* 11, 976.

Berdasco, M., Alcázar, R., García-Ortiz, M.V., Ballestar, E., Fernández, A.F., and Roldán-Arjona, T. (2008). Promoter DNA hypermethylation and gene repression in undifferentiated *Arabidopsis* cells. *PLoSONE* 3, e3306.

Blödner, C., Skroppa, T., Johnsen, Ø., and Polle, A. (2005). Freezing tolerance in two Norway spruce (*Picea abies* [L.] Karst.) progenies is physiologically correlated with drought tolerance*. J. Plant Physiol.* 162, 549-558.

Bokszczanin, K.L., and Fragkostefanakis, S. (2013). Perspectives on deciphering mechanisms underlying plant heat stress response and thermotolerance. *Front. Plant Sci*. 4, 1-20.

Bouché, F., Woods, D.P., and Amasino, R.M. (2017). Winter memory throughout the plant kingdom: different paths to flowering. *Plant Physiol. 173*, 27-35.

Boyko, A., and Kovalchuk, I. (2008). Epigenetic control of plant stress response. *Environ. Mol. Mutagen.* 49, 61-72.

Boyko, A., Blevins, T., Yao, Y., Golubov, A., Bilichak, A., Ilnytskyy, Y. et al. (2010). Transgenerational adaptation of *Arabidopsis* to stress requires DNA methylation and the function of dicer-like proteins. *PLoSONE* 5, e9514.

Bravo, S., Bertín, A., Turner, A., Sepúlveda, F., Jopia, P., Parra, M.J., et al. (2017). Differences in DNA methylation, DNA structure and embryogenesis-related gene expression between embryogenic and non-embryogenic lines of *Pinus radiata* D. don. *Plant Cell Tiss. Organ Cult.* 130, 521-529.

Browne, L., Mead, A., Horn, C., Chang, K., Celikkol, Z.A., Henriquez, C.L., et al. (2020). Experimental DNA demethylation associates with changes in growth and gene expression of oak tree seedlings. *G3* 10, 1019-1028.

Businge, E., and Egertsdotter, U. (2014). A possible biochemical basis for fructose-induced inhibition of embryo development in Norway spruce (*Picea abies*). *Tree Physiol.* 34, 657-669.

Castander-Olarieta, A., Montalbán, I.A., De Medeiros Oliveira, E., Dell'Aversana, E., D'Amelia, L., Carillo, P., et al. (2019). Effect of thermal stress on tissue ultrastructure and metabolite profiles during initiation of radiata pine somatic embryogenesis. *Front. Plant Sci.* 9, 1-16.

Castander-Olarieta, A., Moncaleán, P., Pereira, C., Pěnčík, A., Petřík, I., Pavlović, I., et al. (2020a). Cytokinins are involved in drought tolerance of *Pinus radiata* plants originating from embryonal masses induced at high temperatures. *Tree Physiol.* 1-15.

Castander-Olarieta, A., Pereira, C., Montalbán, I.A., Pěnčík, A., Petřík, I., Pavlović, I., et al. (2020b). Quantification of endogenous aromatic cytokinins in *Pinus radiata* embryonal masses after application of heat stress during initiation of somatic embryogenesis. *Trees*.

Černý, M., Kuklová, A., Hoehenwarter, W., Fragner, L., Novák, O., Rotková, G., et al. (2013). Proteome and metabolome profiling of cytokinin action in *Arabidopsis* identifying both distinct and similar responses to cytokinin down- and up-regulation. *J. Exp. Bot.* 64, 4193-4206.

Che, P., Love, T.M., Frame, B.R., Wang, K., Carriquiry, A.L., and Howell, S.H. (2006). Gene expression patterns during somatic embryo eevelopment and germination in maize Hi II callus cultures. *Plant Mol. Biol.* 62, 1-14.

Conrath, U., Beckers, G.J., Langenbach, C.J., and Jaskiewicz, M.R. (2015). Priming for enhanced defense. *Annu. Rev. Phytopathol*. 53, 97-119.

Corredoira, E., Cano, V., Bárány, I., Solís, M.T., Rodríguez, H., Vieitez, A.M., et al. (2017). Initiation of leaf somatic embryogenesis involves high pectin esterification, auxin accumulation and DNA demethylation in *Quercus alba*. *J. Plant Physiol*. 213, 42-54.

De-la-Peña, C., Nic-Can, G.I., Galaz-Ávalos, R.M., Avilez-Montalvo, R., and Loyola-Vargas, V.M. (2015). The role of chromatin modifications in somatic embryogenesis in plants. *Front. Plant. Sci*. 6, 635.

Dubin, M.J., Zhang, P., Meng, D., Remigereau, M.S., Osborne, E.J., Paolo Casale, F., et al. (2015). DNA methylation in *Arabidopsis* has a genetic basis and shows evidence of local adaptation. *Elife* 4.

Escandón, M., Valledor, L., Pascual, J., Pinto, G., Cañal, M.J., and Meijón, M. (2017). System-wide analysis of short-term response to high temperature in *Pinus radiata*. *J. Exp. Bot.* 68, 3629-3641.

Fernandez, A.F., Valledor, L., Vallejo, F., Cañal, M.J., and Fraga, M.F. (2018) "Quantification of global DNA methylation levels by mass spectrometry" in DNA Methylation Protocols. Methods in Molecular Biology, eds. Tost, J. (Humana Press: New York), 49-58.

Fraga, M.F., Rodríguez, R., and Cañal, M.J. (2002). Genomic DNA methylation–demethylation during aging and reinvigoration of *Pinus radiata*. *Tree Physiol.* 22, 813-816.

Fraga, M.F., Cañal, M.J., and Rodríguez, R. (2002). Phase-change related epigenetic and physiological changes in *Pinus radiata* D. Don. *Planta* 215**,** 672-678.

Fraga, H.P.F., Vieira, L.N., Caprestano, C.A., Steinmacher, D.A., Micke, G.A., Spudeit, D.A., et al. (2012). 5-Azacytidine combined with 2,4-D improves somatic embryogenesis of *Acca sellowiana* (O. Berg) Burret by means of changes in global DNA methylation levels. *Plant Cell Rep.* 31, 2165-2176.

García-Mendiguren, O., Montalbán, I.A., Goicoa, T., Ugarte, M.D., and Moncaleán, P. (2017). Are we able to modulate the response of somatic embryos of pines to drought stress? *Act. Hortic.* 1155, 77-84.

Iwasaki, M., and Paszkowski, J. (2014). Epigenetic memory in plants. *EMBO J*. 18, 1987-1998.

Jang, H., Shin, H., Eichman, B.F., and Huh, J.H. (2014). Excision of 5-hydroxymethylcytosine by DEMETER family DNA glycosylases. *Biochem. Biophys. Res. Commun.* 446, 1067-1072.

Johnsen, Ø., Fossdal, C.G., Nagy, N., Mølmann, J., Dæhlen, O.G., and Skrøppa, T. (2005). Climatic adaptation in *Picea abies* progenies is affected by the temperature during zygotic embryogenesis and seed maturation. *Plant Cell Environ*. 28, 1090-1102.

Kumar, S., Kumari, R., and Sharma, V. (2013). Roles, and establishment, maintenance and erasing of the epigenetic cytosine methylation marks in plants. *J. Genet.* 92, 629-666.

Kumar, R., Barua, P., Chakraborty, N., and Nandi, A.K. (2020). Systemic acquired resistance specific proteome of *Arabidopsis thaliana*. *Plant Cell Rep.* 39**,** 1549-1563.

Kvaalen, H., and Johnsen, O. (2008). Timing of bud set in *Picea abies* is regulated by a memory of temperature during zygotic and somatic embryogenesis. *New Phytol*. 177, 49-59.

Lämke, J., and Bäurle, I. (2017). Epigenetic and chromatin-based mechanisms in environmental stress adaptation and stress memory in plants. *Genome Biol.* 18, 124.

Le Gac, A.L., Lafon-Placette, C., Chauveau, D., Segura, V., Delaunay, A., Fichot, R., et al. (2018). Winter-dormant shoot apical meristem in poplar trees shows environmental epigenetic memory. *J. Exp. Bot*. 14, 4821-4837.

Li, J., Huang, Q., Sun, M., Zhang, T., Li, H., Chen, B., et al. (2016). Global DNA methylation variations after short-term heat shock treatment in cultured microspores of *Brassica napus* cv. Topas. *Sci. Rep.* 6, 38401.

Livak, K.J., and Schmittgen, T.D. (2001). Analysis of relative gene expression data using real-time quantitative PCR and the 2(-Delta Delta C(T)) Method. *Methods* 4, 402-408.

Miguel, C., and Marum, L. (2011). An epigenetic view of plant cells cultured *in vitro*: somaclonal variation and beyond. *J. Exp. Bot.* 62, 3713-3725.

Milla, M.A.R., Townsend, J., Chang, I., and Cushman, J.C. (2006). The *Arabidopsis AtDi19* gene family encodes a novel type of Cys2/His2 zinc-finger protein implicated in ABA-independent dehydration, high-salinity stress and light signaling pathways. *Plant Mol. Biol.* 61, 13-30.

Min, L., Li, Y., Hu, Q., Zhu, L., Gao, W., Wu, Y., et al. (2014). Sugar and auxin signaling pathways respond to high-temperature stress during anther development as revealed by transcript profiling analysis in cotton. *Plant Physiol*. 164, 1293-308.

Montalbán, I.A., de Diego, N., and Moncaleán, P. (2012). Enhancing initiation and proliferation in radiata pine (*Pinus radiata* D. Don) somatic embryogenesis through seed family screening, zygotic embryo staging and media adjustments. *Acta Physiol. Plant.* 34, 451-460.

Montalbán, I.A., and Moncaleán, P. (2018) "*Pinus radiata* (D. Don) somatic embryogenesis" in Step Wise Protocols for Somatic Embryogenesis of Important Woody Plants, eds. Jain, S., Gupta, P. (Springer, Cham, Switzerland), 1-11.

Morcillo, M., Sales, E., Ponce, L., Guillén, A., Segura, J., and Arrillaga, I. (2020). Effect of elicitors on holm oak somatic embryo development and efficacy inducing tolerance to *Phytophthora cinnamomi*. *Sci. Rep.* 10, 15166.

Moricová, P., Ondřej, V., Navrátilová, B., and Luhová, L. (2013). Changes of DNA methylation and hydroxymethylation in plant protoplast cultures. *Acta Biochim. Pol.* 60, 33-36.

Nestor, C.E., Ottaviano, R., Reddington, J., Sproul, D., Reinhardt, D., Dunican, D., et al. (2012). Tissue type is a major modifier of the 5-hydroxymethylcytosine content of human genes. *Genome Res.* 3, 467-77.

Noceda, C., Salaj, T., Pérez, M., Viejo, M., Cañal, M.J., Salaj, J., et al. (2009). DNA demethylation and decrease on free polyamines is associated with the embryogenic capacity of *Pinus nigra* Arn. cell culture. *Trees* 23, *1285*.

Nystedt, B., Street, N., Wetterbom, A., Zuccolo, A., Lin, Y.C., Scofield, D.G. et al. (2013). The Norway spruce genome sequence and conifer genome evolution. *Nature* 497, 579-584.

Pereira, C., Castander-Olarieta, A., Montalbán, I.A., Pěnčík, A., Petřík, I., Pavlović, I., et al. (2020). Embryonal masses induced at high temperatures in Aleppo pine: cytokinin profile and cytological characterization. *Forests* 11, 807.

Perrone, A., and Martinelli, F. (2020). Plant stress biology in epigenomic era. *Plant Sci*. 294, 110376.

Qin, L.X., Li, Y., Li, D.D., Xu, W.L., Zheng, Y., and Li, X.B. (2014). *Arabidopsis* drought-induced protein Di19-3 participates in plant response to drought and high salinity stresses. *Plant Mol. Biol.* 6, 609-625.

Quoirin, M., and Lepoivre, P. (1977). Études des milieux adaptés aux cultures in vitro de *Prunus. Acta Hort.* 78, 437-442.

Santamaría, M.E., Hasbún, R., Valera, M.J., Meijón, M., Valledor, L., Rodríguez, J.L., et al. (2009). Acetylated H4 histone and genomic DNA methylation patterns during bud set and bud burst in *Castanea sativa*. *J. Plant Physiol*. 166, 1360-1369.

Sedaghatmehr, M., Thirumalaikumar, V.P., Kamranfar, I., Marmagne, A., Masclaux-Daubresse, C., and Balazadeh, S. (2019). A regulatory role of autophagy for resetting the memory of heat stress in plants. *Plant Cell Environ*. 42, 1054-1064.

Shi, D.Q., Ali, I., Tang, J., and Yang, W.C. (2017). New insights into 5hmC DNA modification: generation, distribution and function. *Front. Genet.* 8, 100.

Solís, M.T., Rodríguez-Serrano, M., Meijón, M., Cañal, M.J., Cifuentes, A., Risueño, M.C., et al. (2012). DNA methylation dynamics and MET1a-like gene expression changes during stress-induced pollen reprogramming to embryogenesis. *J. Exp.Bot.* 63, 6431-6444.

Sow, M.D., Allona, I., Ambroise, C., Conde, D., Fichot, R., Gribkova, S., et al. (2018). "Epigenetics in forest trees: State of the art and potential implications for breeding and management in a context of climate change" in Advances in botanical research. Plant epigenetics coming of age for breeding applications, eds. Gallusci, P., Bucher, E., Mirouze, M. (Academic Press, Elsevier, Amsterdam), 387-453.

Sow, M.D., Le Gac, A.L., Fichot, R., Lanciano, S., Delaunay, A., Le Jan, I., et al. (2020). Hypomethylated poplars show higher tolerance to water deficit and highlight a dual role

for DNA methylation in shoot meristem: regulation of stress response and genome integrity. *bioRxiv* 045328.

Taïbi, K., del Campo, A.D., Aguado, A., and Mulet, J.M. (2015). The effect of genotype by environment interaction, phenotypic plasticity and adaptation on *Pinus halepensis* reforestation establishment under expected climate drifts. *Ecol. Eng.* 84, 218-228.

Teyssier, C., Maury, S., Beaufour, M., Grondin, C., Delaunay, A., Le Metté, C., et al. (2014). In search of markers for somatic embryo maturation in hybrid larch (*Larix* × *eurolepis*): global DNA methylation and proteomic analyses. *Physiol. Plant.* 150, 271-291.

Thirumalaikumar, V.P., Karina Schulz, M.G., Masclaux-Daubresse, C., Sampathkumar, A., Skirycz, A., Vierstra, R.D., et al. (2020). Selective autophagy regulates heat stress memory in *Arabidopsis* by NBR1-mediated targeting of HSP90 and ROF1. *Autophagy*.

Tittel-Elmer, M., Bucher, E., Broger, L., Mathieu, O., Paszkowski, J., and Vaillant I. (2010). Stress-induced activation of heterochromatic transcription. *PLoS Genet*. 6, 1001175.

Ujino-Ihara, T. Transcriptome analysis of heat stressed seedlings with or without pre-heat treatment in *Cryptomeria japonica*. *Mol. Genet. Genomics* 295, 1163-1172.

Valinluck, V., Tsai, H.H., Rogstad, D.K., Burdzy, A., Bird, A., and Sowers, L.C. (2004). Oxidative damage to methyl-CpG sequences inhibits the binding of the methyl-CpG binding domain (MBD) of methyl-CpG binding protein 2 (MeCP2). *Nucleic Acids Res.* 32, 4100-4108.

Valledor, L., Escandón, M., Meijón, M., Nukarinen, E., Cañal, M.J., and Weckwerth, W. (2014). A universal protocol for the combined isolation of metabolites, DNA, long RNAs, small RNAs, and proteins from plants and microorganisms. *Plant J.* 79, 173-180.

Walter, C., Find, J.I., and Grace, L.J. (2005). "Somatic embryogenesis and genetic transformation in *Pinus radiata*" in Protocols for somatic embryogenesis in woody plants, eds. Jain, S.M., Gupta, P.K. (Springer, Dordrecht), 491-504.

Wang, X.L., Song, S.H., Wu, Y.S., Li, Y.L., Chen, T.T., Huang, Z.Y., et al. (2015). Genome-wide mapping of 5-hydroxymethylcytosine in three rice cultivars reveals its preferential localization in transcriptionally silent transposable element genes. *J. Exp. Bot.* 66, 6651-6663.

Wang, X., Li, Z., Liu, B., Zhou, H., Elmongy, M.S., and Xia, Y. (2020). Combined proteome and transcriptome analysis of heat-primed azalea reveals new insights into plant heat acclimation memory. *Front. Plant Sci.* 11, 1278.

Yakovlev, I.A., Carneros, E., Lee, Y., Olsen, J.E., and Fossdal, C.G. (2016). Transcriptional profiling of epigenetic regulators in somatic embryos during temperature induced formation of an epigenetic memory in Norway spruce. *Planta* 243**,** 1237-1249.

Yakovlev, I.A., and Fossdal, C.G. (2027). *In silico* analysis of small RNAs suggest roles for novel and conserved miRNAs in the formation of epigenetic memory in somatic embryos of Norway spruce. *Front. Physiol.* 8.

Yakovlev, I.A., Gackowski, D., Abakir, A., Viejo, M., Ruzov, A., Olinski, R., et al. (2019). Mass spectrometry reveals the presence of specific set of epigenetic DNA modifications in the Norway spruce genome. *Sci. Rep.* 9, 19314.

GENERAL DISCUSSION

GENERAL DISCUSSION

Trees, as sessile, long-living organisms with complex life cycles, have acquired multiple mechanisms to adapt to constant environmental changes and stress factors. Research carried out during the last decades has demonstrated that plants with the same genetic background can showcase different phenotypes depending on the environment in which they are growing, a phenomenon commonly known as phenotypic plasticity (Pigliucci et al., 2006). Furthermore, those environmental cues can be "remembered" by the plant as a form of mid-term and long-term memory (priming), enhancing plant fitness under sudden stress events and facilitating rapid and sustained acclimation to future constraints (Amaral et al., 2020). The underlaying mechanisms are still largely unknown, but there are now multiple studies supporting that epigenetics have a key role by regulating gene expression and transposable elements mobilization (Zhang et al., 2013; Kijowska-Oberc et al., 2020). This epigenetic footprint can become stable and even transmitted across generations contributing to environmental adaptation.

Besides, embryo development and seed maturation, albeit short periods of time if compared with the lifespan of a tree, appear to be critical stages for the induction of phenotypic plasticity and the establishment of epigenetic memory, as reported in Norway spruce during both zygotic and somatic embryogenesis (SE) (Kvaalen & Johsen, 2008; Yakovlev et al., 2010, 2011). This fact has opened the way for the possibility of modulating the behaviour and stress resilience of the plant at early embryogenic stage. The combination of this idea with a powerful micropropagation technique like SE could be employed in forest biotechnology to improve the productivity and health of economically relevant conifer species under the ongoing global climate warming.

In this context, the present work has shed new insights into phenotypic plasticity and temperature-induced priming, and has confirmed that the application of heat-stress during initial stages of SE can provoke long-lasting effects, determining not only the success of the different phases of the process, but also the performance of the regenerated plants years later. On top of that, this work has revealed that further levels of complexity are potentially underpinning priming and stress memory, which involve

an integrated network of metabolites, phytohormones and proteins acting together to increase phenotypic diversity and regulate abiotic stress tolerance.

In agreement with previous studies carried out in our laboratory (García-Mendiguren et al., 2016; Pereira et al., 2016), one of the first effects of heat during radiata pine SE was the decrease of success at initial steps of the process, especially of embryonal mass induction when moderate temperatures and long-exposures were applied. This compromises the genetic diversity that could be obtained at standard conditions. Microscopical analyses revealed that this effect could be derived from micromorphological changes in embryonal masses (EMs). Heat provoked alterations in the polarity of proembryogenic masses, a reduction of the mitotic activity and an increase in the number vacuoles, Golgi bodies, plastolysome-like structures and starch granules around the nuclei of cells. These features have previously been described as early symptoms of programmed cell death, leading to the formation of supernumerary suspensor cells as a consequence of disturbed polar auxin transport (Abrahamsson et al., 2012).

On the other hand, pulse-like treatments at the highest temperatures (60°C, 5 min) enhanced the formation of big and well-developed embryogenic areas, while at long-term, all treatments increased the production of somatic embryos (Se's), as already observed by García-Mendiguren et al. (2016). This could be used as a tool to improve the efficiency of the process. Besides, it is noticeable that those Se's originating from pulse-like treatments presented better characteristics than those from the longest exposure treatments, reinforcing the importance of EMs morphology in Se's formation. Consequently, short heat exposures at high temperatures are the best option in order not to reduce genetic diversity and increase the number and quality of Se's.

Apart from changes at early and mid-term stages, in this study delayed effects were detected on both the growth of somatic plants in well-watered conditions (increased following treatment at 30°C), and on plant drought resilience (reduced at 30°C and 50°C), as indicated by plant survival and several physiological parameters such as instant net photosynthesis and intrinsic water use efficiency. Despite the reduced

drought resilience of plants originating from high temperatures, the results at control conditions are encouraging as temperature could be employed as a tool to improve the performance of the regenerated plants in terms of growth. Similar results were obtained in other conifer species when leader shoot lengths were measured during the second growth season in somatic plants subjected to high temperatures during SE (Kvaalen & Johnsen, 2008). With regard to drought resilience induction, it would be interesting to test if the adjustment of temperature and exposure periods could revert the results obtained, together with the assessment of thermotolerance acquisition or tolerance to the combination of both heat and drought stresses, as both can activate similar protective molecular pathways (Gimeno et al., 2009).

In line with this information, in this study we observed that the profile of endogenous cytokinins (CKs) in proliferating EMs changed according to the temperature of origin. As a general trend, most of the isoprenoid CKs analysed showed reduced levels (total CK bases, iP, cZR) at moderate temperatures and long exposures, whereas tZR drastically increased at the highest temperature. A similar decreasing pattern was described for some free aromatic CK bases, including BA, oT and pT. The same treatments however, increased the levels of certain ribosides (BAR, pTR), precursors (BARMP) and deactivation forms (BA9G).

While the function of CKs in plant development has extensively been studied (Choi & Hwang, 2007), their role as stress mediators is not fully understood, especially for aromatic CKs like oT and pT, traditionally considered CKs with low biological activity. These results reinforce the idea postulated by Černý et al. (2013) about the involvement of CKs in temperature sensing and remark the function of specific forms such as tZR as protective molecules (Liu et al., 2002) and iP as a molecular marker of embryo formation. In fact, low concentrations of this last phytohormone correlated with high production of Se's in this study and previous ones (Moncaleán et al., 2018). Moreover, the balance between some aromatic free bases like BA and the total amount of ribosides and nucleotides seem to have great impact on EMs proliferation.

Likewise, CKs are known to contribute to the regulation of the WUSHEL related homeobox family (WOX) of genes such as *WUS* (Liu et al., 2018). This gene has important functions along plant embryogenesis, controlling, among others, polar auxin transport during apical-basal patterning through co-regulation by DNA methylation (Maury et al., 2019). This fact could explain the abovementioned alterations in EMs morphologies and the supernumerary suspensor cell phenomenon.

As a putative novel function, results also suggested that CKs may be involved in stress memory acquisition and maintenance. Due to their demonstrated role during plant growth and their function as negative regulators of root growth and lateral root formation (Werner et al., 2001; Perilli et al., 2010), they may have been involved in the delayed effects observed in somatic plants under both control and drought stress conditions. Besides, it has been long described that plant growth regulators can interact with epigenetic mechanisms (Maury et al., 2019). Nonetheless, this remains just as a hypothesis because the levels of CK at plant level were not determined, and thus, further studies are required to confirm it.

Additionally, a crosstalk among CKs and the proteome has been underlined. Certain CKs are known to regulate the expression of heat shock proteins (HSPs) (Černý et al., 2011), whose levels were confirmed to increase at mid-term in Se's. In this regard, HSPs are essential molecules during heat-stress responses and thermotolerance acquisition (Bokszczanin & Fragkostefanakis, 2013). As a counterpoint, the expression pattern of a HSP-coding gene showed a down-regulation tendency throughout the SE process. Nonetheless, these discrepancies may be derived from poor transcript/protein correlations, as already reported in many studies (Correia et al., 2016), or from the fact that all types of HSP may not be involved in regulation of heat acclimation (Ujino-Ihara, 2020). Consequently, it would be of special interest to study the levels of HSP at plant level to determine whether the stress resilience differences observed could be attributed to a differential accumulation of these molecules.

The translasome machinery, including ribosomal proteins, proteasomal subunits and translation elongation factors in Se's was also affected by high temperatures. Some of

these proteins, like the ribosomal subunit 50SR, are known to be connected with the CK signalling network (Černý et al., 2013). The gene encoding this protein was confirmed to present varying expression patterns along the embryogenic process. Moreover, protein synthesis regulation is determinant during embryo formation and certain proteasomal subunits and translation elongations factors have been described as strong molecular markers of embryogenic capacity (Trontin et al., 2016). Thus, the alterations of the translasome machinery together with alterations in the CK profiles could be influencing the maturation efficiency of EMs in terms of embryo quantity/quality.

The epigenetic memory hypothesis was further validated by the detection of varying global DNA methylation levels among EMs and somatic plants originating from different induction temperatures, being the ones from the highest temperatures (60°C) less methylated than the others. DNA methylation has been widely described as having considerable influence on a great variety of biological processes, from plant growth regulation (Ma et al., 2020), to stress response and adaptation (Lafon-Placette et al., 2018). As a result, the differences previously described could be associated with the methylation status of EMs and somatic plants. However, more studies are required to determine in which regions of the DNA are occurring those changes and whether methylation is acting together with other epigenetic mechanisms such as small RNAs or histone modifications to regulate this phenomenon, as reported by Yakovlev & Fossdal (2017) and Lamelas et al. (2020). In this sense, we observed for the first time in a pine species the presence of 5-hydroxymethylcytosine, and although at very low concentrations, this molecule showed tissue specificity and temperature-dependency, indicating that it may take active part in stress response and memory acquisition together with 5-mehylcytosine.

The proteomic study also revealed the presence of proteins related to methylation and posttranscriptional gene regulation via small RNAs, reinforcing the results obtained from the global DNA methylation analysis. This also suggests that multiple epigenetic mechanisms could be working together for the transduction of temperature-induced signals from the early stages of somatic embryogenesis to regenerated plants.

In turn, the combined proteomic, metabolic and gene expression analyses showed that during early phases of stress response, the production of oxidative-stress-related proteins and metabolites seems to be the first response of plant cells, as indicated by the high levels of isoleucine, tyrosine and phenolic compounds in EMs originating from high temperatures after first subculture. Then, during acclimation and memory acquisition in further stages of the process, those molecules appear to be substituted by HSPs, fatty acids and specific carbohydrates such as myo-inositol. The former may play a key role as a compatible solute to cope with osmotic stress (Joshi et al., 2013). Differential synthesis of certain fatty acids and carbohydrates could lead to structural changes in cells. In fact, modification of the composition of cell membrane fatty acids to compensate for membrane fluidity changes produced by heat is a well-known strategy followed by plants during acclimation (Escandón et al., 2017). Similarly, modifications of the components of cell-wall polymers, i.e., changes in the concentration of D-xylose, have been observed in many plant species under heat (Lima et al., 2013).

In conclusion, this study confirmed the feasibility of modulating the characteristics of plants through modifications of the environmental conditions during early stages of SE. This approach could be used to improve the growth of plants at standard conditions, and based on our methylation/hydroxymethylation results, further studies should be carried out to determine if other epigenetic mechanisms such as histone modifications or small RNAs are accounting for phenotypic plasticity and stress memory. It would be of special interest to confirm whether the molecular changes observed in EMs and Se's are maintained during plant conversion to have a broader vision of how memory is maintained and which are the long-term characteristics derived from those molecular readjustments, with special emphasis on structural and compositional changes of cell-walls and membranes.

REFERENCES

Abrahamsson, M., Valladares, S., Larsson, E., Clapham, D., and von Arnold, S. (2012). Patterning during somatic embryogenesis in Scots pine in relation to polar auxin transport and programmed cell death. *Plant Cell Tissue Organ Cult.* 109, 391-400.

Bokszczanin, K.L., and Fragkostefanakis, S. (2013). Perspectives on deciphering mechanisms underlying plant heat stress response and thermotolerance. *Front. Plant Sci.* 4, 1-20.

Černý, M., Dyčka, F., Bobáľová, J., and Brzobohatý, B. (2011). Early cytokinin response proteins and phosphoproteins of *Arabidopsis thaliana* identified by proteome and phosphoproteome profiling. *J. Exp. Bot.* 62, 921-937.

Černý, M., Kuklová, A., Hoehenwarter, W., Fragner, L., Novák, O., Rotková, G., et al. (2013). Proteome and metabolome profiling of cytokinin action in *Arabidopsis* identifying both distinct and similar responses to cytokinin down- and up-regulation. *J. Exp. Bot.* 64, 4193-4206.

Choi, J., and Hwang, I. (2007). Cytokinin: perception, signal transduction, and role in plant growth and development. *J. Plant Biol.* 50, 98-108.

Correia, S.I., Alves, A.C., Veríssimo, P., and Canhoto, J.M. (2016). "Somatic embryogenesis in broad-leaf woody plants: what we can learn from proteomics", in *In Vitro* Embryogenesis in Higher Plants, eds. Germana, M., Lambardi, M. (Humana Press, New York), 117-129.

Escandón, M., Valledor, L., Pascual, J., Pinto, G., Cañal, M.J., and Meijón, M. (2017). System-wide analysis of short-term response to high temperature in *Pinus radiata*. *J. Exp. Bot.* 68, 3629-3641.

García-Mendiguren, O., Montalbán, I.A., Goicoa, T., Ugarte, M.D., and Moncaleán, P. (2016). Environmental conditions at the initial stages of *Pinus radiata* somatic embryogenesis affect the production of somatic embryos. *Trees - Struct. Funct.* 30, 949-958.

Gimeno, T.E., Pas, B., Lemos-Filho, J.P., and Valladares, F. (2009). Plasticity and stress tolerance override local adaptation in the responses of Mediterranean holm oak seedlings to drought and cold. *Tree Physiol.* 29, 87-98.

Joshi, R., Ramanarao, M.V., and Baisakh, N. (2013). *Arabidopsis* plants constitutively overexpressing a myo-inositol 1-phosphate synthase gene (SaINO1) from the halophyte smooth cordgrass exhibits enhanced level of tolerance to salt stress. *Plant Physiol. Biochem.* 65, 61-66.

Kijowska-Oberc, J., Staszak, A.M., Kamiński, J., and Ratajczak, E. (2020). Adaptation of forest trees to rapidly changing climate. *Forests* 11, 123.

Kvaalen, H., and Johnsen, Ø. (2008). Timing of bud set in *Picea abies* is regulated by a memory of temperature during zygotic and somatic embryogenesis. *New Phytol.* 177, 49-59.

Lafon-Placette, C., Le Gac, A.L., Chauveau, D., Segura, V., Delaunay, A., Lesage-Descauses, Irène Hummel, M.C., et al. (2018). Changes in the epigenome and transcriptome of the poplar shoot apical meristem in response to water availability affect preferentially hormone pathways. *J. Exp. Bot.* 69, 537-551.

Lamelas, L., Valledor, L., Escandón, M., Pinto, G., Cañal, M.J., and Meijón, M. (2020). Integrative analysis of the nuclear proteome in *Pinus radiata* reveals thermopriming coupled to epigenetic regulation. *J. Exp. Bot.* 71, 2040-2057.

Lima, R.B., Dos Santos, T.B., Vieira, L.G.E., Ferrarese, M.D.L.L., Ferrarese-Filho, O., Donatti, L., et al. (2013). Heat stress causes alterations in the cell-wall polymers and anatomy of coffee leaves (*Coffea arabica* L.). *Carbohydr. Polym.* 93, 135-143.

Liu, X., Huang, B., and Banowetz, G. (2002). Cytokinin effects on creeping bentgrass responses to heat stress: I. Shoot and root growth. *Crop Sci.* 42, 457-465.

Liu, H., Zhang, H., Dong, Y.X., Hao, Y.J., and Zhang, X.S. (2018). DNA METHYLTRANSFERASE1 - mediated shoot regeneration is regulated by cytokinin-induced cell cycle in *Arabidopsis*. *New Phytol.* 217, 219-232.

Ma, K., Song, Y., Ci, D., Zhou, D., Tian, M., and Zhang, D. (2020). Genome cytosine methylation may affect growth and wood property traits in populations of *Populus tomentosa*. *Forests* 11, 828.

Maury, S., Sow, M.D., Le Gac, A.L., Genitoni, J., Lafon-Placette, C., and Iva Mozgova, I. (2019). Phytohormone and chromatin crosstalk: the missing link for developmental plasticity? *Front. Plant Sci.* 10, 395.

Moncaleán, P., García-Mendiguren, O., Novák, O., Strnad, M., Goicoa, T., Ugarte, M.D., et al. (2018). Temperature and water availability during maturation affect the cytokinins and auxins profile of radiata pine somatic embryos. *Front. Plant Sci.* 9, 1-13.

Pereira, C., Montalbán, I.A., García-Mendiguren, O., Goicoa, T., Ugarte, M.D., Correia, S., et al. (2016). *Pinus halepensis* somatic embryogenesis is affected by the physical and chemical conditions at the initial stages of the process. *J. For. Res.* 21, 143-150.

Perilli, S., Moubayidin, L., and Sabatini, S. (2010). The molecular basis of cytokinin function. *Curr. Opin. Plant Biol.* 13, 21-26.

Pigliucci, M., Murren, C.J., and Schlichting, C.D. (2006). Phenotypic plasticity and evolution by genetic assimilation. *J. Exp. Biol.* 209, 2362-2367.

Trontin, J.F., Klimaszewska, K., Morel, A., Hargreaves, C., and Lelu-Walter, M.A. (2016). "Molecular aspects of conifer zygotic and somatic embryo development: A review of genome-wide approaches and recent insights" in *In Vitro* Embryogenesis in Higher Plants, eds. Germana, M., Lambardi, M. (Humana Press, New York), 167-207.

Ujino-Ihara, T. (2020). Transcriptome analysis of heat stressed seedlings with or without pre-heat treatment in *Cryptomeria japonica*. *Mol. Genet. Genomics* 295, 1163-1172.

Werner, T., Motyka, V., Strnad, M., and Schmülling, T. (2001). Regulation of plant growth by cytokinin. *Proc. National Acad. Sci.* 98, 10487-10492.

Yakovlev, I.A., Fossdal, C.G., and Johnsen, Ø. (2010). MicroRNAs, the epigenetic memory and climatic adaptation in Norway spruce. *New Phytol.* 187, 1154-1169.

Yakovlev, I.A., Asante, D.K.A., Fossdal, C.G., Junttila, O., and Johnsen, T. (2011). Differential gene expression related to an epigenetic memory affecting climatic adaptation in Norway spruce. *Plant Sci.* 180, 132-139.

Yakovlev, I.A.; and Fossdal, C.G. (2017). *In silico* analysis of small RNAs suggest roles for novel and conserved miRNAs in the formation of epigenetic memory in somatic embryos of Norway spruce. *Front. Physiol.* 8.

Zhang, Y.Y., Fischer, M., Colot, V., and Bossdorf, O. (2013). Epigenetic variation creates potential for evolution of plant phenotypic plasticity. *New Phytol.* 197, 314-322.

CONCLUSIONS

CONCLUSIONS

1. High temperatures at initial stages of radiata pine somatic embryogenesis determine the success of the different phases of the process. Long exposures at high temperatures have detrimental effects in terms of initiation and proliferation rates caused by micromorphological alterations in embryonal masses. However, all high temperature treatments assayed enhance the production of somatic embryos.
2. Heat-stress at initiation of somatic embryogenesis provokes long-lasting effects at plant level. Long exposure treatments (30°C, 4 weeks) increase the growth rate of somatic plants at standard conditions, presenting no physiological differences under drought conditions.
3. Pulse-like treatments (50°C, 5 min) decrease the drought resilience of somatic plants.
4. Heat leads to a long-term reduction in the amount of total isoprenoid cytokinin base forms, N^6-Isopentenyladenine, and *cis*-Zeatin riboside in embryonal masses, together with an increment in the levels of *trans*-Zeatin riboside. This could be determining the growth and physiology of the resulting somatic plants under both control and stress conditions.
5. The profile of aromatic cytokinins in embryonal masses is influenced by the temperature at which they are induced: bases like N^6-benzyladenine, *ortho*-Topolin and *para*-Topolin decrease, while ribosides, nucleotides and N-glucosides increase.
6. During early stress responses in radiata pine embryonal masses the synthesis of free branched-chain amino acids (isoleucine) and tyrosine is enhanced, which could serve as substrate for the synthesis of stress induced proteins and secondary metabolites such as phenolic compounds.
7. At long-term in somatic embryos, heat provokes changes in the profile of heat shock proteins, and proteins involved in translation, methylation, post-transcriptional regulation, and sugar/lipid metabolism.

8. High temperatures during induction of somatic embryogenesis lead to hypomethylation of embryonal masses and somatic plants and to sustained alterations in the expression patterns of stress-related genes. In particular, it is noticeable the down-regulation of a gene encoding a heat shock protein.
9. It is demonstrated for the first time the presence of 5-hydroxymethylcytosine in the genome of radiata pine, as well as its tissue specificity and temperature-sensitivity.

Temperature-induced priming during *Pinus radiata* somatic embryogenesis: integrating proteomic, metabolic and physiological approaches

Ander Castander Olarieta

eman ta zabal zazu
Universidad del País Vasco
Euskal Herriko Unibertsitatea
NEIKER
MEMBER OF BASQUE RESEARCH & TECHNOLOGY ALLIANCE
Euskadi, auzolana, bien común
EUSKO JAURLARITZA
GOBIERNO VASCO